Autoimmunity due to molecular mimicry as a cause of neurological disease

MICHAEL C. LEVIN[1,2,3], SANG MIN LEE[2,3], FRANCK KALUME[2,4], YVETTE MORCOS[2,3], F. CURTIS DOHAN JR[5], KAREN A. HASTY[1,6,8], JOSEPH C. CALLAWAY[2,4], JOSEPH ZUNT[9], DOMINIC M. DESIDERIO[3,7] & JOHN M. STUART[1,8]

[1]*Research Service, Veterans Affairs Medical Center, Memphis, Tennessee, USA*
[2]*Center for the Neurobiology of Brain Disease, Departments of [3]Neurology, [4]Anatomy, [5]Pathology, [6]Orthopedics-Campbell Clinic, Molecular Science and The Charles B. Stout Neuroscience Mass Spectrometry Laboratory, [7]Medicine and Center of Excellence in Connective Tissue Diseases, University of Tennessee Health Sciences Center, Memphis, Tennessee, USA*
[8]*Department of Neurology, University of Washington, Seattle, Washington, USA*
Correspondence should be addressed to M.C.L.; email: mlevin@utmem.edu

One hypothesis that couples infection with autoimmune disease is molecular mimicry. Molecular mimicry is characterized by an immune response to an environmental agent that cross-reacts with a host antigen, resulting in disease[1,2]. This hypothesis has been implicated in the pathogenesis of diabetes, lupus and multiple sclerosis (MS)[1-4]. There is limited direct evidence linking causative agents with pathogenic immune reactions in these diseases. Our study establishes a clear link between viral infection, autoimmunity and neurological disease in humans. As a model for molecular mimicry, we studied patients with human T-lymphotropic virus type 1 (HTLV-1)-associated myelopathy/tropical spastic paraparesis (HAM/TSP), a disease that can be indistinguishable from MS (refs. 5–7). HAM/TSP patients develop antibodies to neurons[8]. We hypothesized these antibodies would identify a central nervous system (CNS) autoantigen. Immunoglobulin G isolated from HAM/TSP patients identified heterogeneous nuclear ribonuclear protein-A1 (hnRNP-A1) as the autoantigen. Antibodies to hnRNP-A1 cross-reacted with HTLV-1-tax, the immune response to which is associated with HAM/TSP (refs. 5,9). Immunoglobulin G specifically stained human Betz cells, whose axons are preferentially damaged[7]. Infusion of autoantibodies in brain sections inhibited neuronal firing, indicative of their pathogenic nature. These data demonstrate the importance of molecular mimicry between an infecting agent and hnRNP-A1 in autoimmune disease of the CNS.

To test for molecular mimicry between an environmental agent and the central nervous system (CNS), we isolated immunoglobulin G (IgG) from the serum of patients with human T-lymphotropic virus type 1 (HTLV-1)-associated myelopathy/tropical spastic paraparesis (HAM/TSP) and tested it for reactivity with human tissues (Fig. 1*a*). There was intense staining of neurons in brain and no staining of glia, dorsal root ganglion (peripheral nervous system) or systemic organs. A monoclonal antibody to HTLV-1-tax (tax mAb) mimicked IgG staining of neurons. To identify the protein, cortical neurons were isolated, proteins extracted and subjected to SDS–PAGE and western-blot analysis. The IgG recognized a band of approximately 33 kD (Fig. 1*b*), whereas IgG isolated from controls did not. Importantly, the tax mAb that stained CNS neurons reacted with the antigen. All patients with HAM/TSP (13/13) developed antibodies recognizing the neuronal antigen[8]. Nine of ten HTLV-1-seropositive patients without neurological symptoms and 12 HTLV-1-seronegative controls showed no reactivity ($P < 0.0001$ versus HAM/TSP)[8]. Clinically, the HAM/TSP patients presented with progressive neurological disease in which corticospinal tract damage (weakness, spasticity and pathological reflexes) predominated[9]. Many of our patients were originally diagnosed with MS. In fact, one of our patients was diagnosed with MS for 20 years before HTLV-1 testing[10].

To establish a direct link between the immune response to HTLV-1 and the neurological disease, we purified the proteins recognized by the immune sera. Neuronal proteins were extracted under high salt conditions, separated by centrifugation and subjected to SDS–PAGE followed by western-blot analysis. Under these conditions, HAM/TSP IgG reacted with an antigen of 38 kD (Fig. 1*c*). Thus, depending on the extraction conditions, either a 33- or 38-kD autoantigen was recognized. Subsequently, the supernatant was subjected to two-dimensional (2-D) gel electrophoresis followed by western blot. HAM/TSP IgG was immunoreactive with proteins at a molecular weight of 33 and 38 kD and a pI of 9.3 (Fig. 1*d*). The proteins were dissected from 2-D gels, digested with trypsin and analyzed by matrix-assisted laser desorption ionization mass spectroscopy[11]. The molecular weights of the tryptic peptides aligned with hnRNP-A1 and A1[B]. Approximately 93% of the molecular weights matched these proteins with probability scores as high as 3.13×10^3 (data not shown). Heterogeneous nuclear ribonuclear protein-A1 (hnRNP-A1) and A1[B] are identical except for an additional 50 amino acids in hnRNP-A1. There were no matches with this unique sequence of hnRNP-A1. These data strongly suggest that HAM/TSP patients had autoimmunity to a common epitope in hnRNP-A1 and A1[B]. The calculated molecular weight and pI of these proteins approximate what we found by western blot (A1 = 38.8, A1[B] = 34.2, pI = 9.3). To prove that the immunoreactivity was specific for hnRNP-A1, we cloned and expressed recombinant hnRNP-A1 (rhnRNP-A1) from human brain. HAM/TSP IgG reacted with rhnRNP-A1 and the neuronal extract at an identical molecular weight (Fig. 2*a*). Pre-incubation of HAM/TSP IgG with rhnRNP-A1 abolished immunoreactivity of the western blots (Fig. 2*b* and *c*). This confirms that the protein dissected from the gel was the same protein identified by western blot and that the neuronal antigen recognized by HAM/TSP IgG is hnRNP-A1. IgG isolated from the cerebrospinal fluid (CSF) and brain of a HAM/TSP patient reacted with hnRNP-A1 (Fig. 2*d*). These data indicate that there is IgG specific for hnRNP-A1 intrathecally and within the brain parenchyma of HAM/TSP patients. Finally, the tax mAb that was immunoreac-

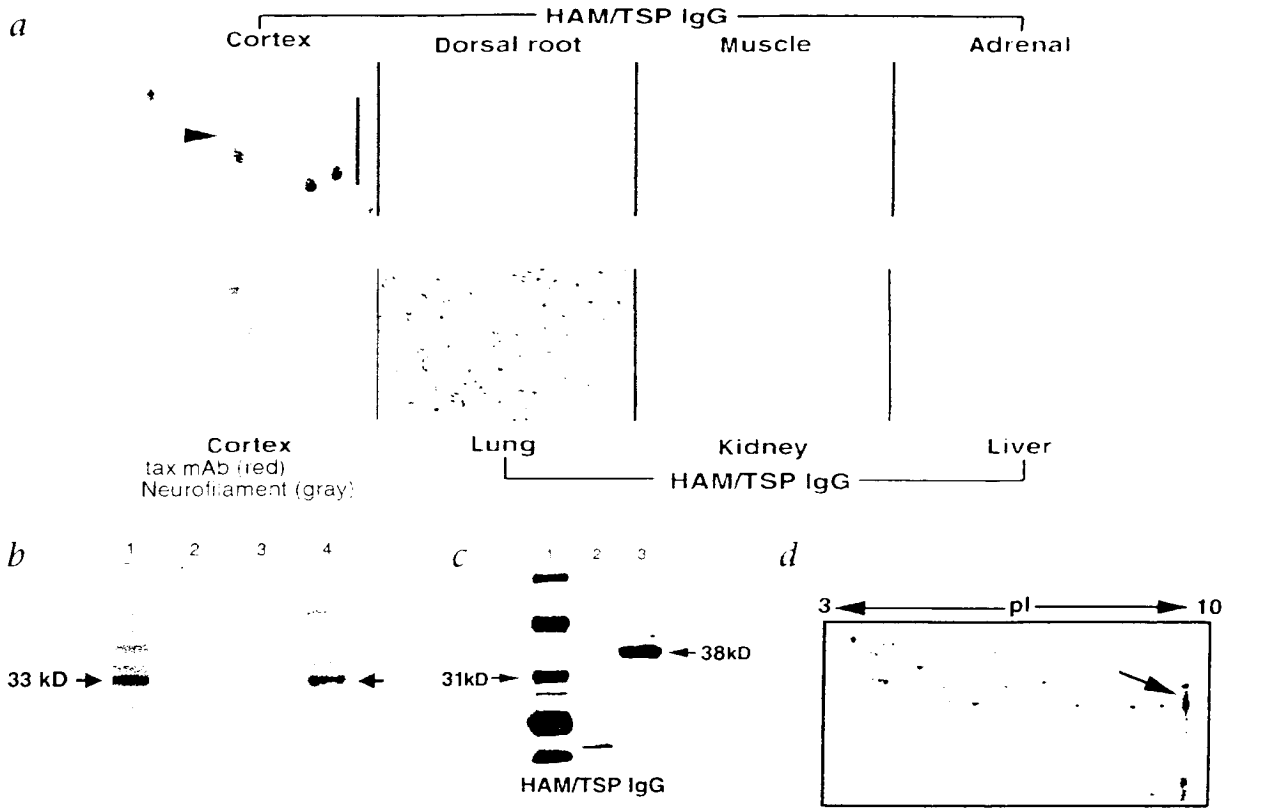

Fig. 1 Specificity of HAM/TSP IgG for CNS neurons and isolation of the neuronal antigen. ***a***, Immunohistochemistry of human tissues. Biotinylated HAM/TSP IgG stained CNS neurons (cortex, brown reaction product) (scale bar, 100 μm). There was no staining of glia (arrowhead), dorsal root ganglion or systemic organs. A tax mAb mimicked HAM/TSP IgG staining indicated by the red stain. Neurofilament (gray) confirmed localization of tax mAb to neurons. ***b***, Western blots of proteins derived from CNS neurons. HAM/TSP IgG showed an intense signal at 33 kD (lane 1). There was no reactivity using IgG isolated from HTLV-1 seronegative (lane 2) or HTLV-1 seropositive, neurologically asymptomatic individuals (lane 3). The tax mAb recognized the 33-kD neuronal antigen (lane 4). ***c***, Purification and western blots of the neuronal protein following high salt extraction and centrifugation. Molecular weight markers (lane 1), precipitate (lane 2) and supernatant (lane 3). HAM/TSP IgG reacted with the supernatant (lane 3), but not the precipitate (lane 2). ***d***, 2-D gel electrophoresis and western blot of the neuronal protein purified from the supernatant. Coomassie stain of gel (left). Western blot of the neuronal extract (right), HAM/TSP IgG reacted at 33–38 kD, pI ~ 9.3 (arrow).

tive with neurons reacted with hnRNP-A1 (Fig. 2*e*), suggesting molecular mimicry between the epitope recognized by the mAb and hnRNP-A1. The epitope specificity of the mAb includes the C-terminus of tax (tax$^{346-353}$) (M.C.L., personal communication) which is coincident with the immunodominant epitope in HAM/TSP patients[7]. Database analysis showed no exact match between tax$^{346-353}$ (KHFRETEV) and hnRNP-A1. Molecular mimicry due to immunologic cross-reactivity as shown by these and other data may have increased biological significance compared with mimics defined by primary sequences[13,14]. Importantly, all of the HAM/TSP patients and none of the HTLV-1-seronegative patients reacted with rhnRNP-A1 (Fig. 2*f*).

The hnRNPs are a group of approximately 30 nuclear riboproteins associated with systemic, but not neurological, autoimmune diseases. Autoantibodies against hnRNP-A1 and A2/B1 have been found in patients with lupus, mixed connective tissue disease and rheumatoid arthritis[12]. hnRNP-A1 is critical to transport of mRNA from the nucleus to the cytoplasm and cellular processes[15,16]. In the CNS, hnRNP-A1 shows greater expression in neurons compared with glia[17]. We hypothesized that hnRNP-A1 would be highly expressed in large cells of the CNS in which efficient transport of mRNA is critical, such as pyramidal neurons of the precentral gyrus, including Betz cells. These motor neurons control movement and their axons comprise most of the corticospinal tract. Betz cells are the largest neurons in the human CNS with cell bodies that are 60–120 μm in height and axons up to a meter long[18]. To determine if these cells preferentially bound HAM/TSP autoantibodies, we separated neurons of the precentral gyrus from other areas of brain (Fig. 3). Trypan blue staining confirmed the presence of pyramidal and Betz cells in the pre-central gyrus and cortical neurons in the parietal-occipital lobe (Fig. 3*a* and *d*). All cells stained with neurofilament, indicating there was no contamination by non-neuronal cells (Fig. 3*d*, inset). Western blots of pre-central gyrus neurons including Betz cells, in contrast to smaller cortical neurons, showed

an intense signal with HAM/TSP IgG (Fig. 3*b* and *e*). This correlated with immunohistochemical staining (Fig. 3*c* and *f*). These data suggest that HAM/TSP IgG is specific for neurons of the corticospinal tract, the major target of neurological dysfunction in HAM/TSP.

We have determined that HAM/TSP patients develop antibodies to CNS neurons that cross-react with HTLV-1-tax. The neuronal autoantigen is hnRNP-A1. The distribution of hnRNP-A1 in the CNS corresponds to structures affected in HAM/TSP. These data establish a strong relationship between the autoimmune response and the neurological disease. To provide further proof that the autoimmune reaction contributes to the neurological disease, we used patch-clamp studies to test the ability of autoantibody to alter neuronal function. Here, we studied individual neurons in rat brain sections that maintain interactions with other neurons and non-neuronal cells[18]. Infusion into the extracellular space with HAM/TSP IgG (at concentrations of IgG in human CSF) completely inhibited neuronal firing (Fig. 3*g*). HAM/TSP IgG localized only to the neuronal cytoplasm, suggesting that IgG entered the cell, bound hnRNP-A1 and resulted in decreased neuronal firing. A monospecific antibody against hnRNP-A1 purified from HAM/TSP patients replicated this response. These data are consistent with HAM/TSP IgG being biologically active and pathogenic. Infusion of IgG from normal individuals showed no change in neuronal firing (Fig. 3*h*). Importantly, inhibition was reproduced by the infusion of tax mAb (Fig. 3*i*), suggesting that biological activity is dependent upon an immunodominant cross-reactive epitope between HTLV-1-tax and hnRNP-A1.

How CNS damage develops in HAM/TSP is incompletely understood. It does not seem to result from direct infection with HTLV-1 but infection associated with an autoimmune mechanism. The immune response to tax differentiates patients with HAM/TSP from controls[19,20]. Specifically, HAM/TSP patients develop a $CD8^+$ cytotoxic T-lymphocyte (CTL) response specific for the N terminus of HTLV-1-tax (tax^{11-19}) associated with human leukocyte antigen-$A2^+$ and an antibody response to its C terminus ($tax^{301-353}$)[21]. Viral load may be important in stimulating these responses since HAM/TSP patients have elevated viral loads of tax[19]. In addition to tax, antibodies from HTLV-1 infected patients react with several intracellular autoantigens[20]. These data suggest that a cross-reactive immune response between HTLV-1-tax and a CNS autoantigen may exist and contribute to the pathogenesis of HAM/TSP. Until now, a specific CNS autoantigen that may act as a target for cellular or antibody-mediated autoimmune responses had not been identified in HAM/TSP patients.

How antibodies enter the CNS and bind to intracellular antigens such as neuronal hnRNP-A1 in autoimmune diseases such as HAM/TSP and MS is not clear. Data indicate that IgG has a significant role in the pathogenesis of these diseases[22,23]. In HAM/TSP, patients are infected with HTLV-1, which is tropic for $CD4^+$ T-lymphocytes[3]. Infection of $CD4^+$ T-lymphocytes results in their activation and may allow them to cross the blood-brain barrier (BBB)[22,24]. Interaction of these cells with the CNS results in cytokine expression, adhesion molecule and receptor upregulation, and metalloproteinase secretion[22,24]. These events are associated with disrup-

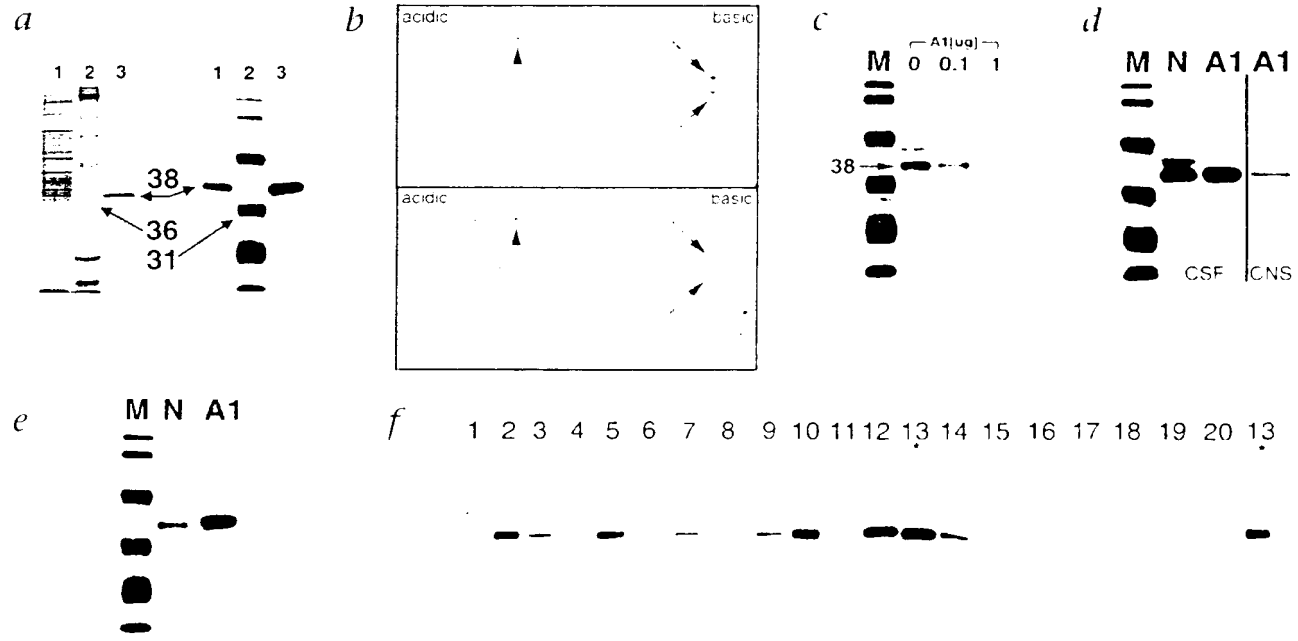

Fig. 2 Immunoreactivity of HAM/TSP IgG with the neuronal extract and hnRNP-A1. ***a***, Left panel, Coomassie staining; right panel, HAM/TSP IgG immunoreactivity by western blot. Neuronal extract (lane 1), molecular weight markers (lane 2) and rhnRNP-A1 (lane 3). rhnRNP-A1 is identified as a 38-kD band that is recognized by HAM/TSP IgG (right panel, third lane) and corresponds to an immunoreactive band in the neuronal extract (right panel, lane 1). ***b***, Reactivity by western blot following 2-D gel electrophoresis of neuronal extract is adsorbed by pre-incubation with rhnRNP-A1. Immunoreactivity of HAM/TSP IgG with neuronal proteins (top panel) was adsorbed by pre-incubation with rhnRNP-A1 (bottom panel, arrows). There was immunoreactivity to other neuronal proteins that did not adsorb with rhnRNP A1 (arrowheads). M, molecular weight markers; N, neurons; A1, rhnRNP A1. ***c***, Pre-incubation of HAM/TSP IgG with 0, 0.1 and 1.0 μg rhnRNP A1 followed by western blot of the neuronal extract demonstrated concentration-dependent adsorption of immunoreactivity. ***d***, IgG purified from the CSF and CNS of a patient with HAM/TSP reacted with neurons and rhnRNP A1. ***e***, The tax mAb reacted with neurons and rhnRNP-A1. ***f***, Screening of patient sera demonstrated 10/10 HAM/TSP patients (numbers 2, 3, 5–7, 9, 10 and 12–14) and 0/10 HTLV-1 seronegative controls (1, 4, 8, 11 and 15–20) reacted with rhnRNP A1. *, patient 13 was used as a positive control for the assay that tested patients 15–20.

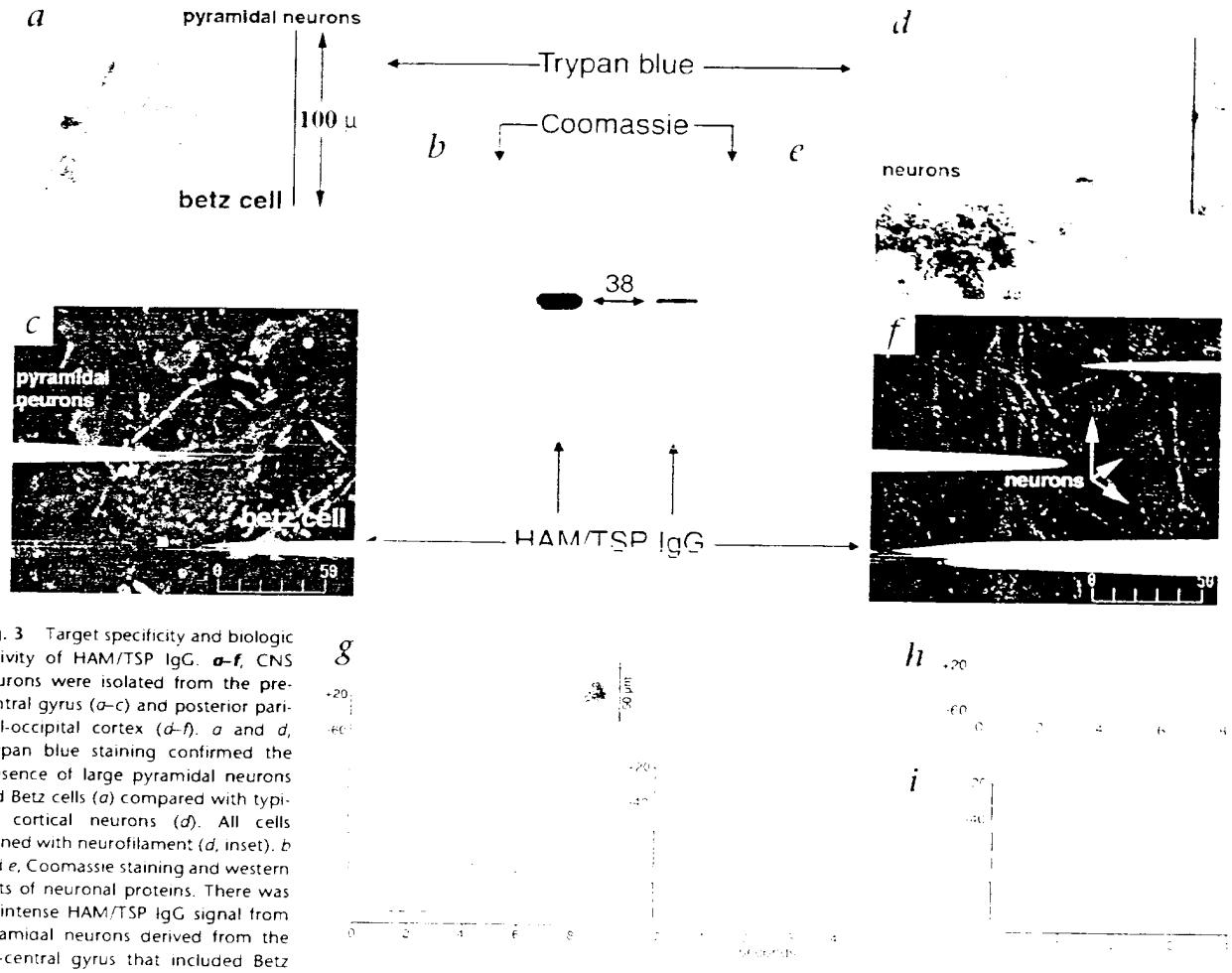

Fig. 3 Target specificity and biologic activity of HAM/TSP IgG. ***a–f***, CNS neurons were isolated from the pre-central gyrus (*a–c*) and posterior parietal-occipital cortex (*d–f*). *a* and *d*, Trypan blue staining confirmed the presence of large pyramidal neurons and Betz cells (*a*) compared with typical cortical neurons (*d*). All cells stained with neurofilament (*d*, inset). *b* and *e*, Coomassie staining and western blots of neuronal proteins. There was an intense HAM/TSP IgG signal from pyramidal neurons derived from the pre-central gyrus that included Betz cells (*b*), compared with parietal-occipital cortex (*e*). Coomassie staining shows comparable protein loading. *c* and *f*, Immunohistochemistry of the pre-central gyrus of human motor cortex and of the parietal-occipital cortex. *c*, A Betz cell is shown surrounded by pyramidal neurons. Staining is present throughout the cytoplasm and extends into neuronal processes (arrow). *f*, Staining is less intense in parietal-occipital cortex. ***g–i***, Patch clamp recording of neurons in rat brain following extracellular infusion of antibodies (normal CSF – red). *g*, Left, Physiological concentrations of HAM/TSP IgG (5, 10, 15 and 20 µg/ml, respectively) decreased neuronal firing without affecting calcium (data not shown). HAM/TSP IgG localized to the cytoplasm of neurons (inset). Right, Experiments were replicated using the monospecific antibody to hnRNP-A1 (5 and 10 µg/ml, respectively). *h*, Application of normal IgG (10 µg/ml; green) showed no slowing in neuronal firing. *i*, The tax mAb decreased (10 µg/ml; green), then completely inhibited neuronal firing (20 µg/ml; blue).

tion of the BBB after which CTLs and antibodies against tax may enter the CNS (refs. 5–9). Tax-specific antibodies may home to and enter corticospinal neurons that express high levels of hnRNP-A1. Antibodies can disrupt neuronal function, as suggested by this and other studies[34].

Our data show that there is molecular mimicry between HTLV-1 and neuronal hnRNP-A1. This mimicry is likely to be significantly involved in the pathogenesis of HAM/TSP. The data establish a clear link between chronic viral infection, autoimmunity and neurological disease in humans. Recently, investigators have shown that hnRNP-A2, a ribonucleoprotein with significant homology to hnRNP-A1, has a critical role in the transport of myelin basic protein (MBP) mRNA to the processes of oligodendrocytes[35]. Many studies implicate molecular mimicry involving MBP in the pathogenesis of MS (refs. 1–4). Future studies may find that cellular and humoral autoimmunity to hnRNP-A complexes are involved in the pathogenesis of other immune-mediated diseases of the CNS such as MS.

Methods

IgG isolation and immunohistochemistry. IgG was isolated from serum or CSF by adsorption to protein A Sepharose (Sigma) and biotinylated (biotin-N-hydroxysuccinimide, Vector, Burlingame, California). Autopsy tissues were obtained from HTLV-1 seronegative individuals. Immunohistochemistry was performed on formalin-fixed, paraffin-embedded 5-µm sections. IgG (1:50) was detected with avidin biotin peroxidase/diamino benzidine HCl or Texas Red Avidin-D (Vector). Fluorescence was imaged by confocal microscopy (Bio Rad MRC-1024, Hercules, California). The tax mAb (1:50) was coupled with secondary antibody followed by Alkaline Phosphatase (Vector Red). Neurofilament was detected with NCL-NF68 antibody (Novocastra, Newcastle upon tyne, UK) and secondary antibody coupled with SG substrate peroxidase or avidin biotin peroxidase/diamino benzidine HCl (Vector). IgG was isolated from HAM/TSP brain[36]. A monospecific antibody to hnRNP-A1 was produced by purifying HAM/TSP IgG with rhnRNP-A1 bound to sepharose.

Neuronal preparations and western blots. Human cortex was dissected, suspended in Ficoll/sucrose buffer, filtered through nylon mesh and neurons isolated by centrifugation. Whole neurons were mixed with TRYPAN blue, adhered to slides and photographed. For initial SDS–PAGE/western blots, neurons were mixed in reducing buffer and boiled before loading onto 12% SDS–PAGE gels[7]. To purify the antigen, neurons were subjected to guanidinium hydrochloride (6 M, 125 mM Tris/HCl, pH 6.8) and centrifuged (10,000*g*). The supernatant was used for subsequent studies. After SDS–PAGE, proteins were transferred to polyvinylidene fluoride (PVDF) membranes for western blotting with biotinylated IgG (1:5,000) and detected with avidin-horseradish peroxidase followed by enhanced chemiluminescence (ECL, Amersham, Piscataway, New Jersey). The tax mAb (1:5,000) was detected with biotinylated-goat anti-mouse antibody and ECL. For adsorption studies, HAM/TSP IgG was incubated with 0, 0.1 or 1.0 μg rhnRNP-A1 prior to western blotting.

2-D gel electrophoresis and purification and mass spectroscopy of dissected proteins. Samples were solubilized in 0.5% (v/v) immobilized pH gradient (IPG) buffer (pH 3–10, Pharmacia) and bromophenol blue. A 17-cm IPG strip was used for isoelectric focusing of 30 μg samples. The first-dimension isoelectric focusing program was as follows: 0 V, 12 h; 500 V, 1 h; 1,000 V, 1 h; and 8,000 V, 4 h. After equilibration in buffer with DTT and iodoacetamide, the second-dimension was done at 40 mA. Gels were stained with Coomassie (Gel-Code Blue Reagent, Pierce, Rockford, Illinois) or electroblotted onto PVDF membranes for western blotting. Spots identified by western blotting were analyzed by in-gel digestion. Excised plugs were washed with NH_4HCO_3/acetonitrile and dried. Trypsin was added. Supernatant was removed, digestion buffer added, and incubation continued (37 °C, 12 h). The sample was centrifuged and transferred to a tube containing hydrophilic peptides. Peptides were extracted with 60% acetonitrile/0.01% trifluoracetic acid (TFA). Samples were dried, TFA and water were added. Peptides were eluted, purified with ZipTip C18-microcolumns (Millipore, Bedford, Massachusetts) and deposited directly on the MALDI (Matrix-Assisted Laser Desorption Ionization) target. MALDI-time-of-flight mass spectroscopy was used to obtain mass fingerprinting for proteins using a Voyager DE-ER instrument (Applied Biosystems, Framingham, Massachusetts). Spectra were acquired in the delayed extraction (DE), reflectron (R) mode. 100-200 scans were averaged to produce final spectra. The mass scale was calibrated using the masses of trypsin autodigestion products. Protein identification was performed by searching peptide masses in a comprehensive non-redundant protein sequence database (Protein Prospector)[8]. Primary sequences were compared using Pustell Protein Matrix (MacVector) and Patrwise-Blast, NCBI.

Cloning of human hnRNP-A1. Human brain mRNA was isolated using a commercial kit (Clontech, San Francisco, California). hnRNP-A1 cDNA was prepared by RT-PCR using primers representing the coding region (sense, 5′-GGATCCATGTCTAAGTCAGAGTCTCCTAAA-3′, antisense, 5′-AAGCTTTTAAAATCTTCTGCCACTGCCATA-3′). PCR product size was confirmed by agarose gel electrophoresis. PCR product was excised from the gel, purified, and subcloned into TOPO PCR 2.1 vector (Invitrogen, Carlsbad, California). Positive clones were selected by white/blue screening. Plasmids were purified (Wizard Plus SV Miniprep, Promega, Madison, Wisconsin), subjected to *Bam*HI/*Hin*dIII double digestion and cloned into pQE 30 vector (Qiagen, Valencia, California) in which the gene product was expressed with 6 X His tag for purification. The recombinant hnRNP-A1 was expressed by adding IPTG (1 mM) in M15 (pRep4), an *E. coli* strain (Qiagen), and purified using Ni-chelating affinity chromatography.

Patch-clamp experiments. 300-μm brain slices dissected from Sprague–Dawley rats were prepared in ice-cold artificial cerebrospinal fluid (ACSF). Slices were submerged in the recording chamber and perfused with ACSF, followed by the test antibody (in ACSF). Neurons were visualized with a Photometrics PXL charge-coupled camera and patched with a glass electrode filled with a physiologic intracellular solution. Neurons were held below −50 mV and constant depolarization with 1–10 Hz pacemaker firing (IgG) and below −40 mV and constant depolarization of 5–15 Hz (tax mAb and monospecific ab). Electrode resistance was between 5 and 8 MΩ. Recordings were made in a current clamp mode synchronously with calcium imaging and analyzed by Igor Pro 3.13 (ref. 18).

Acknowledgments

We thank K. Troughton, E. Umstot and J. Berk for technical assistance; C. Rainey for autopsy material; S. Jacobson for some of the serum samples; and B. Langston for the HTLV-1-tax monoclonal antibody obtained through the AIDS Research and Reference Reagent Program, Division of AIDS, NIAID, NIH. This material is based upon work supported by the Office of Research and Development, Medical Research Service, Department of Veterans Affairs. This study was funded by the VA Career Development Award and NIH RO1-NS-38876 (to M.C.L.) and NIH RR 10522 and NSF-DBI-9604633 (to D.M.D.).

Competing interests statement

The authors declare that they have no competing financial interests.

RECEIVED 18 SEPTEMBER 2001; ACCEPTED 18 MARCH 2002

1. Oldstone, M. Molecular mimicry and immune mediated disease. *FASEB J.* **12**, 1255–1265 (1998).
2. Albert, L.J. & Inman, R.D. Molecular mimicry and autoimmunity. *New. Engl. J. Med.* **341**, 2068–2074 (1999).
3. Gran, B., Hemmer, B., Vergelli, M., McFarland, H. & Martin, R. Molecular mimicry and multiple sclerosis: Degenerate T-cell recognition and the induction of autoimmunity. *Ann. Neurol.* **45**, 559–567 (1999).
4. Fujinami, R. & Oldstone, M. Amino acid homology between the encephalitogenic site of myelin basic protein and virus: A mechanism for autoimmunity. *Science* **230**, 1043–1045 (1985).
5. Jacobson, S., Shida, H., McFarlin, D., Fauci, A. & Koenig, S. Circulating CD8 cytotoxic lymphocytes specific for HTLV-1 in patients with HTLV-1 associated neurological disease. *Nature* **348**, 245–248 (1990).
6. Levin, M. *et al.* Immunopathogenesis of HTLV-I associated neurologic disease based on a spinal cord biopsy from a patient with HTLV-1 associated myelopathy/tropical spastic paraparesis (HAM/TSP). *New. Engl. J. Med.* **336**, 839–845 (1997).
7. Levin, M. & Jacobson, S. HTLV-I associated myelopathy/tropical spastic parapareus (HAM/TSP): A chronic progressive neurologic disease associated with immunologically mediated damage to the central nervous system. *J. Neurovirol.* **3**, 126–140 (1997).
8. Levin, M. *et al.* Neuronal molecular mimicry in immune mediated neurologic disease. *Ann. Neurol.* **44**, 87–98 (1998).
9. Lal, R., Giam, C., Coligan, J. & Rudolph, D. Differential immune responsiveness to the immunodominant epitopes of regulatory proteins (tax and rex) in human T-cell lymphotropic virus type I associated myelopathy. *J. Infect. Dis.* **169**, 496–503 (1994).
10. Kahn, R., Bertonni, T. & Levin, M. Neurologic complications of HTLV-1 infection. *The Neurologist* **7**, 271–278 (2001).
11. Beranova-Giorgianni, S. & Desiderio, D. Mass spectrometry of the human pituitary proteome: Identification of selected proteins. *Rapid Commun. Mass Spectrom.* **14**, 161–167 (2000).
12. Biamonti, G., Ghigna, C., Caporali, R. & Montecucco, C. Heterogeneous nuclear ribonucleoproteins (hnRNPs): An emerging family of autoantigens in rheumatic diseases. *Clin. Exp. Rheumatol.* **16**, 317–326 (1998).
13. Krecic, A.M. & Swanson, M.S. hnRNP complexes: Composition, structure, and function. *Curr. Opin. Cell Biol.* **11**, 363–371 (1999).
14. Nakielny, S. & Dreyfuss, G. Nuclear export of proteins and RNAs. *Curr. Opin. Cell Biol.* **9**, 420–429 (1997).
15. Shyu, A.B. & Wilkinson, M.F. The double lives of shuttling mRNA binding proteins. *Cell* **102**, 135–138 (2000).
16. Kamma, H., Portman, D.S. & Dreyfuss, G. Cell type-specific expression of hnRNP proteins. *Exp. Cell Res.* **221**, 187–196 (1995).
17. Lassek, A.M. The human pyramidal tract. IV. A study of the mature, myelinated fibers of the pyramid. *J. Comp. Neurol.* **76**, 217–225 (1942).
18. Callaway, J., Lasser-Ross, N., Stuart, N. & Ross, W. Dynamics of intracellular free calcium concentration in the presynaptic arbors of individual barnacle photoreceptors. *J. Neurosci.* **13**, 1157–1166 (1993).
19. Nagai, M. *et al.* Analysis of HTLV-1 proviral load in 202 HAM/TSP patients and 243 asymptomatic HTLV-1 carriers: High proviral load strongly predisposes to HAM/TSP. *J. Neurovirol.* **4**, 586–593 (1998).
20. Muller, S. *et al.* IgG Autoantibody response in HTLV-I infected patients. *Clin. Immunol. Immunopathol.* **77**, 282–290 (1995).
21. Warren, K., Catz, I. & Steinman, L. Fine specificity of the antibody response to myelin basic protein in the central nervous system in multiple sclerosis: The minimal B-cell epitope and a model of its features. *Proc. Natl. Acad. Sci. USA* **92**, 11061–11065 (1995).
22. Romero, I. *et al.* Interactions between brain endothelial cells and human T-cell leukemia virus type I infected lymphocytes: Mechanisms of viral entry into the central nervous system. *J. Virol.* **74**, 6021–6030 (2000).
23. Giraudon, P. *et al.* T lymphocytes activated by persistent viral infection differentially modify the expression of metalloproteinases and their endogenous inhibitors, TIMPs, in human astrocytes: Relevance of HTLV-I-induced neurologic disease. *J. Immunol.* **164**, 2718–2727 (2000).
24. Chen, W., Elias, R.V., Cao, W., Lerious, V. & McGinnis, J.F. Anti-recoverin antibodies cause the apoptotic death of mammalian photoreceptor cells *in vitro*. *J. Neurosci. Res.* **57**, 706–718 (1999).
25. Munro, T.P. *et al.* Mutational analysis of a heterogeneous nuclear ribonucleoprotein A2 response element for RNA trafficking. *J. Biol. Chem.* **274**, 34389–34395 (1999).

Immunity, Vol. 15, 137–147, July, 2001, Copyright © 2001 by Cell Press

Analysis of the Relationship between Viral Infection and Autoimmune Disease

Vily Panoutsakopoulou,[1,2,5] Marie E. Sanchirico,[1,2,5] Katharina M. Huster,[1,2] Marianne Jansson,[1,2] Francesca Granucci,[1,6] David J. Shim,[1] Kai W. Wucherpfennig,[1,3] and Harvey Cantor[1,2,4]
[1]Department of Cancer Immunology and AIDS Dana-Farber Cancer Institute
[2]Department of Pathology
[3]Department of Neurology
Harvard Medical School
Boston, Massachusetts 02115

Summary

The clinical association between viral infection and onset or exacerbation of autoimmune disorders remains poorly understood. Here, we examine the relative roles of molecular mimicry and nonspecific inflammatory stimuli in progression from infection to autoimmune disease. Murine herpes virus 1 (HSV-1 KOS) infection triggers T cell-dependent autoimmune reactions to corneal tissue. We generated an HSV-1 KOS point mutant containing a single amino acid exchange within the putative mimicry epitope as well as mice expressing a TCR transgene specific for the self-peptide mimic to allow dissection of two pathogenic mechanisms in disease induction. These experiments indicate that viral mimicry is essential for disease induction after low-level viral infection of animals containing limited numbers of autoreactive T cells, while innate immune mechanisms become sufficient to provoke disease in animals containing relatively high numbers of autoreactive T cells.

Introduction

Two general explanations have been put forward to explain the clinical association between microbial infection and induction or exacerbation of autoimmune disease. One mechanism depends on evidence that the immune response to pathogens provides a nonspecific stimulus of the innate immune system that promotes activation and expansion of autoreactive T cells (Horwitz and Sarvetnick, 1999). A second holds that the pathogen itself may provide a counterfeit antigenic stimulus that provokes autoreactive T cells (Oldstone, 1987; von Herrath and Oldstone, 1996). The contribution of nonspecific inflammatory mechanisms has received extensive experimental support in several different animal models of autoimmune disease (Horwitz and Sarvetnick, 1999). The role of antigenic mimicry has also received extensive support. For example, viral peptides can cross-stimulate autoreactive human T cells, and mice that express a viral protein in a relevant target tissue develop autoimmune disease after viral infection (Hemmer et al., 1997; Wucherpfennig and Strominger, 1995; Ohashi et al., 1991). Cross-reactive T cell activation (mimicry) has also been implicated in the pathogenesis of Lyme disease (Gross et al., 1998) and a murine model of heart disease (Bachmaier et al., 1999).

The issue of self-mimicry by microbial agents has been studied in murine Herpes Stromal Keratitis (HSK), a T cell-dependent autoimmune response that destroys corneal tissue after HSV-1 KOS infection (Avery et al., 1995; Streilein et al., 1997). Viral mimicry may provoke this disorder because Th1 cell clones that initiate HSK respond to both a corneal self-antigen and a peptide derived from the UL6 protein of HSV-1 KOS. Moreover, a replication-defective HSV-1 KOS virus that does not express the UL6 protein fails to induce HSK in adoptive hosts given virus-immune T cells (Zhao et al., 1998). However, the inability of this replication-defective mutant to induce disease compared with a glycoprotein B-deficient strain may have reflected a difference in virulence between the two deletion mutants and/or inhibitory effects of low levels of UL6 expressed at the protein level by the replication-defective virus.

A direct test of the contribution of an HSV-1 peptide mimic to the development of disease after viral infection depends on generation of a replication-competent virus containing a single amino acid exchange that alters the putative mimicry epitope and analysis of mice that express a TCR transgene (C1-6) specific for a potential viral mimic (Zhao et al., 1998). We find that this exchange virtually abrogates disease induction, while disease susceptibility is increased dramatically in mice expressing the C1-6 TCR. This mutant virus and TCR transgenic mouse model are used to delineate the relative contribution of antigen-specific and innate immune mechanisms to the pathogenesis of autoimmune disease after viral infection.

Results

Generation of a Replication-Competent HSV-1 KOS Mutant Containing a Single Amino Acid Exchange

A previous comparison of several replication-defective HSV-1 mutants suggested that expression of the UL6 protein was important for induction of HSK following HSV-1 infection (Zhao et al., 1998). However, impaired replication or other functional defects of the HSV-1 KOS/UL6^{m}-mutant virus might have contributed to its failure to induce disease. A decisive test of the putative UL6-derived peptide mimic requires generation of a UL6 amino acid exchange mutant that alters the UL6 T cell epitope but spares HSV-1 replication and function.

A mutation that converts the *UL6* Ser at position 309 to Leu (S309L) and disrupts the predicted class II binding frames of the postulated mimic was induced by an alteration of AGC (encoding Ser) to CTT (encoding Leu) after site-directed mutagenesis (Figure 1A). The HindIII restriction site created by this mutation was used to moni-

[4]Correspondence: harvey_cantor@dfci.harvard.edu
[5]These authors contributed equally to this work.
[6]Present address: Department of Biotechnology and Bioscience, University of Milan, Milan, Italy.

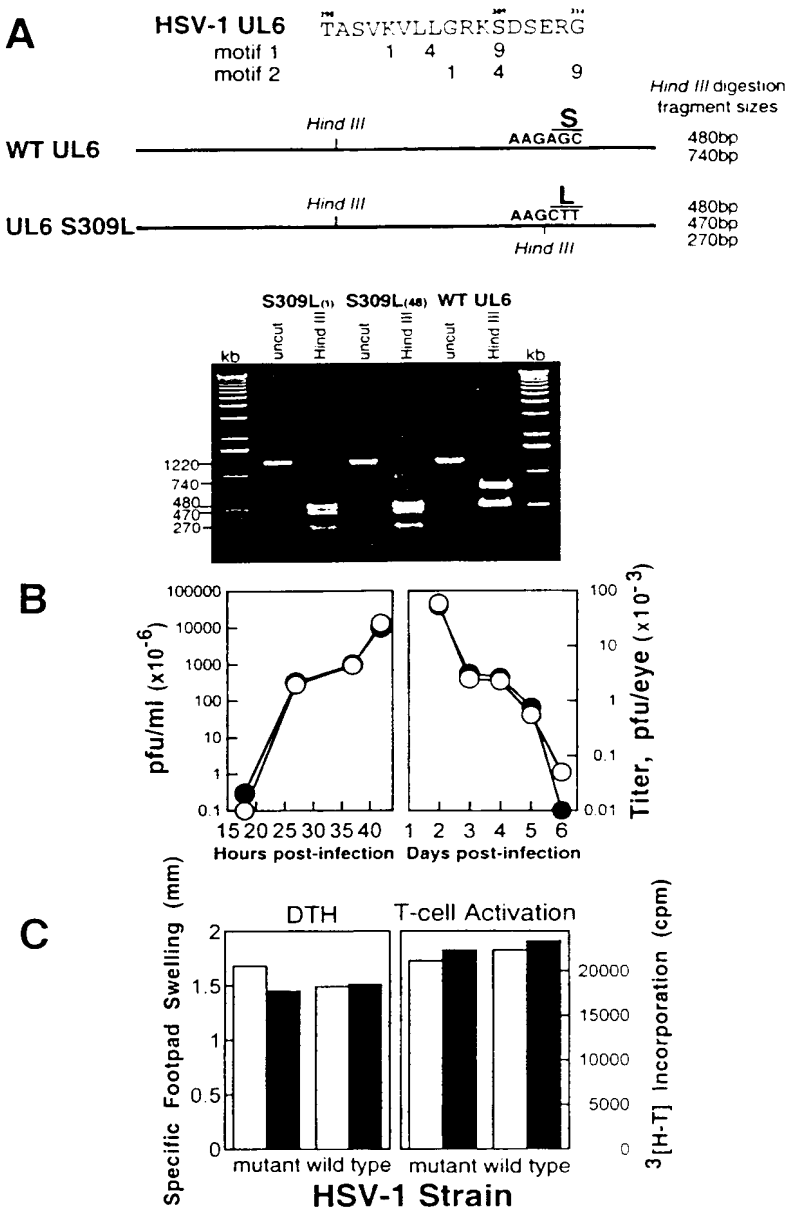

Figure 1. Generation and Analysis of KOS UL6^{S309L}

(A) Two potential binding motifs for the UL6 peptide (aa 298–314; TASVKVLLGRKSDS ERG), based on preferred amino acid anchors and the I-A^d crystal structure (top). The introduction of an AGC→CTT mutation in an epitope-coding region of the *UL6* gene in HSV-1 KOS creates a HindIII site at bp 922 (middle). Viral DNA extracted from Vero cells infected with isolates of wild-type KOS or the mutant KOS/UL6^{S309L} (1,48) was used as template for PCR amplification of a 1.2 kb fragment of *UL6* (bottom), which was gel purified and digested to test for the presence of the HindIII site within the epitope coding region (480 and 740 bp for wild-type and 480, 470, and 270 bp for KOS/UL6^{S309L}).

(B) KOS/UL6^{S309L} replicates at the same rate as wild-type KOS. Vero cell monolayers were infected with ten viral particles of KOS (closed circles) or KOS/UL6^{S309L} (open circles) per cell and harvested at 18, 27, 37, and 42 hr post-infection (left). Samples were analyzed for virus yields as described (Sandstrom et al., 1986). Data points represent the mean of duplicate samples. Viral titers in eyes of infected mice during the period of acute replication (right). C.AL-20 mice were ocularly infected with 4 × 10^6 PFU wild-type KOS (closed circles) or KOS/UL6^{S309L} (open circles); eyes were harvested on days 2, 3, 4, 5, and 6 and assayed for viral particles as described (Sandstrom et al., 1986). Data points represent the mean of duplicate samples.

(C) The T cell response to the KOS/UL6^{S309L} is similar to the response to wild-type KOS. DTH response to KOS/UL6^{S309L}. (Left panel) C.AL-20 mice were infected in the right eye with either HSV-1 KOS or KOS/UL6^{S309L} (4 × 10^6 PFU), and, 5 days later, individual groups of infected mice were challenged in the left footpad with 5 × 10^7 PFU UV-inactivated HSV-1 KOS (white bars) or KOS/UL6^{S309L} (black bars). The right and left footpads of each mouse were measured 24 hr later, and the data are given as average specific swelling calculated by subtracting the width of the control right footpad of four mice per group. (Right panel) In vitro proliferation to KOS/UL6^{S309L}. The right superficial cervical draining lymph nodes of C.AL-20 mice were harvested 15 days after ocular infection of the right eye with 4 × 10^6 PFU HSV-1 KOS or KOS/UL6^{S309L}. Cells from these lymph nodes were cultured with syngeneic BALB/c irradiated spleen cells in the presence of UV-inactivated HSV-1 KOS (white bars) or KOS/UL6^{S309L} (black bars). Results are shown as cpm of incorporated [^{3}H]thymidine that was added to each well during the last 16 hr of culture.

tor recombination after cotransfection of Vero cells with a linear S309L DNA fragment and infectious nonreplicating KOS/UL6^m DNA (containing a stop codon in the UL6 gene) (Figure 1A). Recombination between linear S309L DNA and purified KOS/UL6^m DNA allows viral replication and functional selection of recombinants containing repaired UL6 genes. Replication-competent viral isolates (48) were subcloned after cotransfection, and all contained the S309L mutation according to PCR amplification and HindIII digestion (Figure 1A). Sequencing of the PCR product containing the epitope region was performed to confirm conversion of AGC to CTT in two isolates used for further study.

Characterization of the T Cell Response to Mutant Virus KOS/UL6^{S309L}

KOS/UL6^{S309L} grew to titers that were at least as high as wild-type (wt) KOS, and the replication rate of KOS/UL6^{S309L} was indistinguishable from KOS wt after infection of Vero cells in vitro or murine cornea in vivo (Figure 1B). The effect of this amino acid exchange on the ability of the mutant virus to interact with T cells was also measured. T cells from lymph nodes draining HSV-1 KOS- or HSV-1 KOS/UL6^{S309L}-infected corneas responded equally well to wt KOS or mutant KOS/UL6^{S309L}, according to [^{3}H]thymidine incorporation (Figure 1C). Infection with HSV-1 KOS or KOS/UL6^{S309L} also provoked

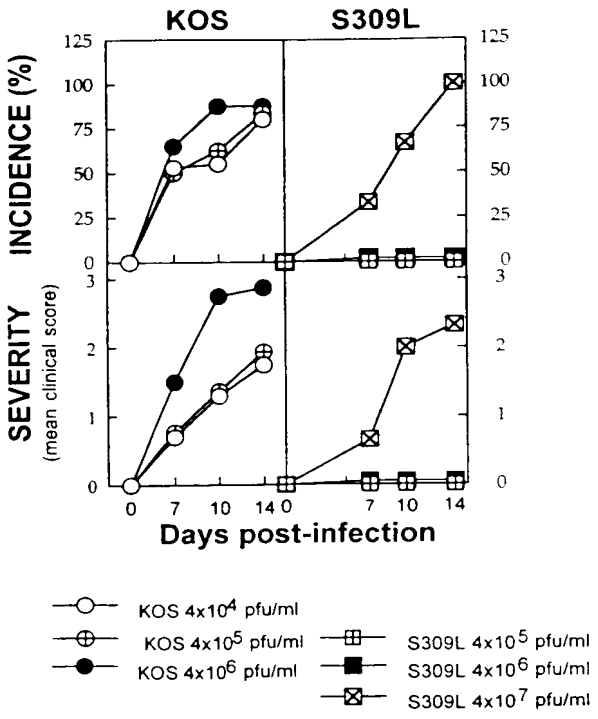

Figure 2. HSK Induction by KOS/UL6^{S309L}

The right eyes of C.AL-20 mice were infected with HSV-1 wild-type KOS at 4 × 10^4 PFU (open circles), 4 × 10^5 PFU (plus symbols within circles), or 4 × 10^6 PFU (closed circles) or KOS/UL6^{S309L} at 4 × 10^5 PFU (plus symbols within squares), 4 × 10^6 PFU (closed squares), or 4 × 10^7 PFU (x within squares), followed by disease assessment on days 0, 7, 10, and 14 after infection. The percentage of each group with detectable disease (i.e., incidence [%]) on days 0, 7, 10, and 14 (minimum score 1) and disease severity shown is based on analysis of HSK in four to eight mice per data point.

similar levels of tuberculin-type delayed-type hypersensitivity (DTH) upon challenge with either UV-inactivated KOS or KOS/UL6^{S309L} (Figure 1C). Since the *UL6* mutation did not inhibit the ability of the virus to replicate, interact with T cells, or induce DTH (cellular) immunity, we were able to ask whether the local inflammatory response provoked by a virus lacking a putative mimic epitope (HSV-1 KOS/UL6^{S309L}) caused HSK.

HSK Induction by KOS/UL6^{S309L}

Corneal infection with 4 × 10^4 PFU wild-type KOS was sufficient to induce HSK. However, KOS/UL6^{S309L} did not induce detectable HSK in concentrations less than 4 × 10^7 PFU (Figure 2). Thus, an amino acid exchange that affected the UL6 T cell epitope but not other viral functions decreased the efficiency of disease induction by approximately 10^3-fold compared to wild-type KOS virus. Histologic analysis of corneas from mice infected with 4 × 10^6 PFU KOS wt or KOS/UL6^{S309L} revealed that both viruses provoked similar levels of inflammatory response 5 days after infection (Figure 3A) during the period of active HSV-1 expression (the virus is no longer detectable in the cornea at the RNA or protein level after day 6) (Daheshia et al., 1997). The KOS/UL6^{S309L}-induced

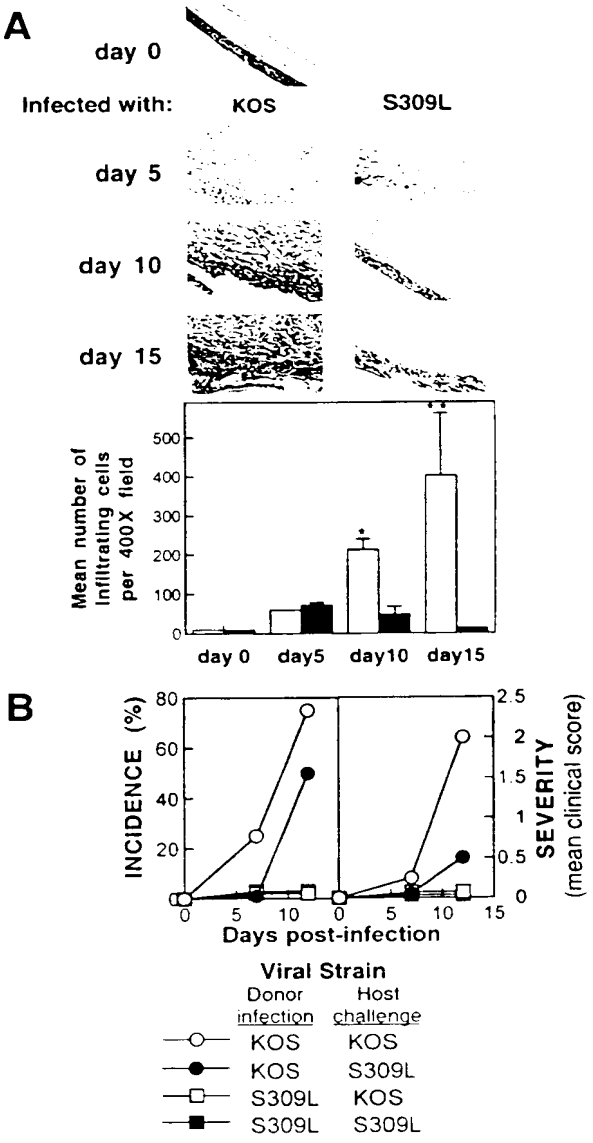

Figure 3. HSK Induction by the KOS/UL6^{S309L} Mutant

(A) Histologic analysis of the inflammatory response of C.AL-20 mice. After ocular infection by HSV-1/KOS (white bars) and S309L mutant (black bars); infected eyes were fixed at the indicated days after infection, sectioned, and stained with hematoxylin-eosin. Infiltrating cells per field (400 ·) were counted (standard error shown). Numbers indicate average of five fields. *, p 3 · 10 ; **, p 0.008.

(B) Adoptive transfer of HSK by CD4 cells from mice infected with KOS or KOS/UL6^{S309L}. The right eyes of C.AL-20 mice were infected with 4 · 10^6 PFU/eye of wild-type KOS or the KOS/UL6^{S309L} mutant virus. After infection (7 days), CD4 T cells were isolated (as described in Experimental Procedures) from the draining lymph nodes of these mice, and 10^6 CD4 cells from KOS-infected (circles) or KOS/UL6^{S309L}-infected (squares) mice were transferred intravenously into syngeneic BALB/c-*RAG2* mice. After T cell transfer (2 days), recipient mice were ocularly infected with 4 · 10^5 PFU/eye of either KOS (open circles, open squares) or KOS/UL6^{S309L} (closed circles, closed squares) virus and scored for disease on days 7 and 12 as described in Experimental Procedures. Each point represents at least six mice.

inflammatory response diminished and resolved over the next 10 days, while the KOS-induced inflammatory response progressively increased during this time in the absence of detectable HSV-1.

Adoptive Transfer of HSK by CD4 Cells from KOS/UL6^{S309L}-Infected Mice

We then defined the ability of the S309L mutant virus to stimulate pathogenic CD4 cells according to transfer of HSK. CD4 cells from donors infected with KOS/UL6^{S309L} were unable to transfer detectable HSK to *RAG-2*$^{-/-}$ recipients challenged with wt KOS in contrast to CD4 cells from donors infected with wt KOS, which reproducibly transferred robust HSK into *RAG-2*$^{-/-}$ recipients upon infection with HSV-1 KOS (Figure 3B). The 10^3-fold reduction in HSK activity of the KOS/UL6^{S309L} virus and its failure to induce pathogenic CD4 cells indicate that the UL6 viral mimic critically contributes to activation and expansion of T cells that initiate this autoimmune disease.

Initiation of HSK by CD4 Cells Bearing the C1-6 TCR

These findings suggest that CD4 T cells that express a TCR that recognizes the UL6 mimic and a corneal autoantigen can initiate HSK after viral infection. We have previously defined a $V_\beta8^+V_\alpha11^+CD4^+$ T cell clone (C1-6) that expressed this pattern of crossreactivity and transferred HSK into syngeneic *RAG-2*$^{-/-}$ hosts (Zhao et al., 1998). We therefore expressed the C1-6 or control DO11.10 TCR (which recognizes an OVA-derived peptide) transgene in BALB/c-*RAG2*$^{-/-}$ mice to generate "monoclonal" mice that do not contain other T cell clones because of a blocked endogenous TCR recombination (Chen et al., 1993a, 1993b) to directly test the contribution of this TCR to disease.

T cells that develop in BALB/c-*RAG2*$^{-/-}$ C1-6 TCR Tg mice are composed entirely of $V_\beta8^+CD4^+$ T cells (as predicted from the class II reactivity of the C1-6 TCR) (data not shown), and ocular infection by 10^3 PFU HSV-1 KOS provoked HSK in all BALB/c-*RAG-2*$^{-/-}$ C1-6 mice. In contrast, a 10^4-fold increase in viral titer to 10^7 PFU (the highest titer technically feasible) failed to induce detectable HSK in BALB/c-*RAG-2*$^{-/-}$ DO11.10 mice (Table 1A). Histologic analysis of the inflammatory response at day 10 showed a substantial mononuclear cell infiltration of the corneas of BALB/c-*RAG-2*$^{-/-}$ C1-6 mice (69.8 ± 13/hpf) but virtually none in the corneas of BALB/c-*RAG-2*$^{-/-}$ DO11.10 mice (3 ± 1.8/hpf).

Increased HSK susceptibility of BALB/c-*RAG-2*$^{-/-}$ C1-6 mice reflected enhanced T cell reactivity because 2×10^4 CD4 cells from BALB/c-*RAG-2*$^{-/-}$ C1-6 mice transferred HSK to naive BALB/c-*RAG-2*$^{-/-}$ hosts, while 2×10^6 CD4 cells from nontransgenic BALB/c mice were required for efficient transfer of HSK, and as many as 2×10^7 CD4 cells from BALB/c-*RAG-2*$^{-/-}$ DO11.10 mice failed to transfer detectable disease (Table 1B). These data indicate that small numbers of CD4 cells that express the C1-6 TCR are sufficient to confer disease while much larger numbers of T cells bearing an irrelevant TCR cannot.

We have previously suggested that mouse strains that are resistant to HSK following HSV-1 KOS infection lack the T cell clones that recognize the C1-6 peptide (Avery et al., 1995; Zhao et al., 1998). A direct test of this hypothesis comes from an analysis of HSK induction in the resistant C.B-17 mouse strain that expresses the C1-6 TCR transgene. We find that the C.B-17 C1-6 TCR tg mice develop severe HSK following HSV-1 KOS infection (4×10^5 PFU), while age- and sex-matched control C.B-17 mice do not develop detectable disease (Figure 4A). Thus, insertion of the C1-6 TCR into the T cell repertoire converts the phenotype of C.B-17 mice from resistant to highly susceptible.

Amelioration of HSK Using V_β Antibody or Peptides

One prediction of these data is that purging of CD4 cells containing the pathogenic $V_\beta8^+V_\alpha11^+$ TCR from the T cell repertoire might ameliorate HSK upon viral infection. We found that depletion of $V_\beta8.1/8.2^+$ cells but not $V_\beta6^+$ cells from C.AL-20 mice markedly reduced disease intensity after corneal infection with HSV-1 KOS without affecting the T cell response to HSV-1 (Figures 4B and 4C). Moreover, removal of $V_\beta8^+$ but not $V_\beta6^+$ cells from CD4 cells infused into BALB/c-*RAG2*$^{-/-}$ hosts virtually eliminated their ability to transfer HSK into adoptive hosts (Figure 4B). Depletion of $V_\beta8^+$ CD4 cells did not affect antiviral activity, because *RAG-2*$^{-/-}$ recipients of $V_\beta8$-depleted CD4 cells were fully protected from the lethal HSV-1 encephalitis that routinely follows ocular infection of mice that are deficient in T cells (Altmann and Blyth, 1985). Moreover, T cells from mice treated with $V_\beta8$ antibody displayed unimpaired proliferative responses to HSV-1 in vitro (Figure 4C). These data extend conclusions drawn from analysis of C1-6 TCR transgenic mice concerning the primacy of $V_\beta8^+$ C1-6 TCR in disease induction and suggest new therapeutic approaches based on depletion of a restricted portion of the T cell repertoire.

A second consequence of the view that C1-6 TCR$^+$ CD4 cells play a critical role in disease induction is that engagement of this TCR by a peptide ligand leading to anergy or apoptosis should inhibit disease development in vivo. The peptide SYFMYSKLRVQKS represents a superagonist that efficiently activates the C1-6 T cell clone at concentrations of less than 0.05 μM (Zhao et al., 1998) and, at concentrations greater than 20 μM, induces CD4 cells from C1-6 TCR transgenic mice to undergo anergy and apoptosis (Figures 5A and 5B). We therefore asked whether this ligand might induce resistance to HSK in both C1-6 TCR and in susceptible (nontransgenic) C.AL-20 mice. Intravenous injection of high concentrations of soluble C1-6 (400 μg/mouse) but not a mutant peptide that no longer activates the C1-6 TCR resulted in almost complete resistance to the development of HSK after infection with HSV-1 (Figure 5C).

Role of Antigen-Specific and Inflammatory Stimuli in the Induction of HSK

The finding that *RAG-2*$^{-/-}$ hosts reconstituted with KOS-primed CD4 cells developed mild but significant disease when challenged with KOS/UL6^{S309L} (Figure 3B) opened the possibility that LPS-induced stimulation of innate immunity and APC may induce disease in hosts containing sufficient numbers of autoreactive T cells. To test this hypothesis, we examined a series of mice that

Table 1. Analysis of HSK after Ocular Infection of BALB/c-*RAG-2*$^{-/-}$ CI-6 Transgenic Mice

A. Mouse Strain	HSV-1 Challenge (PFU/Eye)	Herpes Stromal Keratitis	
		Percent	Severity
C.AL-20	4×10^3	0	0
	4×10^4	100	2.7
	4×10^5	100	3.3
BALB/c-*RAG-2*$^{-/-}$ CI-6 tg	4×10^2	20	0.5
	4×10^3	100	2.1
	4×10^4	100	3.2
	4×10^5	100	4.0
BALB/c-*RAG-2*$^{-/-}$ DO11.10 tg	4×10^6	0	0
	4×10^7	0	0

B. CD4 Cell Donor	Disease Incidence (%): CD4 Cells Infused into *RAG-2*$^{-/-}$ Hosts			
	2×10^4	2×10^5	2×10^6	2×10^7
BALB/c-*RAG-2*$^{-/-}$ CI-6 tg	100	100	100	100
BALB/c-*RAG-2*$^{-/-}$ DO11.10 tg	0	0	0	0
BALB/c	0	20	90	100

(A) Mice were infected with HSV-1 KOS in the right eye, and disease was scored on day 10 and 14 after infection, as described in Experimental Procedures. The percentage of each group with detectable disease on day 14 (minimum score 1) and disease severity shown is based on analysis of HSK in four to eight mice per data point. (B) Purified CD4$^+$ cells from BALB/c, BALB/c-*RAG-2*$^{-/-}$ CI-6 TCR Tg, or BALB/c-*RAG-2*$^{-/-}$ DO11.10 TCR Tg were adoptively transferred into BALB/c-*RAG-2*$^{-/-}$ mice. Recipient mice were infected with 4×10^5 PFU/eye HSV-1 KOS and scored for HSK. The percentage of each group with detectable disease on day 14 (minimum score 1) shown is based on analysis of HSK in five to eight mice per data point.

contained increasing numbers of autoreactive T cells (naive C.AL-20; <KOS-immune C.AL-20; BALB/c-*RAG-2*$^{-/-}$ C1-6; <KOS-immune BALB/c-*RAG-2*$^{-/-}$ C1-6). While inoculation of LPS or infection by the HSV-1 KOS/UL6^{S309L} mutant virus onto scratched corneas fails to cause disease in naive C.AL-20 or BALB/c mice, 60% of KOS-immune C.AL-20 mice developed HSK after inoculation of LPS into the cornea. Moreover, 100% of BALB/c-*RAG-2*$^{-/-}$ C1-6 transgenic mice but not control BALB/c-*RAG-2*$^{-/-}$ DO11.10 mice developed intense keratitis after inoculation of LPS or infection with KOS/UL6^{S309L} (Figures 6A and 6C). Finally, provision of a mild inflammatory stimulus (corneal scratch) induced severe keratitis in BALB/c-*RAG-2*$^{-/-}$ C1-6 mice that had been immunized with UV-inactivated HSV-1 (Figure 6B). These experiments indicate that (1) direct activation of T cells by the molecular mimic is required to induce disease in normal nonprimed animals containing limiting numbers of autoreactive T cells (naive C.AL-20); and (2) innate immune mechanisms are sufficient to trigger disease in animals that contain expanded numbers of C1-6 TCR$^+$ T cells. Moreover, development of intense HSK in BALB/c-*RAG-2*$^{-/-}$ C1-6 but not DO11.10 transgenic mice after LPS-dependent activation of innate immune mechanisms reemphasizes the autoimmune nature of HSK in this model.

Discussion

Microbial infection often precedes the clinical onset of diabetes (Gamble and Taylor, 1973; Gamble, 1980; Nagata and Yoon, 1992) and relapses of multiple sclerosis (Sibley et al., 1985) and can precipitate murine diabetes (Nagata and Yoon, 1992), demyelinating disease (Rodriguez et al., 1987; Dal Canto and Rabinowitz, 1982; Miller et al., 1990), herpes stromal keratitis (Streilein et al., 1997; Zhao et al., 1998), and myocarditis (Bachmaier et al., 1999). However, there is no consensus view of the relative importance of antigen-specific stimuli (microbial mimics) and nonspecific innate immune mechanisms to the genesis of autoimmune disease, in part because both mechanisms are likely to contribute to most autoimmune disorders, while one or the other may play a dominant role under particular circumstances (Cantor, 2000). Our studies delineate the conditions that determine the importance of these two mechanisms to the development of HSK.

Viral Infection and Molecular Mimicry

The HSK system is particularly well-suited for studying the inciting role of viral infection, because stimulation of the immune system by the virus is limited to an acute period of approximately 5–7 days, after which the virus becomes undetectable at the protein and RNA level (Streilein et al., 1997; Figure 1), in contrast to other viral infections that may provoke chronic immune reactions through smoldering infection (e.g., HSV-1 encephalitis). A direct test of a peptide mimic in HSK induced by HSV-1 KOS comes from analyses of a replication-competent KOS point mutant as well as studies of mice that express a TCR specific for this mimic. The S309L amino acid exchange in the HSV-1 KOS UL6 protein alters the predicted UL6 T cell epitope without affecting viral replication, stimulatory activity for T cells, or induction of DTH and is thus equipped to provide an unimpaired inflammatory milieu (Figure 1). Nevertheless, this viral mutant did not cause HSK in susceptible C.AL-20 mice unless viral concentrations were increased 10^3-fold, achieving levels not normally seen in nature (Figure 2). Histologic analysis of the cornea showed that cellular infiltration after KOS/UL6^{S309L} and wt KOS infection was similar at day 5, when virus was present. However, over the next 10 days, when the virus is no longer detectable, cell infiltration initiated by wt virus progressively increased, while the KOS/UL6^{S309L} virus-initiated cellular response was markedly reduced by day 10 and absent at day 15.

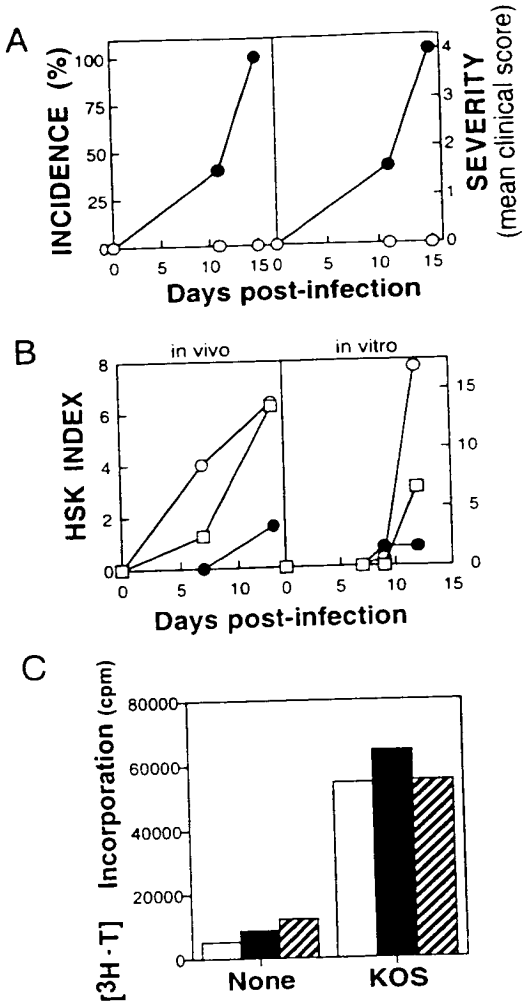

Figure 4. Regulation of HSK Response to HSV-1/KOS by the C1-6 TCR

(A) Effect of C1-6 TCR transgene. C.B-17 (open circles) and C.B-17 C1-6 TCR transgenic (closed circles) mice were infected with HSV-1 (KOS; 4 × 10^5 PFU). Data shown represent two independent experiments based on analysis of four to five mice per group.

(B and C) Depletion of V_β^+ T cell subpopulation and HSK. (B) (Left panel) C.AL-20 mice were depleted in vivo of $V_\beta6^+$ cells (open circles) and $V_\beta8^+$ cells (closed circles) by i.p. injection of monoclonal antibodies (four doses of 25 μg each), resulting in 98%–99% depletion, or untreated (open squares), before ocular infection with HSV-1 KOS (4 × 10^6 PFU/eye). (Right panel) Purified $CD4^+$ cells from BALB/c mice were transferred (3 × 10^6/mouse) into BALB/c-*RAG2*$^{-/-}$ mice after in vitro depletion (99%) of $V_\beta6^+$ cells (open circles) or $V_\beta8^+$ cells (closed circles) or untreated (open squares). All mice were ocularly infected 24 hr later with HSV-1 KOS (4 × 10^6 PFU/eye) followed by disease assessment as described in Experimental Procedures. HSK index = percent incidence × mean severity of clinical stromal keratitis ÷ 10. Each data point represents the average of at least five mice.

(C) The lymph nodes of HSV-1 KOS-infected, $V_\beta6$-depleted (hatched bars), $V_\beta8$-depleted (black bars), or untreated (white bars) C.AL-20 mice were harvested and cultured with syngeneic C.AL-20 irradiated spleen cells in the presence of UV-inactivated HSV-1 KOS (as described in Experimental Procedures). Results are shown as cpm of incorporated [^{3}H]thymidine that had been added to each well during the last 16 hr of culture.

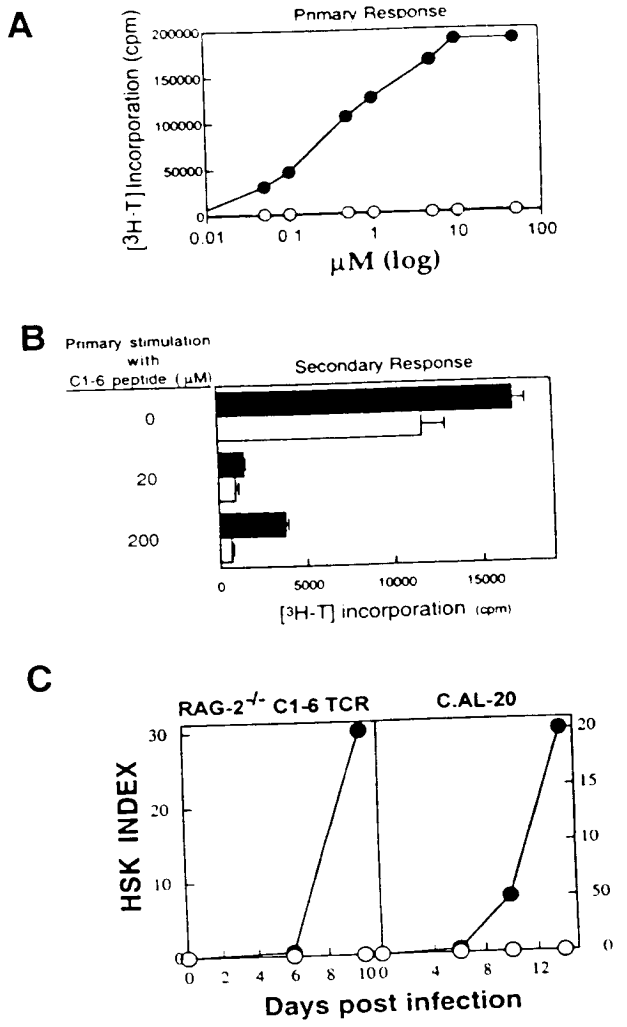

Figure 5. Effect of a Peptide Superagonist on C1-6 T Cell Responses

(A) Stimulation of CD4 cells from BALB/c-*RAG-2*$^{-/-}$ C1-6 mice in vitro. Proliferative response of CD4 cells from BALB/c-*RAG-2*$^{-/-}$ C1-6 mice (10^4/well plus 10^5 irradiated BALB/c splenic cells) to the indicated concentrations of peptide: C1-6 (292-308; SYFMYSK LRVQKS) (closed circles) or K8S mutant (SYFMYSKLRVQSS) (open circles), as described in Experimental Procedures.

(B) Induction of unresponsiveness by C1-6 peptide. After stimulation (5 days) of C1-6 CD4 cells (5 × 10^4/well) with the indicated concentrations of the C1-6 peptide, cells were restimulated with immobilized anti-CD3 (5 μg/ml; black bars) or C1-6 peptide (100 μM; white bars) and [^{3}H]thymidine incorporation was determined 24–36 hr later. The levels of apoptosis as judged by annexin staining 24 hr after anti-CD3 stimulation of cells primed with 0, 20, and 200 μM peptide were 11, 74, and 82, respectively.

(C) Effect of soluble C1-6 peptide on HSK. BALB/c-*RAG2*$^{-/-}$ C1-6 TCR Tg and C.AL-20 mice were intravenously injected (400 μg/mouse) with either normal C1-6 (open circles) or a mutant C1-6 peptide, K8S (closed circles) twice prior to ocular infection with HSV-1 (4 × 10^6 PFU/eye), and HSK was scored on the indicated days.

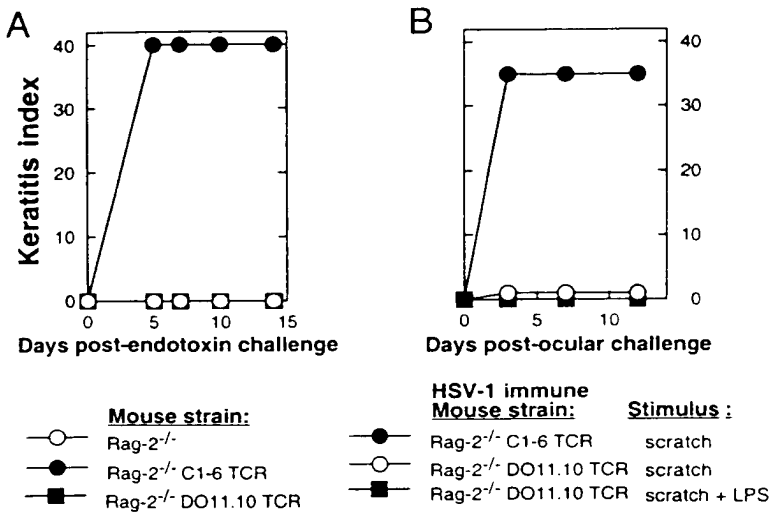

Figure 6. Nonspecific Stimuli Induces Keratitis in Mice Containing Large Numbers of Self-Reactive T Cells

(A) The right eyes of BALB/c-*RAG2*$^{-/-}$ (open circles), BALB/c-*RAG2*$^{-/-}$ DO11.10 Tg (closed squares), or BALB/c-*RAG2*$^{-/-}$ C1-6 TCR Tg (closed circles) mice were scratched with a 27 gauge needle, and 16 μg of LPS (Sigma, St. Louis, MO) was added in an 8 μl volume. Clinical keratitis was scored on day 5, 7, 10, and 15. Each point represents at least eight mice.

(B) BALB/c-*RAG2*$^{-/-}$ C1-6 TCR Tg (closed circles) and BALB/c-*RAG2*$^{-/-}$ DO11.10 TCR Tg (open circles, closed squares) mice were immunized three times with 2×10^5 PFU irradiated KOS virus weekly prior to ocular scarification or scarification and LPS (16 μg) treatment. Clinical keratitis was scored on day 3, 7, and 12. Each point represents at least five mice per group.

(C) The indicated strains were infected with increasing titers of HSV-1 (KOS or S309L) in the right eye, and disease was scored on day 10 after infection, as described in the Experimental Procedures. The percent with detectable disease on day 10 (minimum score 1) is shown based on analysis of four to eight mice per group.

C

Viral challenge (pfu x 10^3/eye)		HSK (%) BALB/c RAG-2$^{-/-}$ C1-6 Tg	BALB/c RAG-2$^{-/-}$ DO11.10	C.AL-20
KOS	.4	20	0	0
	4	100	0	0
	40	100	0	100
	400	100	0	100
S309L	.4	20	0	0
	4	100	0	0
	40	100	0	0
	400	100	0	0

This truncated response reflected the inability of KOS/UL6^{S309L} to stimulate disease-inducing T cells; purified CD4$^+$ T cells from the draining lymph nodes of KOS/UL6^{S309L}-infected mice were unable to transfer significant disease to recipient BALB/c-*RAG2*$^{-/-}$ mice compared with the robust activity of CD4 cells from KOS-wt-infected mice (Figure 3B).

Comparative analyses of HSK after HSV-1 infection of *RAG-2*$^{-/-}$ mice expressing the C1-6 and DO11.10 TCR strengthened the conclusion that HSK induction after HSV-1 (KOS) infection depended on activation of a restricted set of CD4 clones. This hypothesis also received support from the finding that insertion of the C1-6 TCR into the T cell repertoire converted the phenotype of C.B-17 mice from resistant to highly susceptible. The hypothesis that the interaction between the C1-6 TCR and the viral mimic played a critical role in disease induction predicted several targeted approaches to immunotherapy of the disease. We found that depletion of $V_\mu 8.1/8.2^+$ cells (the V_β expressed by C1-6) but not $V_\beta 6^+$ cells markedly diminished disease intensity after corneal infection with HSV-1 KOS without affecting the overall antiviral immune response and that intravenous injection of a C1-6 peptide at concentrations that induce apoptosis in vitro ameliorated disease in vivo (Figures 5 and 6).

Viral Infection and Innate Immunity

Understanding the conditions that determine the contribution of innate and adaptive immune mechanisms to the pathogenesis of autoimmunity following infection remains a central and unresolved issue in this field (Horwitz and Sarvetnick, 1999; Medzhitov and Janeway, 1998). The role of nonspecific inflammatory responses is most clearly evident from the finding that tissue-specific expression of cytokine transgenes can provoke autoimmune disease without the need for microbial infection (Horwitz et al., 1997; Akassoglou et al., 1997). In most cases, microbial infection increases the efficiency of T cell activation through enhanced expression of costimulatory molecules, upregulation of MHC expression on professional APC, and attraction of dendritic cells from peripheral to secondary lymphoid tissues (Bachman et al., 1997). Continued activation of innate immunity can also potentiate autoimmune disorders through chronic immune-mediated tissue damage and autoantigen release without the need for specific activation of autoreactive T cells by a microbial mimic (Miller et al., 1990, 1995, 1997; Vanderlugt, 1996; Vanderlugt et al., 1998).

We have compared the relative importance of inflammatory and antigen-specific aspects of infection according to the level of autoreactive T cells in the host. A mild inflammatory stimulus (corneal trauma) is suffi-

cient to provoke disease in animals containing high levels of autoreactive memory T cells (Figure 6C), while a stronger nonspecific stimulus (mutant KOS/UL6^{S309L} virus or LPS) elicits disease in mice that harbor high numbers of naive autoreactive T cells (Figures 6A and 6C). Similarly, MBP1-11 TCR transgenic mice spontaneously develop experimental autoimmune encephalomyelitis (EAE) after exposure to pertussis toxin without specific antigen (Goverman et al., 1993; Linthicum et al., 1982; Munoz et al., 1984). All these observations emphasize that the need for a specific antigenic stimulus is greatest when the host contains limiting numbers of autoreactive T cells, while nonspecific stimuli are sufficient for disease induction in hosts containing expanded numbers of autoimmune T cells. These conclusions are also consistent with observations that Coxsackie B (CB4) virus infection can induce diabetes in BDC2.5^{+} mice provided that that host has developed an expanded population of autoreactive CD4 memory cells (Horwitz et al., 1998; Serreze et al., 2000).

Molecular Mimicry and Autoimmune Disease

Why is expression of a molecular self-mimic essential for efficient disease induction in hosts containing limited numbers of autoreactive T cells? The target self-antigen of HSK is naturally expressed in a nonlymphoid tissue and may not reach levels sufficient for effective cross-presentation to autoreactive T cells, even after microbial infection (Kurts et al., 1998; Ludwig et al., 1999; Sevilla et al., 2000; Serreze et al., 2000). Viruses, on the other hand, are efficiently taken up by professional APC, and peptides derived from them rapidly gain the direct attention of T cells. Presentation of a viral peptide mimic thus bypasses the series of events beginning with release of autoantigen from dying cells and ending with uptake, processing, and cross-presentation by local APC (Ehl et al., 1997; Oxenius et al., 1998). The resulting gain in immunogenicity is reminiscent of the enhanced T cell response achieved after bypassing the need for cross-presentation through expression of tumor antigens in dendritic cells (Klein et al., 2000).

These data open the possibility that subclinical infection by a virus that expresses a mimic can "prime" the host for an autoimmune response upon infection of the target organ by an unrelated virus, thus complicating the search for viral mimics associated with clinical disease. These studies also highlight the importance of testing for viral mimicry early in life (e.g., in genetically predisposed children), since viruses isolated after the onset of clinical disease, such as the dozens identified in MS patients, are likely to contribute to disease pathogenesis through their effects on innate rather than specific immunity. Our studies also indicate that screening for peptide mimics should include assessment of relatively weak microbial ligands. Although the UL6 peptide epitope has a relatively low-affinity interaction with the C1-6 TCR, it is sufficient to induce disease in vivo, while the high-affinity C1-6 peptide (which efficiently stimulates T cells in vitro) inhibits rather than enhances disease in vivo (Figures 4A and 5A). These findings are congruent with the recent observation that MBP-derived peptides that display low-affinity binding to self-MHC efficiently provoke EAE in vivo, while MBP peptide analogs that bind well to self-MHC and strongly stimulate T cells in vitro cause apoptosis of autoreactive T cells and inhibit disease in vivo (Anderton et al., 2001).

Viral Infection and Bystander Damage

In all of the above examples, viral infection through specific or nonspecific mechanisms provokes autoreactive T cells and consequent autoimmune tissue destruction. However, two recent studies by Gangappa and coworkers suggest that a strain of HSV-1 (RE) can induce a nonautoimmune form of keratitis after infection (Gangappa et al., 1998, 2000). In the second study (Gangappa et al., 2000), BALB/c-*RAG2*$^{-/-}$ DO11.10 mice developed keratitis after infection with the HSV-1 RE strain, in apparent contrast to our findings that these mice do not develop HSK after infection by very high titers of HSV-1 KOS (Table 1; Figure 3A). The disparity in these results reflects a difference in the virulence (Thomas and Rouse, 1997) and pathogenicity of the two HSV-1 strains. We have noted that, at relatively high concentrations (4×10^6 PFU), ocular infection by the RE strain can cause clinical keratitis in up to 50% of BALB/c-*RAG2*$^{-/-}$ DO11.10 mice, while infection of the same mice with these titers of HSV-1 KOS fails to induce detectable corneal changes or histological evidence of cellular infiltration. The pathogenicity of HSV-1 RE in BALB/c-*RAG-2*$^{-/-}$ DO11.10 mice may be related to the ability of this strain to attract large numbers of neutrophils (Thomas et al., 1997), in contrast to KOS, which primarily attracts macrophages (Hendricks and Tumpey, 1990), and to its persistence at higher titers in the corneas of immunocompetent mice (Su et al., 1990), leading to attendant damage of the cornea through release of collagenases and/or necrosis of the local vasculature. Alternatively, the intense inflammatory response provoked by the RE virus may allow recognition of low-affinity viral mimics by the DO11.10 TCR.

The development of blindness following clinical herpetic stromal keratitis is marked by intense stromal inflammation leading to irreversible corneal scarring, glaucoma, and cataract. Infection of the mouse strains used here with HSV-1 KOS or RE strains, which model the most destructive and blinding form of this clinical disorder, supports two distinct pathogenic pathways. Infections by relatively nonpathogenic HSV-1 strains such as KOS are translated into an autoimmune attack and blindness through the expression of a viral mimic. A second pathway may result from infection by HSV-1 strains such as RE, which lead to proteolysis and collagen breakdown through nonautoimmune mechanisms that may include bystander damage. Elucidation of the relative roles of these two pathogenic pathways in clinical HSK represents the next step in diagnosis and treatment of a leading cause of human blindness. In a broader context, our studies suggest approaches for evaluation of the relative roles of antigen mimicry and nonspecific inflammation in a variety of clinical syndromes, ranging from bacterial arthritis to some forms of atherosclerosis (Gross et al., 1998; Bachmaier et al., 1999).

Experimental Procedures

Mice

C.AL-20 and C.B-17 female mice were purchased from The Jackson Laboratory (Bar Harbor, ME); DBA/2 and CD1 mice were purchased

from Charles River Laboratory, Inc. (Wilmington, MA); and BALB/c and BALB/c-*RAG2*$^{-/-}$ mice were purchased from Taconic Laboratories, Inc. (Germantown, NY). The OVA-TCR (DO11.10) transgenic mice were crossed into the *RAG2*$^{-/-}$ background (confirmed by PCR and FACS analysis). All mice used for experimentation were 6–8 weeks of age and housed in microisolator cages in the animal biosafety level 2 of the Dana Farber Cancer Institute animal facility.

Construction of KOS/UL6^{S309L} HSV-1 Replication-Competent Mutant Virus

The mutant UL6^{S309L} allele was constructed using the pZZ plasmid (Zhao et al., 1998) containing a 1.3 kb segment of UL6 and the Clonetech Transformer™ Site-directed mutagenesis kit to alter UL6 codon 309 from AGC encoding Ser to CTT encoding for Leu creating plasmid pMES2. These nucleotide changes introduce a HindIII site at bp 922 in the *UL6* coding sequence. The 1 kb MluI-SphI fragment from pMES2 containing the S309L mutation was subcloned into plasmid pMES12, which contains the entire *UL6* coding sequence and a large portion of HSV-1 flanking sequence, to create pMES18.

To integrate the UL6^{S309L} mutation into the HSV-1 KOS genome, 1 μg KOS/UL6^{m} infectious DNA and 5 μg BstBI-AflII-digested pMES18 were cotransfected into 1 × 10^{6} BKK21 cells that had been engineered to express UL6 (Patel et al., 1996). The KOS/UL6^{m} infectious DNA contains a C to T point mutation at nucleotide 136 in the *UL6* coding sequence and does not synthesize UL6 protein (Zhao et al., 1998). Recombination between the BstBI-AflII UL6^{S309L} fragment from pMES18 and the KOS/UL6^{m} infectious DNA introduced the S309L mutation while repairing the UL6^{m} point mutation.

To identify and purify a replication-competent virus that contains the UL6^{S309L} mutation, the transfected G33 cells were harvested 5 days after transfection, virus was isolated by three rounds of freeze thawing, and subsequently used to infect Vero cells. Since KOS/UL6^{m} cannot replicate in Vero cells, only recombinants with a repaired UL6^{m} point mutation could grow. Individual plaques (48) from the Vero cell infection were purified and screened for the presence of the S309L mutation by PCR amplification and digestion with HindIII enzyme. All 48 of the viruses analyzed carried the mutation. Sequencing of an extended region (~500 bp) flanking the 5′ and 3′ boundaries of the recombination sites did not reveal any nucleotide differences compared with the wild-type sequence.

Replication Curve for KOS/UL6^{S309L} and WT KOS

In vitro

To compare the replication rate of the KOS/UL6^{S309L} mutant virus to wild-type KOS, 2 × 10^{5} Vero cells were seeded in wheaton glass vials 4 hr prior to infection with 2 × 10^{6} PFU of virus followed by incubation (1 hr at 37°C) and removal of virus by washing. Cells were resuspended in 1 ml of serum-free DMEM medium, and individual vials were removed at the indicated time points, frozen at −70° C, and prepared by repeated freezing/thawing before assaying for viral PFU/ml by standard methods (Sandstrom et al., 1986).

In vivo

C.AL-20 mice were ocularly infected with 4 × 10^{6} PFU wild-type KOS or KOS/UL6^{S309L}; eyes were harvested on days 2, 3, 4, 5, and 6 and assayed for viral particles as described (Sandstrom et al., 1986).

Ocular Infection and Scoring of HSK

Corneas of mice were scarified using a sterile 27 gauge needle (Avery et al., 1995) before infection with HSV-1 (KOS or KOS/UL6^{S309L}) in the right eye, and disease severity was scored on different days after infection as described (Avery et al., 1995), based on the degree of corneal opacity: ≤25% of cornea, 1; ≤50%, 2; ≤75%, 3; 75%–100%, 4. Corneal opacity represents irreversible and progressive destruction characteristic of necrotizing keratitis resulting from severe stromal edema and necrosis with ulcerations seen on histological sections of the cornea. Neovascularization or corneal clouding were not used to measure stromal keratitis, since these changes may be transient and reversible. Incidence of disease is measured as the percentage of mice with a severity score ≥1. In certain experiments, disease score is summarized as "HSK index" = severity (mean clinical score) × incidence (%) divided by 10.

Histology

Mice were sacrificed on day 5, 10, and 15 postinfection, and infected eyes were enucleated and immediately frozen before tissue sections were stained with hematoxylin-eosin and observed for thickness of cornea and number of infiltrating cells.

Construction of the C1-6 TCR Transgenic Mice

The C1-6 TCR transgenic mouse line was created by cloning the α and β chains from the C1.6 keratogenic T cell clone (Avery et al., 1995). The α-rearranged cDNA (~800 bp) was amplified by anchored PCR as described (Frohman et al., 1988), cloned into SalI-SmaI-digested pSP72 (Promega Corp., Madison, WI) to create α11I, and confirmed by sequence analysis. The XhoI-BglII fragment from α11I containing the complete coding sequence for the α chain was subcloned into the pHSE3′ transgenic vector (Pircher et al., 1989), placing the α chain under the transcriptional control of the H-2K^{b} promoter. Similarly, the β-rearranged cDNA (~930 bp) was amplified by RT-PCR, cloned into SmaI-HindIII-digested pGEM7zf (Promega Corp.) to create BETAI, and sequenced. The XhoI-BamHI fragment from BETAI containing the complete $V_{\beta}8.1/D_{\beta}1.1/J_{\beta}1.4/C_{\beta}1$ sequence was subcloned into the pHSE3′ vector and placed under the control of the H-2K^{b} promoter. The two XhoI fragments from pHSE3′α and pHSE3′β were used to produce the transgenic mice, as described (Hogan et al., 1986). DBA/2 (H-2^{d}) × BALB/c (H-2^{d}) eggs were comicroinjected with α and β chain constructs, implanted in CD1 females to produce mice with a complete C1-6 TCR. These mice were crossed to BALB/c mice for three to four generations before crossing onto the BALB/c-*RAG2*$^{-/-}$ genetic background. The TCR transgene expression and *RAG2* defect were confirmed by both PCR and FACS analysis.

Delayed-Type Hypersensitivity

C.AL-20 mice were infected in the right eye with HSV-1 KOS (4 × 10^{6} PFU), and, 5 days later, individual groups of infected mice were challenged in the left footpad with 5 × 10^{7} PFU UV-inactivated HSV-1 KOS or KOS/UL6^{S309L} (Foster et al., 1986), and the right and left footpads of each mouse were measured 24 hr later with a Fowler micrometer (Schlesinger Tool, Brooklyn, NY).

In Vitro Proliferation to KOS/UL6^{S309L}

The right superficial cervical draining lymph nodes of C.AL-20 mice were harvested 15 days after ocular infection of the right eye with 4 × 10^{6} PFU HSV-1 KOS or KOS/UL6^{S309L}. Cells from these lymph nodes (1 × 10^{5} per well) were cultured with syngeneic BALB/c irradiated (3000 rad) spleen cells (5 × 10^{5}/well) in the presence of 2 × 10^{7} PFU UV-inactivated HSV-1 KOS or KOS/UL6^{S309L}, as described (Zhao et al., 1998). [^{3}H]thymidine (1 μCi) was added to each well during the last 16 hr of culture.

Purification of CD4^{+} Cells and Analysis by Flow Cytometry

CD4^{+} T cells were isolated by magnetic negative selection (Dynal, Lake Success, NY) using antibodies to CD8 (53-6.7), B220 (RA3-6B2), Gr-1 (RB6-8C5), and Mac-1 (M1/70) (PharMingen, San Diego, CA). For certain experiments, anti-$V_{\beta}8$ (F23.1) or anti-$V_{\beta}6$ (RR4-7) was also used (PharMingen). Cells from lymph nodes or blood were stained using FITC- or PE-conjugated anti-$V_{\beta}8$(8.1/8.2), anti-$V_{\beta}6$, anti-$V_{\beta}4$, anti-$V_{\beta}2$, and anti-CD4 as previously described (Pestano et al., 1999).

Depletion of T Cells According to V_{β} Expression

Mice were depleted in vivo of $V_{\beta}6^{+}$ cells or $V_{\beta}8^{+}$ cells by intraperitoneal injection of monoclonal antibodies (RR4-7 or F23.1; four doses of 25 μg each; day −5, −3, 0, and +2; PharMingen), resulting in 98%–99% depletion (as measured by flow cytometric analysis). Depleted mice were ocularly infected with HSV-1 KOS (4 × 10^{6} PFU/eye). In other experiments, purified CD4^{+} cells from BALB/c mice were transferred (3 × 10^{6}/mouse intravenously) into BALB/c-*RAG2*$^{-/-}$ recipient mice after in vitro depletion by magnetic negative selection (99% by flow cytometry) of $V_{\beta}6^{+}$ cells or $V_{\beta}8^{+}$ cells.

Acknowledgments

This work was supported in part by research grants from the National Institutes of Health (NIH) (AI37562, AI12184, AI48125) and the Juvenile Diabetes Foundation International to H.C.; the Diabetes Action Research Council to V.P.; National Research Service Award (NRSA) (F32 EY07032) to M.S.; a Swedish Foundation for International Cooperation in Research and Higher Education (STINT) fellowship to M.J.; Deutsche Forschungemeinschaft Fellowship (HU 890/1-1) to K.M.H.; and NIH (NS 39096) to K.W.W. The authors wish to thank Drs. A. Sharpe for provision of DO11.10 transgenic mice; W. Lucas, Z.-S. Zhao, and L. Yeh for technical advice; as well as A. Angel for manuscript preparation; and E.D. Smith for graphics.

Received February 19, 2001; revised May 17, 2001.

References

Akassoglou, K., Probert, L., Kontogeorgos, G., and Kollias, G. (1997). Astrocyte-specific but not neuron-specific transmembrane TNF triggers inflammation and degeneration in the central nervous system of transgenic mice. J. Immunol. *158*, 438–445.

Altmann, D.M., and Blyth, W.A. (1985). Protection from herpes simplex virus-induced neuropathology in mice showing delayed hypersensitivity tolerance. J. Gen. Virol. *66*, 1297–1303.

Anderton, S.M., Radu, C.G., Lowrey, P.A., Ward, E.S., and Wraith, D.C. (2001). Negative selection during the peripheral immune response to antigen. J. Exp. Med. *193*, 1–11.

Avery, A.C., Zhao, Z.-S., Rodriquez, A., Bikoff, E.K., Soheilian, M., Foster, C.S., and Cantor, H. (1995). Resistance to herpes stromal keratitis conferred by an IgG2a-derived peptide. Nature *376*, 431–434.

Bachmaier, K., Neu, N., delaMaza, L.M., Pal, S., Hessel, A., and Penninger, J.M. (1999). Chlamydia infections and heart disease linked through antigenic mimicry. Science *283*, 1238–1239.

Bachman, M.F., Oxenius, A., Speiser, D.E., Maria-Thasan, S., Hengartner, H., Zinkernagel, R.M., and Ohashi, P.S. (1997). Peptide-induced T cell receptor down-regulation on naive T cells predicts agonist/partial agonist properties and strictly correlates with T cell activation. Eur. J. Immunol. *27*, 2195–2203.

Cantor, H. (2000). T-cell receptor crossreactivity and autoimmune disease. Advan. Immunol. *75*, 209–233.

Chen, J., Lansford, R., Stewart, V., Young, F., and Alt, F.W. (1993a). RAG-2-deficient blastocyst complementation: An assay of gene function in lymphocyte development. Proc. Natl. Acad. Sci. USA *90*, 4528–4532.

Chen, J., Trounstine, M., Alt, F.W., Young, F., Kurahara, C., Loring, J.F., and Huszar, D. (1993b). Immunoglobulin gene rearrangement in B cell deficient mice generated by targeted deletion of the JH locus. Int. Immunol. *5*, 647–656.

Daheshia, M., Kuklin, N., Kanangat, S., Manickan, E., and Rouse, B.T. (1997). Suppression of ongoing ocular inflammatory disease by topical administration of plasmid DNA encoding IL-10. J. Immunol. *159*, 1945–1952.

Dal Canto, M.C., and Rabinowitz, S.G. (1982). Experimental models of virus-induced demyelination of the central nervous system. Ann. Neurol. *11*, 109–127.

Ehl, S., Hombach, J., Aichele, P., Hengartner, H., and Zinkernagel, R.M. (1997). Bystander activation of cytotoxic T cells: studies on the mechanism and evaluation of in vivo significance in a transgenic mouse model. J. Exp. Med. *185*, 1241–1251.

Foster, C.S., Tsai, Y., Monroe, J.G., Campbell, R.C., Cestari, M., Knipe, D., and Greene, M.I. (1986). Genetic studies on murine susceptibility to herpes simplex keratitis. Clin. Immunol. Immunopathol. *40*, 313–325.

Frohman, M.A., Dush, M.K., and Martin, G.R. (1988). Rapid production of full-length cDNAs from rare transcripts: amplification using a single gene-specific oligonucleotide primer. Proc. Natl. Acad. Sci. USA *85*, 8998–9002.

Gamble, D.R. (1980). Relation of antecedent illness to development of diabetes in children. Br. Med. J. *281*, 99–101.

Gamble, D.R., and Taylor, K.W. (1973). Coxsackie B virus and diabetes. Br. Med. J. *1*, 289–290.

Gangappa, S., Babu, J.S., Thomas, J., Caheshia, M., and Rouse, B.T. (1998). Virus-induced immunoinflammatory lesions in the absence of viral antigen recognition. J. Immunol. *161*, 4289–4300.

Gangappa, S., Deshpande, S.P., and Rouse, B.T. (2000). Bystander activation of CD4+ T cells accounts for herpetic ocular lesions. Invest. Ophthalm. Vis. Sci. *41*, 453–459.

Goverman, J., Woods, A., Larson, L., Weiner, L.P., Hood, L., and Zaller, D.M. (1993). Transgenic mice that express a myelin basic protein-specific T cell receptor develop spontaneous autoimmunity. Cell *72*, 551–560.

Gross, D.M., Forsthuber, T., Tary-Lehmann, M., Etling, C., Ito, K., Nagy, Z.A., Field, J.A., Steere, A.C., and Huber, B.T. (1998). Identification of LFA-1 as a candidate autoantigen in treatment-resistant Lyme arthritis. Science *281*, 703–706.

Hemmer, B., Fleckenstein, B.T., Vergelli, M., Jung, G., McFarland, H., Martin, R., and Wiesmuller, K.H. (1997). Identification of high potency microbial and self ligands for a human autoreactive class II-restricted T cell clone. J. Exp. Med. *185*, 1651–1659.

Hendricks, R.L., and Tumpey, T.M. (1990). Contribution of virus and immune factors to herpes simplex virus Type-1 induced corneal pathology. Invest. Ophthalm. Vis. Sci. *31*, 1929–1939.

Hogan, B., Constantini, F., and Lacy, E. (1986). Manipulating the Mouse Embryo: A Laboratory Manual (Cold Spring Harbor, NY: Cold Spring Harbor Laboratories).

Horwitz, M.S., and Sarvetnick, N. (1999). Viruses, host responses, and autoimmunity. Immunol. Rev. *169*, 241–253.

Horwitz, M.S., Evans, C.F., McGavern, D.B., Rodriguez, M., and Oldstone, M. (1997). Primary demyelination in transgenic mice expressing interferon-γ. Nat. Med. *3*, 1037–1041.

Horwitz, M.S., Bradley, L.M., Harbertson, J., Krahl, T., Lee, J., and Sarvetnick, N. (1998). Coxsackie virus-induced diabetes: initiation by bystander damage and not molecular mimicry. Nat. Med. *4*, 781–785.

Klein, C., Bueler, H., and Mulligan, R.C. (2000). Comparative analysis of genetically modified dendritic cells and tumor cells as therapeutic cancer vaccines. J. Exp. Med. *191*, 1699–1708.

Kurts, C., Miller, J.F.A.P., Subramaniam, R.M., Carbone, F.R., and Heath, W.R. (1998). MHC class I-restricted cross-penetration is biased towards high dose antigens and those released during cellular destruction. J. Exp. Med. *188*, 409–414.

Linthicum, D.S., Munoz, J.J., and Blaskett, A. (1982). Acute EAE in mice. I. Adjuvant action of Bordetella pertussis is due to vasoactive amine sensitization and increased vascular permeability of the CNS. Cell. Immunol. *73*, 299–310.

Ludwig, B., Odermatt, B., Ochsenbein, A.F., Zinkernagel, R.M., and Hengartner, H. (1999). Role of dendritic cells in the induction and maintenance of autoimmune diseases. Immunol. Rev. *169*, 45–54.

Medzhitov, R., and Janeway, C. (1998). Innate immune recognition and control of adaptive immune responses. Semin. Immunol. *10*, 351–353.

Miller, S.D., Gerety, S.J., Kennedy, M.K., Peterson, J.D., Trotter, J.L., Tuohy, V.K., Waltenbaugh, C., DalCanto, M.C., and Lipton, H.L. (1990). Class II-restricted T cell responses in Theiler's murine encephalomyelitis virus (TMEV)-induced demyelinating disease. III. Failure of neuroantigen-specific immune tolerance to affect the clinical course of demyelination. J. Neuroimmunol. *26*, 9–23.

Miller, S.D., McRae, B.L., Vanderlugt, C.L., Nikcevitch, K.M., Pope, J.G., Pope, L., and Karpus, W.J. (1995). Evolution of the T-cell repertoire during the course of experimental immune-mediated demyelinating disease. Immunol. Rev. *144*, 225–244.

Miller, S.D., Vanderlugt, C.L., Begolka, W.S., Pao, W., Yauch, R.L., Neville, K.L., Katz-Levy, Y., Carrizosa, A., and Kim, B.S. (1997). Persistent infection with Theiler's virus leads to CNS autoimmunity via epitope spreading. Nat. Med. *3*, 1133–1136.

Munoz, J.J., Bernard, C.C., and Mackay, I.R. (1984). Elicitation of

experimental allergic encephalomyelitis (EAE) in mice with the aid of pertussigen. Cell. Immunol. *83*, 92–100.

Nagata, M., and Yoon, J.-W. (1992). Studies on autoimmunity for T-cell-mediated beta cell destruction. Diabetes *41*, 998–1008.

Ohashi, P.S., Oehen, S., Buerki, K., Pircher, H., Ohashi, C.T., Odermatt, B., Malissen, B., Zinkernagel, R.M., and Hengartner, H. (1991). Ablation of "tolerance" and induction of diabetes by virus infection in viral antigen transgenic mice. Cell *65*, 305–317.

Oldstone, M.B. (1987). Molecular mimicry and autoimmune disease. Cell *50*, 819–820.

Oxenius, A., Zinkernagel, R.M., and Hengartner, H. (1998). $CD4^+$ T-cell induction and effector functions: A comparison of immunity against soluble antigens and viral infections. Advan. Immunol. *70*, 313–367.

Patel, A.H., Rixon, F.J., Cunningham, C., and Davison, A.J. (1996). Isolation and characterization of Herpes Simplex Virus Type 1 mutants defective in the UL6 gene. Virology *217*, 111–123.

Pestano, G.A., Zhou, Y., Daley, J., Trimble, L.A., Weber, G.F., and Cantor, H. (1999). Inactivation of misselected CD8 T cells by CD8 gene methylation and cell death. Science *284*, 1187–1191.

Pircher, H.P., Burki, K., Lang, R., Hengartner, H., and Zinkernagel, R.M. (1989). Tolerance induction in double specific T-cell receptor transgenic mice varies with antigen. Nature *342*, 559–561.

Rodriguez, M., Oleszak, E., and Leibowitz, J. (1987). Theiler's murine encephalomyelitis: a model of demyelination and persistence of virus. Crit. Rev. Immunol. *7*, 325–365.

Sandstrom, I.K., Foster, C.S., Wells, P.A., Knipe, D., Caron, L., and Greene, M.I. (1986). Previous immunization of mice with HSV-1 strain MP protects against secondary corneal infection. Clin. Immunol. Immunopathol. *40*, 326–334.

Serreze, D.V., Ottendorfer, E.W., Ellis, T.M., Gauntt, C.J., and Atkinson, M.A. (2000). Acceleration of type 1 diabetes by a coxsackievirus infection requires a preexisting critical mass of autoreactive T-cells in pancreatic islets. Diabetes *49*, 708–711.

Sevilla, N., Homann, D., von Herrath, M.G., Rodriguez, F., Harkins, S., Whitton, J.L., and Oldstone, M.B.A. (2000). Virus-induced diabetes in a transgenic model: Role of cross-reacting viruses and quantitation of effector T cells needed to cause disease. J. Virol. *74*, 3284–3292.

Sibley, W.A., Bamford, C.R., and Clark, K. (1985). Clinical viral infections and multiple sclerosis. Lancet *1*, 1313–1315.

Streilein, J.W., Dana, M.R., and Ksander, B.R. (1997). Immunity causing blindness: five different paths to herpes stromal keratitis. Immunol. Today *18*, 443–449.

Su, Y.H., Oakes, J.E., and Lausch, R.N. (1990). Ocular avirulence of a herpes simplex virus type 1 strain is associated with heightened sensitivity to alpha/beta interferon. J. Virol. *64*, 2187–2192.

Thomas, J., and Rouse, B.T. (1997). Immunopathogenesis of herpetic ocular disease. Immunol. Res. *16*, 375–386.

Thomas, J., Gangappa, S., Kanangat, S., and Rouse, B.T. (1997). On the essential involvement of neutrophils in the immunopathologic disease: herpetic stromal keratitis. J. Immunol. *158*, 1383–1391.

Vanderlugt, C.L. (1996). Epitope spreading. Curr. Opin. Immunol. *8*, 831–836.

Vanderlugt, C.L., Begolka, W.S., Neville, K.L., Katz-Levy, Y., Howard, L.M., Eagar, T.N., Bluestone, J.A., and Miller, S.D. (1998). The functional significance of epitope spreading and its regulation by co-stimulatory molecules. Immunol. Rev. *164*, 63–72.

von Herrath, M.G., and Oldstone, M.B.A. (1996). Virus-induced autoimmune disease. Curr. Opin. Immunol. *8*, 878–885.

Wucherpfennig, K.W., and Strominger, J.L. (1995). Molecular mimicry in T cell-mediated autoimmunity: Viral peptides activate human T cell clones specific for myelin basic protein. Cell *80*, 695–705.

Zhao, Z.-S., Granucci, F., Yeh, L., Schaffer, P.A., and Cantor, H. (1998). Molecular mimicry by Herpes Simplex Virus-1: autoimmune disease after viral infection. Science *279*, 1344–1347.

tion alters the thermal structure of the deep ocean (25). Calculations for such extended periods are beyond the scope of this study.

REFERENCES AND NOTES

1. Climate: Long-Range Investigation, Mapping, and Prediction (CLIMAP) Project Members, *Map and Chart Series MC-36* (Geological Society of America, Boulder, CO, 1981).
2. T. P. Guilderson, R. G. Fairbanks, J. L. Rubenstone, *Science* **263**, 663 (1994).
3. M. Stute *et al.*, *ibid.* **269**, 379 (1995).
4. D. Rind and D. Peteet, *Quat. Res.* **24**, 1 (1985).
5. L. G. Thompson *et al.*, *Science* **269**, 46 (1995).
6. W. S. Broecker, *Quat. Res.* **26**, 121 (1986); M. W. Lyle, F. G. Prahl, M. A. Sparrow, *Nature* **355**, 812 (1992).
7. J. E. Kutzbach and P. J. Guetter, *J. Atmos. Sci.* **43**, 1726 (1986).
8. N. M. J. Hall, P. J. Valdes, B. Dong, *J. Clim.* **9**, 1004 (1996).
9. S. Manabe and A. J. Broccoli, *J. Geophys. Res.* **90**, 2167 (1985).
10. A. J. Broccoli and S. Manabe, *Clim. Dyn.* **1**, 87 (1987).
11. S. G. H. Philander, *El Niño, La Niña, and the Southern Oscillation*, vol. 46 of *International Geophysics Series* (Academic Press, New York, 1990); J. D. Neelin, M. Latif, F.-F. Jin, *Annu. Rev. Fluid Mech.* **26**, 617 (1994).
12. D. Andreasen and C. Ravelo, *Paleoceanography* **12**, 395 (1997).
13. T. F. Pederson, *Geology* **11**, 16 (1983).
14. See a summary by T. J. Crowley and G. R. North [*Paleoclimatology* (*Oxford Monograph on Geology and Geophysics 18*, Oxford Univ. Press, New York, 1991)], pp. 56–57.
15. The horizontal redistribution of warm surface waters during El Niño alters the topography of the thermocline—it deepens in some regions and shoals in others—while leaving unchanged the spatially averaged depth of and the temperature difference across the thermocline. That is why two-layer models of the ocean are effective tools for studying El Niño.
16. Z. Liu and S. G. H. Philander, *J. Phys. Oceanogr.* **25**, 449 (1995); D. Gu and S. G. H. Philander, *Science* **275**, 805 (1997).
17. C. T. Gordon and W. Stern, *Mon. Weather Rev.* **110**, 625 (1982); R. C. Pacanowski, K. Dixon, A. Rosati, "The GFDL Modular Ocean Model user guide," *GFDL Ocean Group Tech. Rep. 2* (Geophysical Fluid Dynamics Laboratory, Princeton, NJ, 1991).
18. W. R. Peltier, *Science* **265**, 195 (1994).
19. R. G. Fairbanks, *Nature* **342**, 637 (1989).
20. S. Levitus, *NOAA Prof. Pap. 13* (U.S. Government Printing Office, Washington, DC, 1982).
21. S. G. H. Philander *et al.*, *J. Clim.* **9**, 2958 (1996).
22. A. E. Gill, *Q. J. R. Meteorol. Soc.* **106**, 447 (1980).
23. A. B. G. Bush and W. R. Peltier, *J. Atmos. Sci.* **51**, 1581 (1994).
24. W. T. Hyde, T. J. Crowley, K.-Y. Kim, G. R. North, *J. Clim.* **2**, 864 (1989).
25. D. P. Schrag, G. Hampt, D. W. Murray, *Science* **272**, 1930 (1996).

26. This work was supported by a Natural Sciences and Engineering Research Council of Canada grant OGP0194151 (A.B.G.B.) and by the National Oceanic and Atmospheric Administration under contract NOAA-NA56GP0226 (S.G.H.P.). We thank the staff of the Geophysical Fluid Dynamics Laboratory for making this work possible.

7 November 1997; accepted 23 January 1998

Molecular Mimicry by Herpes Simplex Virus–Type 1: Autoimmune Disease After Viral Infection

Zi-Shan Zhao, Francesca Granucci, Lily Yeh, Priscilla A. Schaffer,* Harvey Cantor

Viral infection is sometimes associated with the initiation or exacerbation of autoimmune disease, although the underlying mechanisms remain unclear. One proposed mechanism is that viral determinants that mimic host antigens trigger self-reactive T cell clones to destroy host tissue. An epitope expressed by a coat protein of herpes simplex virus–type 1 (HSV-1) KOS strain has now been shown to be recognized by autoreactive T cells that target corneal antigens in a murine model of autoimmune herpes stromal keratitis. Mutant HSV-1 viruses that lacked this epitope did not induce autoimmune disease. Thus, expression of molecular mimics can influence the development of autoimmune disease after viral infection.

Autoimmune diseases result from a loss of self-tolerance and the consequent immune destruction of host tissues (*1*). Although the pathology of the associated tissue destruction has been well characterized, the mechanisms responsible for initiation and pathogenesis of autoimmune diseases remain unclear. Several mechanisms have been proposed on the basis of the clinical observation that viral infections can induce or exacerbate autoimmune disease (*2*). Virus-induced inflammatory responses that result in release of self antigens and enhancement of costimulatory activity may trigger autoreactive T cells (*3*, *4*). It also has been proposed that viral determinants that mimic host antigens directly stimulate self-reactive T cell clones to attack sequestered host tissues (*5*). Certain viral peptides that cross-react with self peptides can stimulate autoreactive T cells (*6*), and mice genetically engineered to express a viral protein can develop autoimmune disease after infection with the relevant virus (*7*). However, these observations do not provide direct evidence that viral infection can precipitate autoimmune disease by mechanisms that include molecular mimicry. Herpes stromal keratitis (HSK), a disorder induced by HSV-1 infection and characterized by T cell–dependent destruction of corneal tissue, is a leading cause of human blindness (*4*, *8*). To examine the role of viral mimicry in autoimmune disease, we have now studied a murine model of HSK in which corneal HSV-1 infection reproducibly results in a T cell–mediated autoimmune reaction (*8*, *9*).

Murine HSK elicited by HSV-1 (KOS strain) in C.AL-20 mice is mediated by $CD4^+$ T cell clones specific for corneal self antigens but that also recognize a peptide (amino acids 292 to 308) in the C_H3 region of immunoglobulin $G2a^b$ ($IgG2a^b$) (*9*). However, the role of this virus in the induction of HSK disease was not investigated. Given that there are insufficient numbers of T cells in the cornea after HSV-1 (KOS) infection to define potentially cross-reactive cells (*10*), we investigated whether the HSK-inducing C1-6 and C1-15 T cell clones might also recognize HSV-1 epitopes by measuring their proliferative response after stimulation with HSV-1 antigens. Both HSK-inducing clones, but not the ovalbumin (OVA)-reactive clone O3 (*11*), were activated by extracts of HSV-1 (KOS)–infected Vero cells [10^5 ultraviolet (UV)-inactivated plaque-forming units (PFU) per milliliter] but not by extracts of uninfected Vero cells (Fig. 1A).

We searched the GenBank database for HSV-1 proteins that share sequence homology with the keratogenic peptide recognized by C1-6 and C1-15. The best match was with a peptide sequence embedded in the HSV virion-associated protein UL6 (*12*), which contains identical or similar amino acids at seven of eight sequential positions that contribute to T cell recognition (Arg-Lys-Ser-Asp-*Ser*-Glu-Arg-Gly; mismatched residue in italics) (*9*). Both keratogenic clones, but not the OVA-reactive clone, were activated by a synthetic 15-residue viral peptide based on UL6 (amino acids 299 to 314) [UL6-(299–314)] and containing this nested sequence, whereas an unrelated peptide derived from murine mammary tumor virus (MMTV) did not activate these two clones at any concentration tested (Fig. 1B).

The proliferative response of the two keratogenic $CD4^+$ T cell clones to the UL6-(299–314) peptide suggested that in-

Z.-S. Zhao, F. Granucci, H. Cantor, Department of Pathology, Harvard Medical School, and Department of Cancer Immunology and AIDS, Dana-Farber Cancer Institute, Boston, MA 02115, USA.
L. Yeh and P. A. Schaffer, Division of Molecular Genetics, Dana-Farber Cancer Institute, Boston, MA 02115 USA.

*Present address: Department of Microbiology, University of Pennsylvania School of Medicine, Philadelphia, PA 19104 USA.

travenous administration of the soluble peptide into susceptible C.AL-20 mice might inhibit development of HSK. Mice injected twice intravenously with soluble UL6 peptide before corneal inoculation of HSV-1 (5×10^4 PFU per cornea) did not develop HSK; in contrast, mice treated the same way with a control peptide from MMTV developed HSK (Fig. 2A). Immunization of mice with the UL6 peptide in adjuvant also might be expected to result in expansion of T cells capable of inducing HSK. Because immunization of mice with components of HSV-1 can inhibit the HSK response as a result of production of neutralizing antibodies to HSV-1 (*13*), we measured the ability of T cells from peptide-immunized C.AL-20 mice to induce HSK in adoptive syngeneic hosts that lack T cells. T cell–deficient BALB/c *nu/nu* (nude) mice that received T cells (5×10^6) from C.AL-20 mice immunized with UL6-(299–314) peptide in adjuvant developed severe HSK, but *nu/nu* recipients of the same number of T cells from C.AL-20 mice immunized with the MMTV control peptide did not develop significant disease (Fig. 2B).

To further define the role of the UL6-derived peptide in HSK, an HSV-1 (strain KOS) virus containing a mutation in the UL6 gene was produced (*14*). A single base pair substitution introduced by site-directed mutagenesis generated a stop codon in the 5′ end of the UL6 open reading frame (Fig. 3A); this mutation also eliminated a unique Pvu II cleavage site (Fig. 3B). Viral isolates containing this mutation could not replicate in Vero cells but grew to concentrations similar to those of the wild-type virus in G33 cells that stably express the UL6 protein. One isolate (KOS/UL6^m) was selected for further study. The genome of KOS/UL6^m displayed the predicted mutant Pvu II restriction pattern as determined by Southern (DNA) blot analysis (Fig. 3B).

We then tested extracts of cells infected with KOS or KOS/UL6^m for their ability to activate the two keratogenic T cell clones (*15*). Clones C1-6 and C1-15 were activated by protein extracts from Vero cells infected with wild-type HSV-1 (KOS) but not by extracts of cells infected with KOS/UL6^m (Fig. 4A), despite the fact that both extracts contained the same concentration of HSV-1 protein (Fig. 4B). Nude mice that received T cells (5×10^6) from C.AL-20 mice immunized with HSV-1–infected Vero cell extracts developed HSK, whereas recipients of the same number of T cells from mice immunized with KOS/UL6^m-infected Vero cell extracts containing the same concentration of HSV-1 protein (Fig. 4B) did not develop the disease (Fig. 4C).

To further investigate whether the HSV-1 UL6 protein contains a viral epitope that activates keratogenic T cells, we compared HSK induction by KOS/UL6^m with induction by two other replication-defective HSV-1 (KOS) mutant viruses. The HSV-1 (KOS) 5dl1.2 mutant is altered in the UL54 gene of HSV-1 encoding ICP27 and is deficient in expression of late viral proteins including UL6 (*16*). The HSV-1 mutant K082 expresses all viral proteins except the late viral protein glycoprotein B (*17*). The extent of HSK induced after corneal infection by these mutant HSV-1 strains is moderate because nonreplicating antigens placed in the eye have poor access to the immune system (*18*). Moreover, because systemic immunization of mice with HSV-1 does not increase the efficacy of disease induction because it results in production of neutralizing antibodies to HSV-1 that prevent HSK (*13*), we reconstituted CB-17 mice with severe combined immunodeficiency disease (SCID mice), which lack T and B cells and may be more sensitive to HSK induction by T cells than *nu/nu* recipients (*19*), with T cells from HSV-1–immunized C.AL-20 mice immediately before corneal infection with the different mutant HSV-1 strains. Corneal infection by the K082 mutant caused severe HSK in about 85% of these mice, whereas corneal infection with either KOS/UL6^m or KOS/5dl1.2 did not result in detectable HSK (Fig. 4D).

These data indicate that deletion of the HSV-1 (KOS) protein UL6, which stimulates self-reactive T cell clones that initiate HSK, eliminates the ability of this virus to

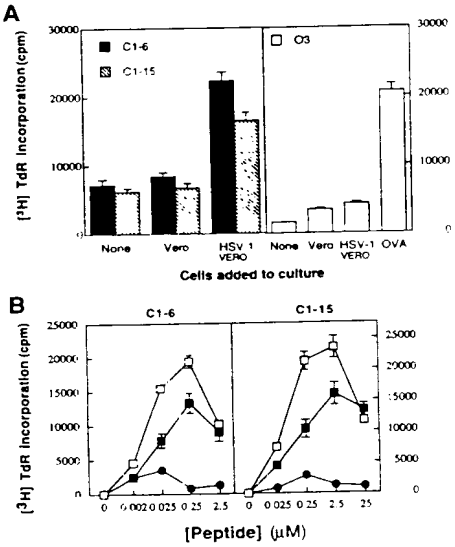

Fig. 1. (**A**) Recognition of UV-irradiated extracts of HSV-1(KOS)–infected cells by cornea-specific CD4+ T cell clones. Cornea-reactive T cell clones (C1-6 and C1-15) or the OVA-specific clone O3 (2×10^4 cells per well) were stimulated with UV-irradiated extracts of HSV-1–infected (*21*) or uninfected Vero cells in the presence of γ-irradiated [33 grays (Gy)] syngeneic BALB/c spleen cells (5×10^5 cells per well). Proliferation was assessed after 2 days by 16 to 18 hours of exposure to 1 μCi of [^{3}H]thymidine ([^{3}H]TdR) and is expressed as mean counts per minute (cpm) ± SEM of triplicate cultures. (**B**) Dose-dependent stimulation of cornea-specific CD4$^+$ T cell clones by HSV UL6-(299–314) peptide CD4$^+$ T cell clones (C1-6 and C1-15) (2×10^4 cells per well) were incubated with the indicated peptides (0.2 μM) in the presence of irradiated (33 Gy) syngeneic BALB/c spleen cells (5×10^5 cells per well): □, p292-308 (IgG2a^b); ■, p299-314 (UL6); ●, p200-222 (MMTV). Proliferation was assessed as in (A).

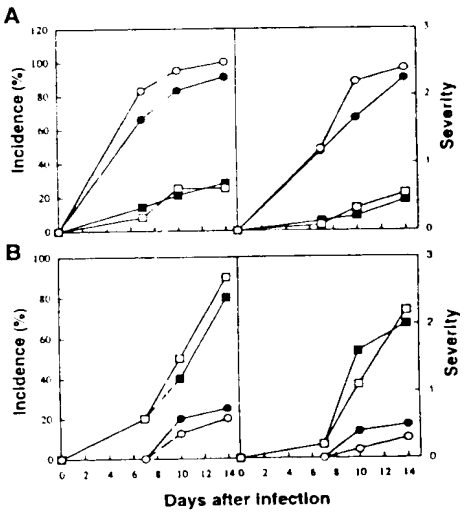

Fig. 2. Effects of HSV-1 UL6-(299–314) peptide on development of HSK. (**A**) C.AL-20 mice were injected intravenously with the indicated synthetic peptides (50 μg per mouse) in PBS 14 and 7 days before corneal infection with HSV-1 (KOS) (5×10^4 PFU per cornea): ■, p299-314 (UL6); □, p292-308 (IgG2a^b); ● p200-222 (MMTV); ○, PBS. Disease was scored on days 7, 10, and 14 after infection as described (*9*); data are means from eight mice per group. The severity of clinical stromal keratitis in anesthetized mice was scored as described (*22*) based on the degree of corneal opacity and neovascularization: <25% of cornea, 1+; <50%, 2+; <75%, 3+; 75 to 100%, 4+. (**B**) C.AL-20 mice were immunized by injection at the base of the tail with the same peptides (50 μg per mouse) as in (A) but in complete Freund's adjuvant. ◇, adjuvant alone. Two weeks later, T cells purified from pooled draining lymph nodes and spleens of immunized mice after passage through Cell-ect columns (Biotex, Edmonton, Alberta, Canada) were injected intraperitoneally into BALB/c *nu/nu* recipients (5×10^6 cells per mouse). Immediately after adoptive transfer, corneas were infected with HSV-1 (KOS) (5×10^4 PFU). Disease was scored on days 7, 10, and 14 after infection for six to eight mice per group. Additional experiments indicated that as many as 15×10^6 T cells specific for control (MMTV) peptides did not induce significant HSK.

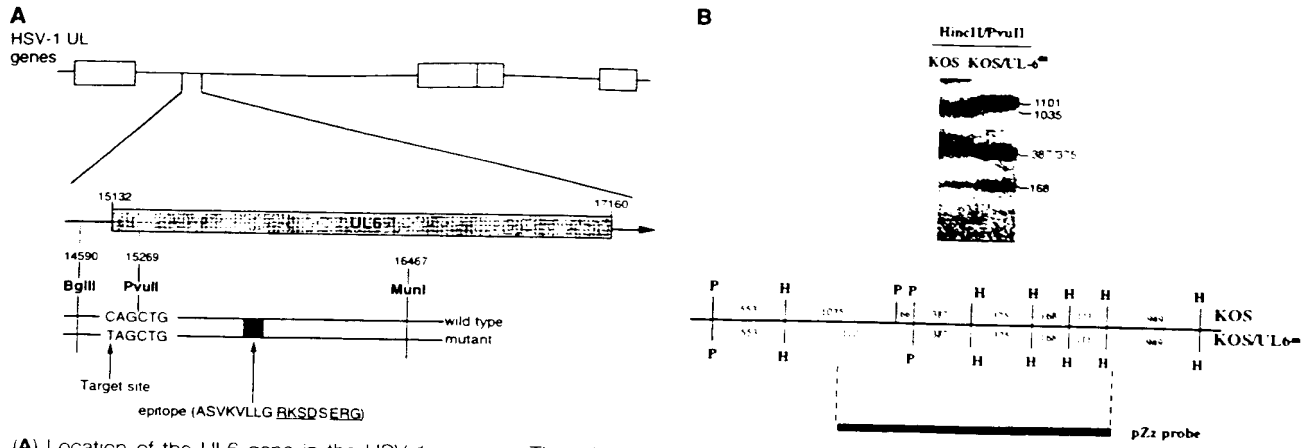

Fig. 3. (**A**) Location of the UL6 gene in the HSV-1 genome. The relative positions of UL6 restriction sites, the target mutation site, and the HSK epitope are also indicated. Amino acids are abbreviated as follows: A, Ala; S, Ser; V, Val; K, Lys; L, Leu; G, Gly; R, Arg; D, Asp; E, Glu. (**B**) Analysis of the genomic structure of the KOS/UL6^m mutant virus. DNA from KOS/UL6^m and wild-type KOS viruses was digested with Pvu II and Hinc II, and genomic fragments were separated by gel electrophoresis, transferred to nylon membranes, and subjected to Southern blot hybridization with the indicated probe (pZz). Below the blot is a restriction map for the enzymes (P, Pvu II; H, Hinc II) used in the Southern blot. The sizes of the relevant restriction fragments are indicated in base pairs.

induce HSK in mice. This effect cannot be attributed to the failure of KOS/UL6^m to replicate in corneal cells because the same concentrations of a second replication-deficient mutant, K082, that lacks a different viral structural protein (glycoprotein B) induced severe HSK. Both UL6 and glycoprotein B are late-appearing viral proteins and deletion mutants at these two loci allow expression of similar sets of HSV-1 genes (*16*, *17*). Moreover, the failure of KOS/UL6^m protein, but not of wild-type HSV-1 protein, to induce expansion of keratogenic T cells after immunization with adjuvant cannot be attributed to a replication defect. Instead, these data implicate a UL6-derived peptide in the pathogenesis of HSK.

Although viral infection can trigger autoimmune T cell responses in mice that express transgenic viral determinants (*5*, *7*), viral mimicry has not been implicated in the etiology of an autoimmune disorder that occurs after viral infection of nontransgenic animals. We have defined a viral peptide that stimulates keratogenic T cell clones in vitro and specifically modifies HSK in vivo. The finding that a mutant HSV-1 virus that lacks this epitope does not induce HSK provides direct evidence that molecular mimicry plays an important role in the development of this virally induced autoimmune disease. The identity of the corneal protein or proteins that correspond to the HSK autoantigen is not apparent from homology searches of protein databases, possibly reflecting the scarcity of structural information on murine corneal proteins in contrast to the abundance of sequence data for viruses (*6*).

The results of this study together with earlier studies suggest that susceptibility to autoimmunity after viral infection may be determined by two opposing mimicry mechanisms. Genetic polymorphisms that affect the sequence (*9*) or tissue expression (*20*) of a protein can generate endogenous molecular mimics that tolerize T cells to sequestered autoantigens and decrease susceptibility to virally induced autoimmune disease. Infection by viruses that carry an exogenous molecular mimic, as shown here, can enhance the development of autoimmunity, presumably by attraction and activation of autoreactive T cell clones to the target tissue.

We do not know whether molecular

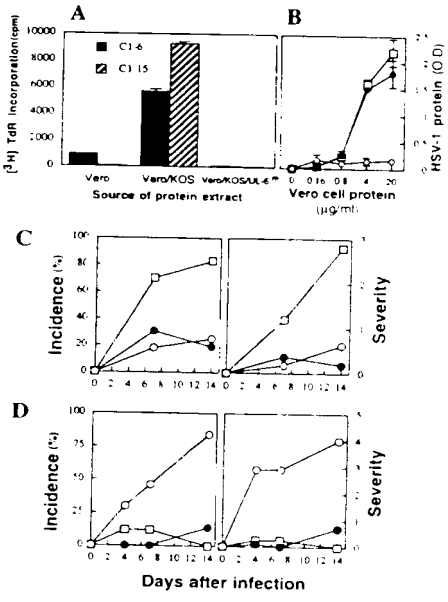

Fig. 4. Analyses of mutant strains of HSV-1 (KOS). (**A**) Keratogenic T cell clones (C1-6 and C1-15) (2×10^4 cells per well) were incubated with Vero cells (200 μg/ml) containing similar amounts of HSV-1 protein after infection with HSV-1 (KOS) or the mutant virus KOS/UL6^m (*21*) in the presence of irradiated (33 Gy) syngeneic BALB/c spleen cells (5×10^5 cells per well). Proliferation was assessed after 2 days by exposure for 16 to 18 hours to 1 μCi of [^{3}H]thymidine ([^{3}H]TdR). Results are expressed as means ± SEM of triplicate cultures. (**B**) Concentration of HSV-1 protein in Vero cell extracts 18 hours after infection with HSV-1 (KOS) (●), KOS/UL6^m (□), or after mock infection (○). HSV-1 protein was measured by a sandwich enzyme-linked immunosorbent assay in which the capture antibody was a rabbit antibody to HSV-1 (D0114, DAKO) and the secondary antibody was a peroxidase-conjugated antibody to HSV-1 (P0175, DAKO). (**C**) C.AL-20 mice were immunized (350 μg per mouse) by injection at the base of the tail with extracts of Vero cells infected with KOS/UL6^m (●) or KOS (□) or with mock-infected cells (○) emulsified in complete Freund's adjuvant. Two weeks later, purified T cells obtained from draining lymph nodes and spleens were adoptively transferred into BALB/c *nu/nu* recipients (5×10^6 cells per mouse). Immediately after adoptive transfer, each cornea was infected with HSV-1 (KOS) (5×10^4 PFU) and disease was scored on days 7, 10, and 14 after infection; data are means from 10 mice per group. (**D**) C.AL-20 mice were immunized with UV-irradiated HSV-1 (5×10^4 PFU per mouse). Two weeks later, T cells from immunized mice were adoptively transferred into CB-17 SCID recipients (5×10^6 cells per mouse). The recipients were immediately subjected to repeated corneal infection with high doses of K082 (○), KOS/UL6^m (●), or 5dl1.2 (□) mutant viruses (5×10^5 PFU per mouse; days 0, 2, and 4) and disease was scored 7, 10, and 14 days after the last infection. Data are means from eight mice per group.

mimicry by HSV-1 (KOS) is essential for disease induction in genetically susceptible hosts under all circumstances. Mimicry mechanisms may be particularly important in translating relatively low level viral infections into an autoimmune response. Infections by higher concentrations of HSV-1 (KOS) or by more virulent strains of HSV-1 may induce inflammatory responses that are sufficient to provoke autoimmune disease without the need for molecular mimicry. A comparison of HSK in transgenic mice with T cells that carry a receptor specific for an HSV-1 (KOS) viral peptide mimic or an unrelated peptide should further clarify the relative roles of mimicry and inflammation in the pathogenesis of virally induced autoimmune disease.

REFERENCES AND NOTES

1. W. M. Ridgway, H. L. Weiner, C. G. Fathman, *Curr. Opin. Immunol.* **6**, 946 (1994).
2. G. Dahlquist *et al.*, *Diabetologia* **38**, 1371 (1995); P. B. Challoner *et al.*, *Proc. Natl. Acad. Sci. U.S.A.* **92**, 7440 (1995). S. Vento *et al.*, *Lancet* **346**, 608 (1995).
3. E. E. Sercarz *et al.*, *Annu. Rev. Immunol.* **11**, 729 (1993).
4. B. T. Rouse, *Adv. Virus Res.* **47**, 353 (1996).
5. M. B. A. Oldstone, *Cell* **50**, 819 (1987); M. G. von Herrath and M. B. A. Oldstone, *Curr. Opin. Immunol.* **8**, 878 (1996).
6. K. W. Wucherpfennig and J. L. Strominger, *Cell* **80**, 695 (1995); B. Hemmer *et al.*, *J. Exp. Med.* **185**, 1651 (1997).
7. M. B. A. Oldstone, M. Nerenberg, P. Southern, J. Price, H. Lewicki, *Cell* **65**, 319 (1991); P. Ohashi *et al.*, *ibid.*, p. 305.
8. J. W. Streilein, M. R. Dana, B. R. Ksander, *Immunol. Today* **18**, 443 (1997).
9. A. C. Avery *et al.*, *Nature* **376**, 431 (1995).
10. M. G. Niemialtowski and B. T. Rouse, *J. Immunol.* **148**, 1864 (1992).
11. S. Friedman, D. Sillcocks, H. Cantor, *Immunogenetics* **26**, 193 (1987).
12. D. J. McGeoch *et al.*, *J. Gen. Virol.* **69**, 1531 (1997); J. Hay and W. T. Ruyechan, *Curr. Topics Microbiol. Immunol.* **179**, 1 (1992); A. H. Patel and J. B. Maclean, *Virology* **206**, 465 (1995).
13. M. B. Raizman and C. S. Foster, *Curr. Eye Res.* **7**, 823 (1988); C. S. Foster *et al.*, *Ocular Immunol. Today* (1990), p. 111.
14. The KOS/UL6^m HSV-1 mutant was constructed by using a plasmid (pSG10) containing the UL6 gene within a 10.6 kb Eco RI–generated DNA fragment derived from the genome of HSV-1 strain KOS [A. L. Goldin *et al.*, *J. Virol.* **38**, 50 (1981)]. A 1.9-kb Bgl II–Mfe I fragment from pSG10 containing a 1.3-kb segment encoding the UL6 NH_2-terminal region was subcloned into the Bam HI–Eco RI sites of pBluescript(K S) (Stratagene) to produce the plasmid pZz. A single point mutation at position 15266 (C → T) of the UL6 gene was introduced with a site-directed mutagenesis kit (Clontech) and the mutant oligonucleotide 5′ GATTCTCCTACGGGTAGCTGGGGTATAC 3′ to generate a stop codon. This substitution was selected because it also eliminates the cleavage site for Pvu II (CAGCTG). The presence of the mutation in the pZz plasmid was confirmed by DNA sequencing with a Sequenase kit (U.S. Biochemical). For isolation of mutant virus, Vero cell monolayers (6×10^5 cells per 60-mm dish) were incubated for 24 hours after seeding and then transfected with 12 μg of DNA (including 0.5 μg of infectious KOS DNA, 5 μg of mutant plasmid DNA, and 6.5 μg of carrier DNA). Five days later, when generalized cytopathic effects were apparent, cultures were harvested and then frozen and thawed three times. The cell suspension was sonicated briefly, diluted 1:10 in medium, passed through a 0.22-μm filter, plated on monolayers of G33 cells—BHK21 cells expressing the UL6 protein [A. H. Patel *et al.*, *Virology* **217**, 111 (1996)]—and overlaid with methylcellulose. After incubation at 37°C for 4 days, plates were stained for 24 hours with medium containing neutral red. Individual plaques were picked, and isolates were screened for their ability to produce cytopathic effects in G33 cells but not in Vero cells. Isolates with this phenotype were plaque-purified three times.
15. Culture flasks (75 cm^2) were seeded at a density of 1×10^6 Vero cells per flask. Cells were infected with wild-type KOS or KOS/UL6^m mutant viruses at a multiplicity of infection of 10 PFU per cell. Uninfected and infected cells were harvested 18 to 20 hours after infection by scraping into the medium and were centrifuged at 1500 revolutions per minute and 4°C for 10 min. The cell pellet was resuspended in 5 ml of phosphate-buffered saline (PBS), repelleted, and resuspended again in 1 ml of PBS. The cell suspension was stored at −70°C overnight, thawed at 37°C, and sonicated for 1 min. Samples were pelleted at 4°C for 10 min, and the supernatant fluid was divided into aliquots and stored at −70°C. Protein concentrations were determined by measuring absorbance at 280 nm and using bovine serum albumin as a standard.
16. A. M. McCarthy, L. McMahon, P. A. Schaffer, *J. Virol.* **63**, 18 (1989).
17. W. Cai, S. Person, S. C. Warner, J. Zhou, N. A. DeLuca, *ibid.* **61**, 714 (1987).
18. J. W. Streilein, G. A. Wilbanks, S. W. Cousins, *J. Neuroimmunol.* **39**, 185 (1992).
19. Y. A. Akova, J. Dutt, A. Rodriguez, N. Jabbur, C. S. Foster, *Curr. Eye Res.* **12**, 1093 (1993); C. M. Maccadal, D. M. Bouley, D. DeStephano, B. T. Rouse, *J. Virol.* **67**, 3404 (1993).
20. M. von Herrath, J. Dockter, M. B. A. Oldstone, *Immunity* **1**, 231 (1994).
21. The antigen used for in vitro stimulation was prepared from extracts of Vero cells infected with HSV-1 (KOS) (0.01 PFU per cell) and harvested 3 days after infection [W. Cai and P. A. Schaffer, *J. Virol* **66**, 2904 (1992)]. The virus suspension was inactivated by UV light (254 nm) for 20 min at a distance of 5 cm [J. Morrison and D. Knipe, *J. Virol.* **68**, 689 (1994)]. Control antigen was prepared in the same way from extracts of uninfected cells.
22. E. M. Opremcak *et al.*, *Invest. Ophthalmol. Vis. Sci.* **29**, 749 (1988).

23. We would like to thank D. Knipe for providing pSG10, A. H. Patel for G33 cells, J. Glorioso for KO82 mutant virus, and A. Angel for assistance in preparation of the manuscript. Supported by NIH grant AI 37562 to H.C.

22 October 1997; accepted 7 January 1998

An Area Specialized for Spatial Working Memory in Human Frontal Cortex

Susan M. Courtney,* Laurent Petit, José Ma. Maisog, Leslie G. Ungerleider, James V. Haxby

Working memory is the process of maintaining an active representation of information so that it is available for use. In monkeys, a prefrontal cortical region important for spatial working memory lies in and around the principal sulcus, but in humans the location, and even the existence, of a region for spatial working memory is in dispute. By using functional magnetic resonance imaging in humans, an area in the superior frontal sulcus was identified that is specialized for spatial working memory. This area is located more superiorly and posteriorly in the human than in the monkey brain, which may explain why it was not recognized previously.

Studies of working memory in monkeys (*1*) and humans (*2–7*) have emphasized the important role of the prefrontal cortex. Physiological evidence for this role comes from studies demonstrating sustained activity in prefrontal cortex during working memory delays (*1*, 6–8). In monkeys, the dorsolateral prefrontal cortex within and surrounding the principal sulcus appears to be involved primarily in working memory for spatial locations, whereas the region ventral to it on the inferior convexity appears to be more involved in working memory for patterns, colors, objects, and faces (*1*, 9). The prefrontal region for spatial working memory in monkeys is located just anterior to a region for the control of eye movements, the frontal eye field (FEF), which is on the anterior bank of the arcuate sulcus (*10*).

Most functional brain imaging studies of spatial working memory in humans have focused on the dorsolateral frontal region defined by Brodmann as area 46 (*5*, *11*, *12*), because the spatial working memory region in monkeys lies within that area (*13*). While performance of spatial working memory tasks activates Brodmann area (BA) 46 (*5*, *11*, *12*), performance of working memory tasks involving other types of information, such as verbal and visual object information, does so as well [for example, see (*3*, *6*, *7*, *12*, *14*, *15*)]. Therefore, the existence of a prefrontal cortical area in humans that is specialized for spatial working memory has been questioned [for example, see (*16*)].

Here we provide evidence that a human frontal area specialized for spatial working

Laboratory of Brain and Cognition, National Institute of Mental Health, Building 10, Room 4C104, 10 Center Drive, Bethesda, MD 20892-1366, USA.

*To whom correspondence should be addressed. E-mail: Susan_Courtney@nih.gov

Cell, Vol. 80, 695–705, March 10, 1995, Copyright © 1995 by Cell Press

Molecular Mimicry in T Cell-Mediated Autoimmunity: Viral Peptides Activate Human T Cell Clones Specific for Myelin Basic Protein

Kai W. Wucherpfennig and Jack L. Strominger
Department of Molecular and Cellular Biology
Harvard University
Cambridge, Massachusetts 02138

Summary

Structural similarity between viral T cell epitopes and self-peptides could lead to the induction of an autoaggressive T cell response. Based on the structural requirements for both MHC class II binding and TCR recognition of an immunodominant myelin basic protein (MBP) peptide, criteria for a data base search were developed in which the degeneracy of amino acid side chains required for MHC class II binding and the conservation of those required for T cell activation were considered. A panel of 129 peptides that matched the molecular mimicry motif was tested on seven MBP-specific T cell clones from multiple sclerosis patients. Seven viral and one bacterial peptide efficiently activated three of these clones. Only one peptide could have been identified as a molecular mimic by sequence alignment. The observation that a single T cell receptor can recognize quite distinct but structurally related peptides from multiple pathogens has important implications for understanding the pathogenesis of autoimmunity.

Introduction

Activation of autoreactive T cells is a critical event in the induction of autoimmunity. In animal models of T cell–mediated autoimmunity, disease can be transferred only with activated but not with resting T cells specific for a central nervous system (CNS)-specific autoantigen (reviewed by Zamvil and Steinman, 1990). Resting autoreactive T cells are part of the normal immune repertoire and do not induce disease as the blood–brain barrier limits access to the CNS to activated T cells (Schluesener and Wekerle, 1985; Burns et al., 1983; Ota et al., 1990; Martin et al., 1990; Pette et al., 1990). This protective mechanism makes circulating self-reactive T cells "ignorant" of the complex set of tissue-specific self-antigens hidden behind the blood–brain barrier. Invasion of the CNS requires autoreactive T cells to be activated in the peripheral immune system. This activation occurs in the absence of their nominal self-antigen, which is sequestered in the CNS (Wekerle et al., 1986; Hickey et al., 1991). Two mechanisms could account for the activation and clonal expansion of autoreactive T cells in the periphery: activation by bacterial or viral superantigens that trigger T cells bearing particular T cell receptor Vβ segments (Brocke et al., 1993; Cole and Griffiths, 1993; Conrad et al., 1994), or activation by viral or bacterial peptides that have sufficient sequence similarity with an immunodominant self-peptide (molecular mimicry) (Oldstone, 1990).

A large body of clinical and epidemiological evidence indicates that infections are important in the induction of autoimmunity. Particular viral infections frequently precede autoimmune myocarditis and type I diabetes (IDDM) (Rose et al., 1986; Ray et al., 1980). Also, an inflammatory CNS disease can follow infection with a number of common viral pathogens, such as measles and rubella. The absence of virus in the CNS and reactivity to myelin basic protein (MBP) in these patients suggest an autoimmune mechanism (Johnson et al., 1984). Environmental agents also influence the risk of developing multiple sclerosis (MS) as demonstrated by migration studies. Individuals that migrate after age 15 carry the risk for developing MS associated with their geographic origin, while individuals who migrate earlier in life acquire the risk of the geographical region to which they migrated (Kurtzke, 1985). These studies are consistent with the hypothesis that a group of pathogens that are relatively ubiquitous in a certain geographic region influence the risk of developing MS.

Recent immunological studies suggest that MBP may be one of the important target antigens in the immunopathogenesis of MS. Several studies have demonstrated that MBP-specific T cells are clonally expanded in MS patients and in an in vivo activated state (Allegretta et al., 1990; Wucherpfennig et al., 1994b; Zhang et al., 1994). Reactivity with the immunodominant MBP(84–102) peptide is found predominantly in subjects carrying HLA-DR2, a genetic marker for susceptibility to MS. The MBP(84–102) epitope can also be presented by other major histocompatibility complex (MHC) class II antigens, including HLA-DQ1 (Ota et al., 1990; Martin et al., 1990; Pette et al., 1990; Wucherpfennig et al., 1994a). In vivo, the T cell response to this peptide appears to be dominated by a few expanded clones. The mechanism(s) leading to clonal expansion of MBP-reactive T cells remains to be identified, but could involve recognition of viral peptides with sufficient structural similarity to the immunodominant MBP peptide. Viruses that cause latent and/or persistent infections (such as the herpes simplex and Epstein–Barr viruses) would be particularly interesting candidates, as they may permit chronic antigenic stimulation of these autoreactive T cell clones. The initiation of autoimmunity by such a mechanism could then lead to sensitization to other CNS self-antigens by determinant spreading (Lehmann et al., 1992; Kaufman et al., 1993; Tisch et al., 1993).

Structural characterization of the immunodominant MBP(85–99) peptide identified residues critical for MHC class II binding and for T cell receptor (TCR) recognition (Wucherpfennig et al., 1994a). The MHC class II and TCR contact residues of the immunodominant MBP(85–99) peptide were then subjected to mutational analysis in order to define the set of amino acids permitted at each critical position. These structural criteria, together with the knowledge that amino acid side chains required for binding to MHC molecules are degenerate, were used to search a protein sequence data base. Selected viral and bacterial peptides were tested for their ability to activate

human MBP(85–99)-specific T cell clones that had been established from blood T cells of MS patients. Of 129 peptides synthesized, seven viral peptides and one bacterial peptide that met the criteria were found to efficiently stimulate MBP-specific T cell clones. These viral and bacterial peptides therefore act as molecular mimics of the immunodominant MBP(85–99) peptide. Molecular mimicry of this immunodominant self-peptide by viruses therefore presents a possible mechanism for the induction of autoimmunity in MS.

Results

Structural Characterization of the Immunodominant T Cell Epitope of Human MBP

Susceptibility to MS is associated with HLA-DR2 (DRA, DRB1*1501, the most common subtype of DR2) (Spielman and Nathenson, 1982; Olerup et al., 1989). This MHC class II molecule may play a critical role in the immunopathogenesis of MS by presenting immunodominant self-peptides to autoreactive T cells. Following injection of MBP in experimental animals, T cells specific for immunodominant peptides of MBP mediate an inflammatory response in the CNS that can be accompanied by marked demyelination (reviewed by Zamvil and Steinman, 1990). In previous studies, two regions of human MBP were found to be immunodominant (residues 84–102 and 143–168) (Ota et al., 1990; Pette et al., 1990; Martin et al., 1990; Wucherpfennig et al., 1994a). Reactivity to the MBP(84–102) peptide was predominantly seen in subjects carrying HLA-DR2. Using L cell transfectants as antigen-presenting cells, HLA-DR2b (DRA, DRB1*1501) was found to serve as the restriction element for these MBP(84–102)-specific T cell clones. The MBP(84–102) peptide bound with high affinity to the HLA-DR2b molecule with two hydrophobic residues serving as the primary anchors (Val-89 and Phe-92 in the MBP(85–99) peptide) (Figure 1) (Wucherpfennig et al., 1994a; Vogt et al., 1994). At the first anchor position, Val-89 could be substituted by other aliphatic amino acids (leucine and isoleucine), as well as by methionine and phenylalanine; alanine was tolerated at this position but reduced the affinity of the peptide for HLA-DR2b. At the second anchor position, all aliphatic and aromatic residues were permitted; again alanine was tolerated but resulted in a loss of binding affinity.

A mutational analysis of putative TCR contact points demonstrated that Phe-91 and Lys-93 were the primary TCR contacts for the MBP(85–99)-specific clones; other residues such as Val-88 and His-90 were important for some clones but not for others. Substitution of Phe-91 by alanine abolished TCR recognition for all clones; some clones tolerated conservative substitutions (e.g., tyrosine or aliphatic amino acids) while other clones did not. Substitution of Lys-93 by arginine was tolerated by most T cell clones, but more drastic changes frequently resulted in a partial or complete loss of T cell reactivity. This analysis demonstrated that His-90, Phe-91, and Lys-93 were the primary TCR contact residues, while Val-89 and Phe-92 were the primary MHC contact residues (Figure 1).

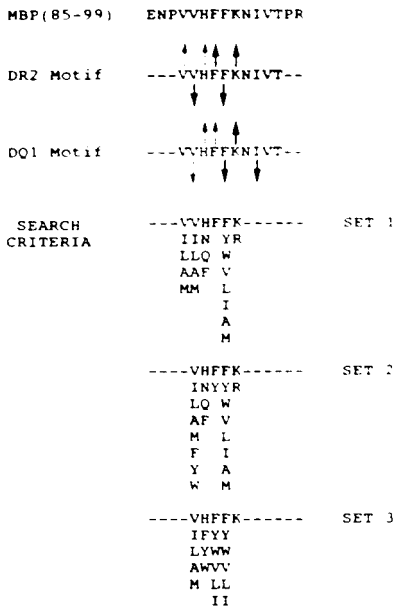

Figure 1. Peptide Motifs Required for MHC Class II Binding and TCR Recognition of the Immunodominant MBP(85–99) Peptide

The MBP(88–97) segment is critical for MHC class II binding and TCR recognition by HLA-DR2- and HLA-DQ1-restricted clones. Peptide residues His-90, Phe-91, and Lys 93 appear to be critical TCR contacts for both sets of clones; hydrophobic amino acids are important for anchoring the peptide to the MHC class II molecules. Based on the recognition motifs and a detailed mutational analysis, molecular mimicry motifs were defined for searching a protein data base for viral and bacterial sequences that fit these criteria. The different sets represent search criteria for different sets of clones with different preferences at TCR contact points (Val-88, His-90, Phe-91, and Lys-93). Hydrophobic amino acids (aliphatic and/or aromatic) were specified for the two major MHC anchor residues (Val-89 and Phe-92). The following number of peptides were synthesized for each set: set 1, 24 peptides; set 2, 46 peptides; set 3, 59 peptides. Random peptide sequences would be expected to match the motifs at the following frequencies: set 1, 1:40,000; set 2, 1:27,750; set 3, 1:3692 sequences

Can Structural Motifs Be Used to Identify Viral Peptides That Activate MBP-Specific T Cells?

Based on this structural characterization of the immunodominant MBP(85–99) peptide, a set of structural criteria (i.e., a molecular mimicry motif) was developed to search a protein data base for viral and bacterial peptides that matched these requirements. These search criteria focused on the core region of the peptide, residues 88–93, which contained the MHC and TCR contacts common to all clones. In the first set, aliphatic amino acids were allowed at the first MHC anchor residue (Val-89); aliphatic and aromatic residues were permitted at the second MHC anchor (Phe-92). For the TCR contacts, Phe-91 was absolutely conserved, Lys-93 could only be substituted by arginine, while His-90 and Val-88 could be substituted by several structurally related amino acids (Figure 1).

The second set of criteria omitted Val-88 as a TCR contact residue (used only by some clones) and also permitted aromatic amino acids at the first MHC anchor (Val-89).

This was done since the MBP(85–99) peptide is presented by different HLA-DR2 subtypes: presentation by DRB1*1501 requires an aliphatic amino acid or phenylalanine at this position, while aliphatic and all aromatic residues at this position can serve as anchor for DRB1*1602 (K. W. W. and J. L. S., unpublished data). This difference relates to the size of the primary pocket binding this hydrophobic residue and is determined by the Val/Gly dimorphism at DRβ86 (Val in *1501 and Gly in *1602) (Busch et al., 1991; Brown et al., 1993).

The third set represented a modification of the TCR contact residues preferred by a subgroup of MBP(85–99)-specific clones. For these clones, Lys-93 was absolutely conserved while Phe-91 could be substituted by some aromatic or aliphatic amino acids (Figure 1).

These search criteria also matched well with the structural requirements for a HLA-DQ1-restricted clone specific for the MBP(85–99) peptide. This clone required the same minimal peptide segment as DR2-restricted clones (residues 87–97). As in the DR2-restricted clones, His-90, Phe-91, and Lys-93 appeared to be the primary TCR contact residues (unpublished data). Based on pool sequencing of naturally processed peptides bound to HLA-DQ1, three hydrophobic positions (at position 1, 4, and 7 relative to the first anchor; Val-89, Phe-92, and Ile 95 in the MBP(85–99) peptide) are thought to contribute to binding (K. Falk and O. Rötschke, submitted). Substitution of these hydrophobic positions by aspartic acid greatly diminished the stimulatory capacity of the peptide, while substitutions by other hydrophobic amino acids were tolerated. These data suggest that the MBP(85–99) peptide is bound in a similar fashion to HLA-DR2b and HLA-DQ1 and that the same peptide residues are critical for interaction with the TCR.

These complex criteria were used to search protein data bases (PIR and SwissProt) using the Genetics Computer Group software (program: findpatterns). More than 600 sequences of viral and bacterial origin were identified that matched these criteria. From this pool, sequences were selected based on the following criteria: one, viruses known to cause human pathology; two, viruses prevalent in the Northern Hemisphere where MS occurs most frequently; three, selected bacterial sequences associated with inflammatory CNS disease (such as Borrelia burgdorferi) and with invasive infections (such as Staphylococcus aureus, Klebsiella pneumoniae, and Pseudomonas aeruginosa). Not included were most viruses that cause infections in tropical countries, sequences derived from vaccinia virus as well as a large number of sequences from Escherichia coli, which is part of the normal intestinal flora. When multiple antigenic variants were present, one or several sequences that best fit the search criteria were chosen. The selected peptides were synthesized by Pin-Technology on a 1 mg scale (Chiron Mimotopes, San Diego); 70 peptides were made for criteria sets 1 and 2 (Figure 1) and 59 peptides for set 3.

Activation of Human MBP(85–99)-Specific T Cell Clones by Viral Mimicry Peptides

Peptides were tested for their ability to activate human MBP(85–99)-specific T cell clones that had been previously established from blood T cells of two patients with relapsing–remitting MS (Wucherpfennig et al., 1994a, 1994b). As previously, homozygous B cell lines that expressed DR2 (DRB1*1501 or DRB1*1602) or DQ1 were used as antigen-presenting cells in these T cell proliferation experiments (Wucherpfennig et al., 1994a). Seven clones were tested with the 70 viral/bacterial peptides from sets 1 and 2. As expected, all clones were activated by the MBP(85–99) peptide that served as the positive control.

Interestingly, three of the seven clones tested were also efficiently activated by several viral/bacterial peptides (Tables 1 and 2, data for five clones are shown). The first clone (Hy.1B11) recognized the MBP(85–99) peptide on HLA-DQ1; clones Hy.2E11 and Hy.1G11 were HLA-DR2 restricted (Wucherpfennig et al., 1994a). Among the first 70 peptides tested, three mimicry peptides stimulated the DQ1-restricted clone; two mimicry peptides from Epstein–Barr virus (EBV) and influenza type A virus stimulated two of the DR2-restricted T cell clones (Table 1). Among the second group of peptides (set 3, 59 peptides), one mimicry peptide from human papillomavirus was identified for the DQ1-restricted clone, while a reovirus peptide and a herpes simplex virus peptide were identified for the DR2-restricted clones (Hy.2E11 and Hy.1G11, respectively) (Table 2; data not shown). This second group of peptides has not yet been tested with the other DR2-restricted clones.

Taken together, the DQ1-restricted T cell clone recognized five structurally related peptides: the immunodominant MBP(85–99) peptide, three viral peptides (from herpes simplex, adenovirus type 12, and human papillomavirus) and a bacterial peptide (Pseudomonas aeruginosa). Two of the DR2-restricted clones were activated by four peptides. Both clones recognized the MBP(85–99) peptide as well as mimicry peptides from EBV and influenza virus. In addition, each clone recognized a viral peptide from reovirus (T cell clone Hy.2E11) and herpes simplex virus (clone Hy.1G11) (Table 2).

Efficient T Cell Stimulation by Mimicry Peptides

If viral/bacterial mimicry peptides are indeed important for the initiation of autoimmunity, they have to be capable of potent T cell stimulation that results in marked clonal expansion of autoaggressive T cell clones. The stimulatory capacity of the mimicry peptides was therefore compared with the MBP(85–99) peptide in a titration experiment (Figure 2). The peptides were found to be efficient stimulators of these MBP-specific T cell clones; in particular, the EBV peptide (DR2-restricted clones) and the adenovirus peptide (DQ1-restricted clone) were similar to the MBP(85–99) peptide in their stimulatory capacity. These results demonstrate that T cell mimicry is not the result of a minor degree of "cross-reactivity" but rather the result of structural similarity sufficient for potent T cell activation.

The efficient stimulation of MBP(85–99)-specific T cell clones by these peptides also argues against the presence of a small contaminating T cell population that responds to these peptides. To ensure that the peptides were indeed seen by a single T cell clone, both T cell clones were

Table 1. Screening of Five MBP (85–99)-Specific T Cell Clones for Reactivity to a Panel of Viral/Bacterial Mimicry Peptides

Peptide	Sequence	Source	Hy.1B11	Ob.1A12	Ob.1C3	Hy.2E11	Hy.1G11
None			6,090	420	452	1,471	200
2	ENPVVHFFKNIVTPR	**MBP(85–99)**	**80,102**	**32,631**	**21,171**	**70,350**	**8,859**
3	GMSLIHFLKGCIISY	Human papillomavirus	4,751	821	769	897	234
4	SGFALHFFRLLPTAS	Epstein–Barr virus	3,850	412	391	772	160
5	FRQLVHFVRDFAQLL	**Herpes simplex virus**	**20,164**	426	402	981	157
6	YQTIIHFARTLNRMY	Parainfluenza virus type 2	4,689	393	443	531	178
7	WRGIVHFLRYQGQEF	Human papillomavirus	4,344	529	436	621	197
8	SCTAAHFIKRFIKDG	Rickettsia prowazekii	5,443	547	438	2,502	219
9	TQRLAHFYRRWTGAK	Yersinia pseudotuberculosis	4,902	414	442	924	143
10	IVVILFFFKIPQRLR	Cytomegalovirus	3,712	444	490	963	175
11	YVVLVQFVKHVALFS	Cytomegalovirus	3,158	441	460	815	201
12	KSLVLNFAKNEELNN	Staphylococcus aureus	3,086	407	449	919	204
13	NSNAINFLKTWAKN	Borellia burgdorferi	3,684	444	442	605	199
14	TRPAAQFVKEAKGFT	Klebsiella pneumoniae	2,912	419	454	797	221
15	YEAMAQFFRGELRAR	Herpes simplex	4,626	430	400	1,058	193
16	SPGLVQFARATDTYF	Adenovirus type 40 and 41	4,987	474	509	1,235	213
17	ACIVLFFARRAFNKK	Human cytomegalovirus	7,969	376	412	959	171
18	ILGLLNFARNFIPNF	Human spuma retrovirus	5,259	415	430	936	144
19	VVALVNFLRHLTQKP	Human cytomegalovirus	6,103	401	408	926	154
20	PVHLLNFARLDLIKQ	Varizella–Zoster virus	5,620	340	437	858	163
21	FRDLLNFIRQRLCCE	Human cytomegalovirus	2,619	426	510	967	144
22	DLRVLNFIRGTKVIP	Influenza A virus	3,517	486	451	741	191
23	TVDVANFLRAYSWSD	Marburg virus	3,660	434	427	1,045	175
24	LQKALNFVRMGDRFI	Staphylococcus aureus	4,868	354	344	977	213
25	TLLLIFFYRFMRPLI	Staphylococcus aureus	3,884	420	455	834	200
26	HELLANFLRQQGGVR	Pseudomonas aeruginosa	3,738	388	442	987	195
27	SDDFIHFFKAKSYDD	Dhori virus	3,373	431	459	879	651
28	LVDEAHFIKKEAFNT	Human cytomegalovirus	3,553	425	429	2,306	208
29	TGGVYHFVKKHVHES	**Epstein-Barr virus**	3,667	503	435	**96,613**	**8,915**
30	EACNAHFWRDLQGEA	Herpes simplex virus	3,517	494	446	1,214	224
31	IGSQVHFYRDLSSIN	Human papillomavirus	2,562	398	456	1,172	207
32	EQVLFHFARKNGVMR	Human papillomavirus	5,127	510	421	1,115	189
33	PLGRIHFFRRGFWTL	Human cytomegalovirus	6,459	231	417	973	122
34	ISIFLHFVRIPTHRH	LCMV	8,921	342	341	944	162
35	NGQYIHFYREPTDIK	LCMV	4,408	371	401	948	209
36	SGCYVHFFREPTDLK	Lassa virus	4,687	359	388	1,094	175
37	QESYAHFIRDSVGLP	Adenovirus type 7	4,307	415	399	957	245
38	SKYLYHYLRTLALGT	HTLV-I	4,404	326	468	1,049	159
39	NFEDWHYAKFGFTPL	Human corona virus	4,809	434	367	944	184
40	LAYSLNFLKVIQQIL	Measles virus	5,383	443	393	936	223
41	DFEVVTFLKDVLPEF	**Adenovirus type 12**	**57,504**	393	445	1,148	194

(continued)

recloned by limiting dilution. The subclones had the same specificity for MBP(85–99) and for the viral peptides as the parental T cell clones. Two subclones were obtained for Hy.1B11 (DQ1 restriction); these reacted with the MBP(85–99) peptide as well as with the herpesvirus, adenovirus, and Pseudomonas peptides (the papillomavirus peptide from the second synthesis was not tested on the subclones). One subclone was obtained for Hy.2E11 (DR2 restriction); this clone reacted with MBP(85–99) as well as with the EBV and the influenza peptides as did the parental clone (the reovirus peptide from the second synthesis was not tested). In addition, previous polymerase chain reaction (PCR) analysis of these T cell clones using a panel of TCR Vα and Vβ family-specific primers had indicated that they represented clonal populations (Wucherpfennig et al., 1994b). Surface staining of clone Hy.1G11 with a monoclonal antibody specific for the Vβ17.1 segment (MAb C1, Friedman et al., 1991) showed that all cells expressed the Vβ17.1 segment, proving that it represented a clonal population.

Mimicry Peptides Have Conserved Features but Are Quite Distinct from the MBP Peptide

Comparison of peptide sequences that stimulate the same TCR revealed several interesting points. First, only one peptide (from human papillomavirus L2 protein) had striking sequence similarity with the MBP(85–99) peptide, in that all amino acids in the MBP(89–95) segment except position 94 (asparagine to aspartic acid) were identical (Table 2). For all other sequences, simple alignment would not have predicted them to be efficient stimulators of MBP(85–99)-specific T cell clones. Second, at positions not specified by the search criteria, the selection for particular amino acids was apparent (Table 2). For example, for the DQ1-restricted clone, aspartic acid was selected at position 94 (probably a TCR contact) in all four mimicry peptides. This position is occupied by asparagine in the MBP peptide (similar size, but no negative charge). Substitution of Asn-94 for aspartic acid in the MBP peptide markedly increased its stimulatory capacity for the DQ1-restricted clone but reduced it for the DR2-restricted clone. Selection also oc-

Table 1. (*continued*)

Peptide	Sequence	Source	Hy.1B11	Ob.1A12	Ob.1C3	Hy.2E11	Hy 1G11
42	RTLVLAFVKTCAVLA	Adenovirus type 2	3,756	405	400	962	156
43	TLMVIPFVKLDYADT	Coxsackie A9 virus	3,411	427	451	744	188
44	VEGVATFLKNPFGAF	Human cytomegalovirus	3,137	426	458	786	148
45	VGGVVSFLKNPFGGG	Human herpes virus 6	3,710	338	469	774	193
46	DSHLICFYKRGEGLS	Human cytomegalovirus	3,936	371	416	921	203
47	VLNLLEFLKDWSGHL	Epstein–Barr virus	3,913	371	410	1,055	201
48	INTVLCFVKSGILLY	Hepatitis A virus	4,472	374	430	1,088	197
49	GFIAALFYKHGFNSS	Hepatitis C virus	4,180	397	418	1,332	168
50	GFLAALFYKHKFNAS	Hepatitis C virus	3,581	360	468	987	202
51	YRNLVWFVKKGNSYP	Influenza A virus	3,628	371	399	567	183
52	YRNLVWFIKKNTRYP	**Influenza type A virus**	3,911	368	420	**45,094**	**5,885**
53	DLRVLSFIKGTKVVP	Influenza A virus	4,315	406	414	438	214
54	SGRLIDFLKDVIESM	Influenza A virus	3,982	380	488	720	205
55	GEILIDFFKKGNLSA	Influenza C virus	4,908	355	425	884	161
56	VLALITFFKFTALAP	Japanese encephalitis virus	11,189	329	415	1,128	159
57	ILQVLSFFKGTIING	Newcastle disease virus	3,895	389	392	1,121	195
58	CAAMVRFYKRGQMRE	Human papillomavirus	3,428	365	410	587	161
59	NSNAAAFLKSNSQAK	Human papillomavirus	3,698	433	476	665	189
60	TLDILVFLKTFGGLL	Parainfluenza virus type 3	4,138	399	499	708	206
61	DLPMVTFLKDELRKK	Rhinovirus type 89	4,375	365	426	453	211
62	PKAAALFAKTYNLVP	Sindbis virus	4,156	404	443	571	200
63	DTKLAGFLKHYNSVW	Rotavirus	4,185	398	376	775	169
64	FVIVLPFIKAQNYGI	Rotavirus	4,350	399	468	1,015	212
65	YARVIDFAKFREIAD	Campylobacter jejuni	2,769	379	447	1,034	181
66	EQFKAHYFRNVTKGE	Hemophilus influenza	2,961	312	392	828	132
67	PRAAAAFVKFNCAAL	Klebsiella	5,096	355	364	631	134
68	ERFLARFVKDYGRPA	Pseudomonas aeruginosa	4,894	350	374	899	143
69	APGAILFAKAKHEVG	Pseudomonas aeruginosa	3,965	390	305	983	163
70	DRLLMLFAKDVVSRN	**Pseudomonas aeruginosa**	**32,872**	311	373	887	169
71	NQEAAGFIKHFEQLL	Staphylococcus aureus	3,830	345	413	956	202
72	EEKLLAFAKADKTYS	Streptococcus pneumoniae	4,916	325	445	1,061	191

The MBP(85–99) peptide (peptide 2) was used as a positive control; mimicry peptides 3–26 were from peptide set 1, mimicry peptide 27–72 from peptide set 2. T cell clone Hy.1B11 is HLA-DQ1 restricted, clones Ob.1A12, Ob.1C3, Hy.2E11, and Hy.1G11 are HLA-DR2 restricted. Irradiated homozygous B cell lines were used as antigen-presenting cells: 9001 (DQ1) for clone Hy.1B11; MGAR (DR2 [DRB1*1501]) for clones Ob.1A12, Ob.1C3, Hy6.2E11, and Hy.1G11. B cells were pulsed with peptides for 2 hr at a concentration of approximately 60 μg/ml (clones Hy.1B11, Ob.1A12, and Hy.1G11) and at approximately 12.5 μg/ml for clones Ob.1C3 and Hy.2E11. After the 2 hr pulse, T cells were added (50×10^3/well; final peptide concentrations: 12.5 μg/ml and 3.1 μg/ml, respectively). Numbers represent incorporation of [^{3}H]thymidine that was determined after a 3 day culture period. Two other T cell clones (Hy.2B6 and Ob.3D1) were also tested and responded only to the MBP(85–99) peptide (data not shown).

curred at the neighboring MHC contact (Ile-95) for which isoleucine, valine, or phenylalanine were selected (all hydrophobic). Third, different selection events occurred for the DQ1- and the DR2-restricted clones: at position 94 (selection of aspartic acid [negative charge] for DQ1 peptides), a positive charge (lysine) was selected in two of the three mimicry peptides presented by DR2. Fourth, in the flanking segments (residues 85–87 and 97–99), no apparent selection took place as amino acids with different size and charge were allowed.

The majority of the viruses are common human pathogens: influenza type A frequently causes respiratory tract infections; human papillomavirus infects epithelial tissues and has been linked to cervical carcinomas; EBV causes an acute viral syndrome (infectious mononucleosis) in young adults. Human herpesvirus I (herpes simplex), EBV, and human papillomavirus cause latent/persistent infections; the respective reservoirs are neurons (herpes simplex), B cells (EBV), and epithelial cells (papillomavirus). Virus expression can be reactivated by UV exposure and stress (herpes simplex) and by B cell activation (EBV) (Schwarz et al., 1985; Epstein and Achong, 1977; Spruance, 1985; Tovey et al., 1978). For the induction and maintenance of an autoimmune response, these persistent viral infections are of particular interest as they could explain the chronicity of the clinical disease and the clonal expansion and persistence of MBP-specific T cells. Reactivation of viral expression may also be involved in triggering clinical relapses. By this mechanism, viral mimicry peptides could activate resting MBP-specific T cells in periphery and allow them to invade the CNS (Figure 4).

Presentation of a Naturally Processed Viral Mimicry Peptide

Are these mimicry epitopes actually presented to autoreactive T cells during a viral infection? The mimicry peptide from the EBV DNA polymerase allowed this question to be addressed. In EBV-transformed B cells (which were used as antigen-presenting cells in the T cell assays), the lytic viral cycle is repressed. The DNA polymerase gene

Table 2. Sequence Alignment of Viral/Bacterial Mimicry Peptides That Stimulate MBP-Specific T Cell Clones That Are DQ1 or DR2 Restricted

	85 90 94 99
Peptides Recognized by Clone Hy.1B11 (DO1 Restricted)	
MBP(85–99)	ENPVVHFFKNIVTPR
Herpes simplex, UL15 protein	FRQLVHFVRDFAQLL
Adenovirus type 12, ORF	DFEVVTFLKDVLPEF
Pseudomonas, phosphomannomutase	DRLLMLFAKDVVSRN
Human papillomavirus type 7, L2 protein	IGGRVHFFKDISPIA
Peptides Recognized by Clone Hy.2E11 (DR2 Restricted)	
MBP(85–99)	ENPVVHFFKNIVTPR
EBV, DNA polymerase	TGGVYHFVKKHVHES
Influenza type A, hemagglutinin	YRNLVWFIKKNTRYP
Reovirus type 3, sigma 2 protein	MARAAFLFKTVGFGG
Peptides Recognized by Clone Hy.1G11 (DR2 Restricted)	
MBP(85–99)	ENPVVHFFKNIVTPR
EBV, DNA polymerase	TGGVYHFVKKHVHES
Influenza type A, hemagglutinin	YRNLVWFIKKNTRYP
Herpes simplex, DNA polymerase	GGRRLFFVKAHVRES

Only the human papillomavirus peptide has obvious sequence similarity with the MBP(85–99) peptide (residues identical in the 89–95 segment are underlined). All mimicry peptides that stimulate the DQ1-restricted clones have aspartic acid (D) at position 94 (a putative TCR contact); hydrophobic residues were selected at position 95 (a putative MHC contact). In contrast, two of three mimicry peptides for the DR2-restricted clones have a positive charge (lysine) at position 94.

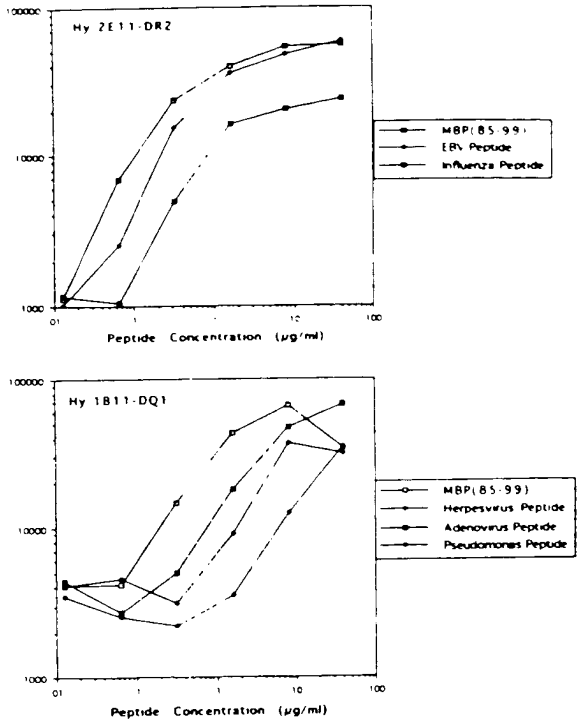

Figure 2. Efficient Stimulation of MBP(85–99)-Specific Clones by Mimicry Peptides

Peptides were compared with the MBP(85–99) peptide in a titration experiment. The top panel shows the DR2-restricted clone (Hy.2E11) with MGAR (DRB1*1501) as antigen-presenting cells, while the bottom panel shows the DQ1-restricted clone (Hy.1B11) with 9001 (DQ1) as antigen-presenting cells. B cells were pulsed with peptides for 2 hr, washed, and cocultured with T cells for 3 days. Numbers represent cpm of incorporated [^{3}H]thymidine as a measure of T cell proliferation.

is not transcribed in this latent state; however, B cell activation results in activation of the lytic cycle and in the expression of the DNA polymerase gene (Datta et al., 1980). To examine MHC class II–restricted presentation of the EBV DNA polymerase, an HLA-DR2$^+$ EBV-transformed B cell line (MGAR) and an MHC-mismatched control (9001, HLA-DR1) were pretreated for 36 hr with phorbol ester, which was removed by extensive washing prior to coculture of antigen-presenting cells with T cells. T cell clones Hy.2E11 and Hy.1G11, which recognize the EBV DNA polymerase peptide presented by HLA-DR2, were activated by a HLA-DR2$^+$ EBV-transformed B cell line pretreated with phorbol ester. This effect was specific because MHC-mismatched B cells did not activate the clones; also, a control clone (Ob.1A12) that recognized MBP(85–99) but not the EBV peptide was not activated (Figure 3). In a separate experiment, T cell activation was blocked by a MAb specific for HLA-DR (MAb L243) but not by a MAb specific for HLA-DQ (G2a.5). These results demonstrate that the MBP-specific T cell clones recognize not only the viral peptide but also antigen-presenting cells infected with the virus. In vivo, this recognition event could lead to chronic antigenic stimulation of MBP-specific T cells as B cell activation results in the reexpression of EBV genes, including the DNA polymerase gene.

Viral Variants Differ in Their Capacity to Activate MBP-Specific T Cell Clones

Two peptides from different strains of influenza type A matched the initial search criteria; only one of them was stimulatory for clone Hy.2E11. These two viral sequences were derived from the hemagglutinin subtype H13 (there are 13 serologically defined hemagglutinin subtypes of influenza type A) (Chambers et al., 1989). These hemagglutinin peptides differed at four positions: the first substitution was at position 92 (isoleucine for valine), which anchors the peptide to DR2; the other substitutions were at positions 95–97 (Table 3). Single amino acid substitutions demonstrated that the change at position 97 (arginine to serine) was responsible for the loss of reactivity (Table 3). This was surprising since threonine is present in the MBP peptide (which is structurally similar to serine) and since peptide position 97 was not subject to strong selection among the mimicry peptides (the stimulatory peptides have threonine, histidine, arginine, or phenylalanine at this position). Therefore, it is likely that this substitution affects the overall peptide conformation as described for MHC class I–bound peptides (Madden et al., 1993). These effects on the overall peptide conformation are probably responsible for the fact that the majority of viral peptides do not stimulate MBP(85–99)-specific clones.

The observation that certain viral strains are capable of stimulating MBP-specific T cells while other strains are

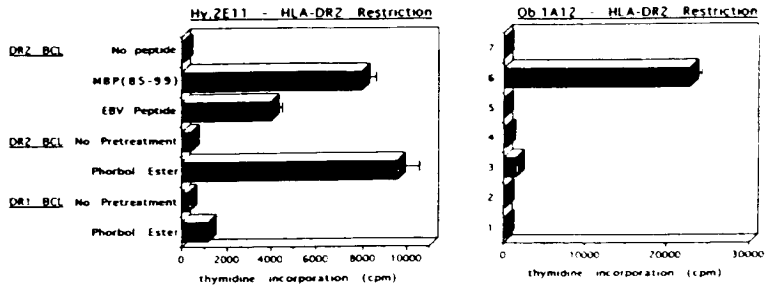

Figure 3. Recognition of the Naturally Processed EBV DNA Polymerase Peptide by MBP-Specific T Cells Following Reactivation of EBV Transcription in B Cells

The EBV lytic cycle is suppressed in EBV-transformed B cells; however, B cell activation results in reactivation of the lytic cycle and in transcription of the DNA polymerase gene. A HLA-DR2 B cell line (MGAR) and a MHC-mismatched control (9001, HLA-DR1) were pretreated with phorbol ester (PMA, 25 ng/ml for 36 hr), washed, and cocultured with MBP(85–99)-specific T cell clones. T cell clone Hy.2E11 recognized both the MBP(85–99) and the EBV DNA polymerase peptide; clone Ob.1A12 that recognized only MBP(85–99) in the context of HLA-DR2 served as a control. Clone Hy.2E11 was activated by phorbol ester–pretreated B cells that expressed HLA-DR2 but not by MHC-mismatched B cells. In a separate experiment, this effect could be blocked by a MAb specific for HLA-DR (L243) but not by a MAb specific for HLA-DQ (G2a.5). T cell clone Hy.1G11 that also recognized MBP(85–99) and the EBV DNA polymerase peptide were also activated by phorbol ester–pretreated, HLA-DR2$^+$ B cells (data not shown). T cell proliferation assays were performed as described in Table 4.

not may be important in defining the epidemiology of the disease. "Epidemic" outbreaks of MS have been noted (for example on the Faroe islands [Kurtzke and Hyllestad, 1979]) that may be related to particular viral strains that possess strongly cross-reactive T cell epitopes. These results also indicate that epidemiological studies will have to take viral subtypes and viral antigenic variation into account. Influenza viruses are among the interesting candidates as presentation of the influenza hemagglutinin (from which the mimicry peptide is derived) by MHC class II molecules is well documented (Brown et al., 1991).

MBP(85–99) and Its Viral Mimicry Peptides Are Efficiently Presented by the Disease-Associated DR2 Molecule

The presentation of the viral mimicry peptides by different DR2 subtypes was compared to determine whether they are efficiently presented by the disease-associated molecule (DRB1*1501, the most common DR2 subtype). The MBP peptide was presented by three of the four DR2 subtypes; the peptide was not presented by DRB1*1601, which differs from DRB1*1602 by a single amino acid substitution (at position DRβ67, a possible TCR contact). The two viral peptides were presented much better by the DR15 molecules (DRB1*1501 and 1502, which differ only at position DRβ86) than by DRB1*1602. This was particularly evident for the influenza peptide, which only activated the T cell clone when presented by the DRB1*1501/1502 molecules but not by DRB1*1602 (Table 4). These results indicate that the viral mimicry peptides identified here are more effectively presented by the MS-associated DR2 molecules (DRB1*1501/1502).

Discussion

This study establishes that some TCRs actually recognize not a single peptide but rather a limited repertoire of structurally related peptides derived from different antigens. This was true for three of the seven MBP(85–99)-specific T cell clones studied. One of these clones recognized five different peptides; the other clone recognized four peptides from different antigens. This recognition did not merely represent a minor degree of cross-reactivity, since these peptides efficiently activated the MBP(85–99)-specific clones. The other T cell clones were probably negative because the search criteria had focused only on the core region of the peptide (residues 88–93) that contained the most important MHC and TCR contact points common to all clones. Several clones for which no mimicry peptides were identified do, however, need a longer peptide segment than the positive clones (residues 85–97 versus residues 87–97). It is therefore likely that mimicry peptides could also be identified for these clones if all positions of the peptide were subjected to a detailed mutational analysis. As only a small fraction of the peptides that matched the criteria were synthesized, it is likely that many more peptides capable of activating MBP(85–99)-specific T cells could be identified.

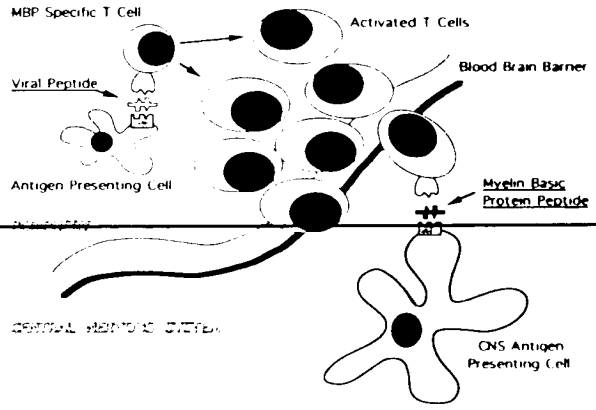

Figure 4. Proposed Mechanism for Activation of MBP-Specific T Cells in the Peripheral Immune System by Molecular Mimicry

Since only activated T cells can cross the blood–brain barrier, activation of T cells specific for CNS-specific antigens occurs in the peripheral immune system in the absence of the self-antigen. Viral peptides with sufficient structural similarity to the immunodominant MBP peptide activate these autoreactive T cells allowing them to undergo clonal expansion and CNS infiltration. Recognition of the MBP peptide in the CNS initiates the autoimmune destruction of myelin in the white matter (modified after Wucherpfennig et al., 1991).

Table 3. Antigenic Variation of Viral Epitopes Determines Capacity for T Cell Stimulation by Molecular Mimicry

MBP(85–99)	ENPVVHFFKNIVTPR
Influenza peptide 52 (Stimulatory)	YRNLVWFIKKNTRYP
Influenza peptide 51 (Nonstimulatory)	YRNLVWFVKKGNSYP
Point mutation position 92 (Ile to Val)	YRNLVWFVKKNTRYP
Point mutation position 95 (Asn to Gly)	YRNLVWFIKKGTRYP
Point mutation position 96 (Thr to Asn)	YRNLVWFIKKNNRYP
Point mutation position 97 (Arg to Ser)	YRNLVWFIKKNTSYP
	Hy.2E11
No Peptide	1,025
MBP(85–99)	**40,532**
Influenza peptide 52	**20,116**
Influenza peptide 51	805
Influenza peptide 52 (92 Val)	**16,070**
Influenza peptide 52 (95 Gly)	**13,998**
Influenza peptide 52 (96 Asn)	**14,604**
Influenza peptide 52 (97 Ser)	1,299

Two influenza type A hemagglutinin peptide sequences obtained from different viral isolates matched the search criteria; one of these sequences stimulated the DR2-restricted clone, the other peptide did not. Using single amino acid substitutions of the four positions different between these two peptides, the defective stimulation of peptide 51 was mapped to position 97 (Arg to Ser). These results indicate that antigenic variation of viruses can have a profound influence on molecular T cell mimicry. Numbers represent cpm of incorporated [^{3}H]thymidine as a measure ot T cell proliferation (mean of triplicates).

Table 4. Presentation of Viral Peptides by Subtypes of the Disease-Associated HLA-DR2 Molecule

Peptide	DRB*1501	DRB*1502	DRB*1601	DRB*1602
No peptide	310	1,064	360	423
MBP(85–99)	11,487	10,189	601	14,557
EBV peptide	12,005	11,277	521	3,389
Influenza peptide	6,266	10,079	456	412

B cell lines homozygous for different DR2 subtypes (DRB1*1501, 1502, 1601, and 1602) were compared for their ability to present viral mimicry peptides. B cell lines were pulsed with peptides at a concentration of 60 μg/ml for 2 hr, followed by washing to remove free peptide. Irradiated B cells (25 × 10^3) were cocultured with 50 × 10^3 T cells for 3 days. T cell proliferation was quantitated by [^{3}H]thymidine incorporation. Numbers represent cpm of incorporated [^{3}H]thymidine as a measure of T cell proliferation (mean of triplicates).

It was, however, surprising that the majority of peptides did not result in T cell activation. Most likely, amino acid substitutions at single positions have only limited predictive value as the simultaneous substitution of multiple neighboring positions may profoundly affect the peptide conformation. This has been elegantly demonstrated for MHC class I–bound peptides by comparing the crystal structures of HLA-A2 complexed with five different peptides (Madden et al., 1993). The effect of multiple simultaneous substitutions on peptide conformation makes peptides structurally more unique than appreciated by simple sequence comparison. The power and the novelty of the approach chosen in the present study is, however, demonstrated by the fact that the stimulatory mimicry peptides identified only have limited primary sequence similarity and would not have been predicted (with the exception of the papilloma virus peptide) based on simple alignments between MBP(85–99) and viral antigens. A better understanding of the structural consequences of multiple simultaneous substitutions on peptide conformation will certainly enhance the predictive power of this approach.

How specific is T cell recognition of MHC–peptide complexes? The molecular mimicry hypothesis postulates that there is significant cross-reactivity between viral T cell epitopes and human self-peptides. At first sight, TCR recognition appears to be exquisitely specific, since even minor substitutions in a T cell epitope can diminish or abrogate T cell activation (Reay et al., 1994). Several lines of evidence do, however, indicate that there is a significant degree of cross-reactivity. In shaping the TCR repertoire, two conflicting requirements have to be met. The first is comprehensive coverage of pathogen-derived epitopes by production of a large panel of specificities that can deal with the rapidly changing antigenic composition of pathogens. The second is elimination of TCRs that react with self-antigens that could initiate autoimmune responses. However, tolerance achieved by clonal deletion cannot be complete due to the complexity of self-antigens expressed in some organs, in particular the brain. The T cell receptor repertoire generated represents a compromise between these conflicting needs and allows a certain degree of self-reactivity in return for reasonably comprehensive coverage of foreign antigens.

Cross-reactivity is part of the positive selection process in the thymus that selects T cells with low affinity for self-MHC molecules (plus peptide) and deletes T cells with higher affinity for their ligand (Kappler et al., 1987; Kisielow et al., 1988; Sebzda et al., 1994). The relatively high frequency of alloreactive T cells also indicates that T cell recognition is not absolutely specific. Cytotoxic T cells specific for an EBV peptide bound to HLA-B8 were found to cross-react with HLA-B44 (Burrows et al., 1994). This alloreactivity is probably the result of molecular mimicry between the HLA-B8-bound EBV peptide and a HLA-B44-bound self-peptide that remains to be identified.

Molecular mimicry may also be an important mechanism in experimental autoimmune diseases. Immunization of Lewis rats with complete Freund's adjuvant induces a strong T cell response to a mycobacterial heat shock protein 65 (hsp65) peptide. Hsp65-reactive T cell clones mediate arthritis by cross-reacting with a joint proteoglycan (van Eden et al., 1985, 1988). While the cross-reacting joint peptide remains to be biochemically defined, molecular mimicry between hsp65 and a joint proteoglycan appears to be the underlying pathogenetic mechanism. Significant sequence similarity had also been noted between a T cell epitope of rabbit MBP and hepatitis B virus. Administration of this hepatitis B virus peptide was found to induce histological signs of CNS inflammation and T cell reactivity to MBP in a polyclonal population (Fujinami and Oldstone, 1985).

The diverse nature of the molecular mimicry peptides and the ubiquitous presence of some of these pathogens may make it difficult to establish a direct epidemiological

link between these viral infections and the occurrence of MS. In addition, the temporal relationship between a viral infection and the initiation of MS is not clear in most cases, as the clinical diagnosis is frequently made at a time when magnetic resonance scans demonstrate a relatively large number of old lesions (Stadt et al., 1990). It may, however, be possible to directly demonstrate the causal relationship in patients with postinfectious encephalomyelitis by establishing both virus-specific and MBP-specific T cell clones. The importance of molecular mimicry could also be demonstrated in MS patients with a recent viral infection (high IgM antibody titers to a particular virus) and magnetic resonance scans indicative of a recent onset of disease.

The diverse nature of the viral peptides that stimulate MBP(85–99)-specific T cell clones makes it unlikely that a single virus is responsible for initiating autoimmunity in MS. The observation that several pathogens carry mimicry epitopes of MBP(85–99) could explain why it has been so difficult to link the immunopathogenesis of MS to a single viral agent. Rather, it appears that a group of common viral pathogens, in particular the herpes virus family (EBV, herpes simplex, and cytomegalovirus), influenza viruses, and papillomaviruses could be involved in initiating the autoimmune process. This notion is supported by clinical and epidemiological data that suggest the involvement of several pathogens; the observation that oligoclonal immunoglobulins in the cerebrospinal fluid of MS patients are specific for several different viruses also points in this direction (Kurtzke, 1985; Baig et al., 1989). Childhood immunization against viral pathogens that carry mimicry T cell epitopes may reduce the risk of developing MS later in life. Genetic modifications of viral vaccines that eliminate proven mimicry epitopes could make viral vaccines safer and reduce the frequency of postvaccinal encephalomyelitis.

Experimental Procedures

Cell Lines

Homozygous EBV-transformed B cell lines used were the following: MGAR (DRB1*1501), 9011 (DRB1*1502), 9009 (DRB1*1601), 9016 (DRB1*1602), and 9001 (DQ1 [DQA1*0101, DQB1*0501]).

Peptide Synthesis

Mimicry peptides were synthesized on a 1 mg scale using the Multipin Peptide Synthesis System (Chiron Mimotopes). Peptides were synthesized on pins with a cyclic dipeptide (diketopiperazine, DKP) group attached to the C-terminus of the peptide that allowed cleavage in aqueous solution at a neutral or slightly basic pH. Peptide synthesis was monitored by including a standard peptide sequence as a control, which was subjected to HPLC and mass spectroscopy analysis. The immunodominant MBP(85–99) peptide was also included as a positive control for the T cell experiments.

Pin peptides were lyophilized and resuspended at a concentration of 2 mg/ml in 40% acetonitrile, 100 mM HEPES (pH 7.4). These conditions allowed the majority of peptides to be completely solubilized. Preliminary experiments had indicated that adding acetonitrile to a final concentration of 2% or less had no detrimental effect on the degree of T cell stimulation observed in the proliferation assay.

Viral and bacterial peptides that stimulated MBP(85–99)-specific clones were resynthesized by conventional methods (free C-terminus instead of the DKP group); the identity of peptides was further confirmed by mass spectroscopy (using a API III Sciex Ionspray Spectrometer) and by amino acid analysis.

Cloning of MBP(84–102)-Specific T Cells

Previously established MBP-specific T cell clones specific for the immunodominant MBP(85–99) peptide were used in this study (Wucherpfennig et al., 1994a, 1994b). These clones had been generated from blood mononuclear cells of two patients with relapsing–remitting MS carrying HLA-DR2 (DR2 subtypes: DRB1*1501 for patient Ob; DRB1*1602 for patient Hy). In both patients, the T cell response was focused on the immunodominant MBP(84–102) peptide. T cell lines specific for MBP had been generated from blood mononuclear cells by stimulation with MBP (100 μg/ml) in RPMI 1640 supplemented with 10% human serum, 2 mM L-glutamine, 10 mM HEPES, 100 U/100 μg/ml penicillin/streptomycin in 96-well plates at 2×10^5 cells/well (Ota et al., 1990). On day 3, IL-2 was added to 5% (Human T-Stim, Becton Dickinson, Bedford, MA). On day 14, an aliquot of each cell line was assayed for reactivity to human MBP followed by proliferation assays with a panel of 13 synthetic peptides encompassing the human MBP sequence. Following a third round of stimulation (generally two stimulations with MBP and one stimulation with peptide), T cell lines were cloned by limiting dilution using allogeneic feeder cells and phytohemagglutinin (PHA) (1 μg/ml) (Murex Diagnostics, Dartford, England) for stimulation. Allogeneic MNC were irradiated with 5000 rad and cocultured in 96-well plates (10^5 cells/well) with T cells. IL-2 was added on day 3, and cells were fed every 3–4 days with media containing 5% IL-2-containing supernatant. On day 12–14, growth-positive wells were expanded by restimulation with PHA, IL-2, and allogeneic feeder cells.

Recloning of MBP-specific clones was also done by limiting dilution using allogeneic feeder cells, PHA, and recombinant human IL-2 (Boehringer Mannheim). Clones were maintained by weekly stimulation with irradiated allogeneic feeder cells, PHA, and rIL-2. Alternatively, clones were expanded by stimulation with MBP(85–99) peptide-pulsed B cells and rIL-2.

T Cell Proliferation Assays

T cell proliferation assays were done using EBV-transformed homozygous B cell lines as antigen-presenting cells. B cells were irradiated (5000 rad) and pulsed with peptide for 2 hr prior to addition of T cells. For screening of pin-peptides, 25×10^3 B cells were added per well of a 96-well microtiter plate in a 50 μl volume (in triplicates). Peptide was added to a concentration of approximately 60 μg/ml. Following a 2 hr incubation at 37°C/5% CO_2, 50×10^3 T cells were added to a total culture volume of 200 μl/well (final peptide concentration approximately 12.5 μg/ml). After 3 days, T cell proliferation was determined with a [^{3}H]thymidine pulse (1 μCi/well) and liquid scintillation counting.

For MHC restriction experiments, irradiated B cells were pulsed with peptide for 2 hr at 37°C, followed by extensive washing. Peptide-pulsed B cells (25×10^3) were cocultured with 50×10^3 T cells for 3 days; T cell proliferation was determined with a [^{3}H]thymidine pulse (1 μCi/well) and liquid scintillation counting.

Acknowledgments

The authors wish to thank Anne L. Wucherpfennig and Mike Parzan for help with the data base searches and Basya Rybalov for expert technical assistance. We acknowledge the important contribution that Dr. David Hafler and members of his laboratory have made toward the generation of the T cell clones used in this study. This work was supported by grants from the National Multiple Sclerosis Society and the National Institutes of Health (CA47554 and NO1.AI 45198). K. W. W. is a Harry Weaver Neuroscience Scholar of the National Multiple Sclerosis Society.

Received November 15, 1994; revised December 15, 1994.

References

Allegretta, M., Nicklas, J. A., Sriram, S., and Albertini, R. J. (1990). T cells responsive to myelin basic protein in patients with multiple sclerosis. Science *247*, 718–721.

Baig, S., Olsson, O., Olsson, T., Love, A., Jeansson, S., and Link, H. (1989). Cells producing antibody to measles and herpes simplex virus in cerebrospinal fluid and blood of patients with multiple sclerosis and

controls. Clin. Exp. Immunol. *78*, 390–395.

Brocke, S., Gaur, A., Piercy, C., Gautam, A., Gijbels, K., Fathman, C. G., and Steinman, L. (1993). Induction of relapsing paralysis in experimental autoimmune encephalomyelitis by bacterial superantigen. Nature *365*, 642–644.

Brown, L. R., Nygard, N. R., Graham, M. B., Bono, C., Braciale, V. L., Gorka, J., Schwartz, B. D., and Braciale, T. J. (1991). Recognition of the influenza hemagglutinin by class II MHC-restricted T lymphocytes and antibodies. I. Site definition and implications for antigen presentation and T lymphocyte recognition. J. Immunol. *147*, 2677–2684.

Brown, J. H., Jardetzky, T. S., Gorga, J. C., Stern, L. J., Urban, R. G., Strominger, J. L., and Wiley, D. C. (1993). Three-dimensional structure of the human class II histocompatibility antigen HLA-DR1. Nature *364*, 33–39.

Burns, J., Rosenzweig, A., Zweiman, B., and Lisak, R. P. (1983). Isolation of myelin basic protein-reactive T-cell lines from normal human blood. Cell. Immunol. *81*, 435–440.

Burrows, S. R., Khanna, R., Burrows, J. M., and Moss, D. J. (1994). An alloresponse in humans is dominated by cytotoxic T lymphocytes (CTL) clones cross-reactive with a single Epstein–Barr virus CTL epitope: implications for graft-versus-host disease. J. Exp. Med. *179*, 1155–1161.

Busch, R., Hill, C. M., Hayball, J. D., Lamb, J. R., and Rothbard, J. B. (1991). Effect of a natural polymorphism at residue 86 of the HLA-DR β chain on peptide binding. J. Immunol. *147*, 1292–1298.

Chambers, T. M., Yamnikova, S., Kawaoka, Y., Lvov, D. K., and Webster, R. G. (1989). Antigenic and molecular characterization of subtype H13 hemagglutinin of influenza virus. Virology *172*, 180–188.

Cole, B. C., and Griffiths, M. M. (1993). Triggering and exacerbation of autoimmune arthritis by the mycoplasma arthritidis superantigen MAM. Arthritis Rheum. *36*, 994–1002.

Conrad, B., Weidmann, E., Trucco, G., Rudert, W. A., Behboo, R., Ricordi, C., Rodriquez-Rilo, H., Finegold, D., and Trucco, M. (1994). Evidence for superantigen involvement in insulin-dependent diabetes mellitus aetiology. Nature *371*, 351–355.

Datta, A. K., Feighny, R. J., and Pagano, J. S. (1980). Induction of Epstein–Barr virus-associated DNA polymerase by 12-O-tetradecanoylphorbol-13-acetate. J. Biol. Chem. *255*, 5120–5125.

Epstein, M. A., and Achong, B. G. (1977). Pathogenesis of infectious mononucleosis. Lancet *ii*, 1270–1272.

Friedman, S. M., Crow, M. K., Tumang, J. R., Tumang, M., Xu, Y., Hodtsev, A. S., Cole, B. C., and Posnett, D. N. (1991). Characterization of human T cells reactive with the mycoplasma arthritidis-derived superantigen (MAM): generation of a monoclonal antibody against Vβ17, the T cell receptor gene product expressed by a large fraction of MAM-reactive human T cells. J. Exp. Med. *174*, 891–900.

Fujinami, R. S., and Oldstone, M. B. A. (1985). Amino acid homology between the encephalitogenic site of myelin basic protein and virus: a mechanism for autoimmunity. Science *230*, 1043–1045.

Hickey, W. F., Hsu, B. L., and Kimura, H. (1991). T-lymphocyte entry into the central nervous system. J. Neurosci. Res. *28*, 254–260.

Johnson, R. T., Griffin, D. E., Hirsch, J. S., Wolinsky, J. S., Rodenbeck, S., Lindo De Soriano, I., and Vaisberg, A. (1984). Measles encephalomyelitis: clinical and immunological studies. N Engl. J. Med. *310*, 137–141.

Kappler, J. W., Roehm, N., and Marrack, P. (1987). T cell tolerance by clonal elimination in the thymus. Cell *49*, 273–280.

Kaufman, D. L., Clare-Salzler, M., Tian, J., Forsthuber, T., Ting, G. S. P., Robinson, P., Atkinson, M. A., Sercarz, E. E., Tobin, A. J., and Lehmann, P. V. (1993). Spontaneous loss of T-cell tolerance to glutamic acid decarboxylase in murine insulin-dependent diabetes. Nature *366*, 69–72.

Kisielow, P., Teh, H. S., Blüthmann, H., and von Boehmer, H. (1988). Positive selection of antigen-specific T cells in thymus by restricting MHC molecules. Nature *335*, 730–733.

Kurtzke, J. F. (1985). Epidemiology of multiple sclerosis. In Handbook of Clinical Neurology. P. J. Vinken, G. W. Bruyn, H. L. Klawans, and J. C. Koetsier, eds. (New York: Elsevier Science Publishing), pp. 259–287.

Kurtzke, J. F., and Hyllestad, K. (1979). Multiple sclerosis in the Faroe Islands: clinical and epidemiological features. Ann. Neurol. *5*, 6–21.

Lehmann, P. V., Forsthuber, T., Miller, A., and Sercarz, E. E. (1992). Spreading of T-cell autoimmunity to cryptic determinants of an autoantigen. Nature *358*, 155–157.

Madden, D. R., Garboczi, D. N., and Wiley, D. C. (1993). The antigenic identity of peptide–MHC complexes: a comparison of the conformation of five viral peptides presented by HLA-A2. Cell *75*, 693–708.

Martin, R., Jaraquemada, D., Flerlage, M., Richert, J., Whitaker, J., Long, E. O., McFarlin, D. E., and McFarland, H. F. (1990). Fine specificity and HLA restriction of myelin basic protein-specific cytotoxic T cell lines from multiple sclerosis patients and healthy individuals. J. Immunol. *145*, 540–548.

Oldstone, M. B. A. (1990). Molecular mimicry and autoimmune disease. Cell *50*, 819–820.

Olerup, O., Hillert, J., Fredrickson, S., Olsson, T., Kam-Hansen, S., Moeller, E., Carlsson, B., and Wallin, J. (1989). Primary chronic progressive and relapsing/remitting multiple sclerosis: two immunogenetically distinct disease entities. Proc. Natl. Acad. Sci. USA *86*, 7113–7117.

Ota, K., Matsui, M., Milford, E. L., Mackin, G. A., Weiner, H. L., and Hafler, D. A. (1990). T-cell recognition of an immunodominant myelin basic protein epitope in multiple sclerosis. Nature *346*, 183–187.

Pette, M., Fujita, K., Wilkinson, D., Altmann, D. M., Trowsdale, J., Giegerich, G., Hinkkanen, A., Epplen, J. T., Kappos, L., and Wekerle, H. (1990). Myelin autoreactivity in multiple sclerosis: recognition of myelin basic protein in the context of HLA-DR2 products by T lymphocytes of multiple sclerosis patients and healthy donors. Proc. Natl. Acad. Sci. USA *87*, 7968–7972.

Ray, C. G., Palmer, J. P., Crossley, J. R., and Williams, R. H. (1980). Coxsackie B virus antibody responses in juvenile-onset diabetes mellitus. Clin. Endocrinol. *12*, 375–378.

Reay, P. A., Kantor, R. M., and Davis, M. M. (1994). Use of global amino acid replacements to define the requirements for MHC binding and T cell recognition of moth cytochrome c (93–103). J. Immunol. *150*, 3946–3957.

Rose, N. R., Wolfgram, L. J., Herskowitz, A., and Beisel, K. W. (1986). Postinfectious autoimmunity: two distinct phases of coxsackie B3-induced myocarditis. Ann. NY Acad. Sci. *475*, 146–156.

Schluesener, H. J., and Wekerle, H. (1985). Autoaggressive T lymphocyte lines recognizing the encephalitogenic region of myelin basic protein: in vitro selection from unprimed T lymphocyte populations. J. Immunol. *135*, 3128–3133.

Schwarz, E., Freese, U. K., Gissman, L., Mayer, W., Roggenbuck, B., Stremlau, A., and zur Hausen, H. (1985). Structure and transcription of human papillomavirus sequences in cervical carcinoma cells. Nature *314*, 111–114.

Sebzda, E., Wallace, V. A., Mayer, J., Yeung, R. S. M., Mak, T. W., and Ohashi, P. S. (1994). Positive and negative thymocyte selection induced by different concentrations of a single peptide. Science *263*, 1615–1618.

Spielman, R. S., and Nathenson, N. (1982). The genetics of susceptibility to multiple sclerosis. Epidemiol. Rev. *4*, 45–65.

Spruance, S. (1985). Pathogenesis of herpes simplex labialis: experimental induction of lesions with UV light. J. Clin. Microbiol. *22*, 366–368.

Stadt, D., Kappos, L., Rohrbach, E., Heun, R., and Ratzka, M. (1990). Occurrence of MRI abnormalities in patients with isolated optic neuritis. Eur. Neurol. *30*, 305–309.

Tisch, R., Yang, X.-D., Singer, S. M., Liblau, R. S., Fugger, L., and McDevitt, H. O. (1993). Immune response to glutamic acid decarboxylase correlates with insulitis in non-obese diabetic mice. Nature *366*, 72–75.

Tovey, M. G., Lenoir, G., and Begon-Lours, J. (1978). Activation of latent Epstein–Barr virus by antibody to human IgM. Nature *276*, 270–272.

van Eden, W., Holoshitz, J., Nevo, Z., Frenkel, A., Klajman, A., and Cohen, I. R. (1985). Arthritis induced by a T-lymphocyte clone that responds to mycobacterium tuberculosis and to cartilage proteogly-

cans. Proc. Natl. Acad. Sci. USA *82*, 5117–5120.

van Eden, W., Thole, J. E. R., van der Zee, R., Noordzij, A., van Embden, J. D. A., Hensen, E. J., and Cohen, I. R. (1988). Cloning of the mycobacterial epitope recognized by T lymphocytes in adjuvant arthritis. Nature *331*, 171–173.

Vogt, A. B., Kropshofer, H., Kalbacher, H., Kalbus, M., Rammensee, H.-G., Coligan, J. E., and Martin, R. (1994). Ligand motifs of HLA-DRB5*0101 and DRB1*1501 molecules delineated from self-peptides. J. Immunol. *151*, 1665–1673.

Wekerle, H., Linington, C., Lassmann, H., and Meyermann, R. (1986). Cellular immune reactivity within the CNS. Trends Neurosci. *9*, 271–277.

Wucherpfennig, K. W., Weiner, H. L., and Hafler, D. A. (1991). T-cell recognition of myelin basic protein. Immunol. Today *12*, 277–282.

Wucherpfennig, K. W., Sette, A., Southwood, S., Oseroff, C., Matsui, M., Strominger, J. L., and Hafler, D. A. (1994a). Structural requirements for binding of an immunodominant myelin basic protein peptide to DR2 isotypes and for its recognition by human T cell clones. J. Exp. Med. *179*, 279–290.

Wucherpfennig, K. W., Zhang, J., Witek, C., Matsui, M., Modabber, Y., Ota, K., and Hafler, D. A. (1994b). Clonal expansion and persistence of human T cells specific for an immunodominant myelin basic protein peptide. J. Immunol. *150*, 5581–5592.

Zamvil, S. S., and Steinman, L. (1990). The T lymphocyte in experimental allergic encephalomyelitis. Annu. Rev. Immunol. *8*, 579–621.

Zhang, J., Markovic, S., Lacet, B., Raus, J., Weiner, H. L., and Hafler, D. A. (1994). Increased frequency of interleukin 2–responsive T cells specific for myelin basic protein and proteolipid protein in peripheral blood and cerebrospinal fluid of patients with multiple sclerosis. J. Exp. Med. *179*, 973–984.